Australian Government
Bureau of Meteorology

East Coast — National Hydrological Projections Assessment report

Vjekoslav Matic, Ulrike Bende-Michl, Pandora Hope, Sri Srikanthan, Alison Oke, Zaved Khan, Steven Thomas, Wendy Sharples, Greg Kociuba, Justin Peter, Elisabeth Vogel, Louise Wilson, Margot Turner

ISBN 978-1-925738-47-6

Version 1.0 July 2022

Published by the Bureau of Meteorology

Cover image: Hawkesbury River near Brooklyn village fishing farms and local marina in aerial view towards bridges and Long Island, Taras Vyshnya, 27 March 2020

Contents

List of figures

List of tables

1 Introduction to the National Hydrological Projections

Australia's climate is changing: temperatures are increasing and precipitation patterns are shifting, as described in the *State of the climate 2020* (CSIRO & Bureau of Meteorology 2020). On average, Australia has warmed by 1.44 ± 0.24 °C since national records began in 1910. Streamflow has changed across the country, broadly increasing in the north and decreasing in the south. The *State of the climate 2020* reports that, in Australia's south-west, cool-season (May–October) precipitation has declined by around 16% since 1970. The decrease is even more pronounced for the winter months (May–July) for the same period. In the south-east of Australia, precipitation started to decline around 1990, and the average cool-season precipitation from 2000 to 2019 was 12% less than last century (CSIRO & Bureau of Meteorology 2020). Along with this observed decline in precipitation, streamflow has declined substantially in both the south-west and south-east; changes in streamflow are typically disproportionally larger than changes in precipitation (Chiew 2006; Wasko et al. 2021; Zhang et al. 2016). In contrast, precipitation has increased across many northern parts of the country, and streamflow follows this trend (Zhang et al. 2016).

With rising greenhouse gas (GHG) levels in the atmosphere, temperature changes are projected to continue and intensify in the future, causing further warming and changes in all components of the climate and hydrological system (CSIRO & Bureau of Meteorology 2015). Given the limited water available for many Australian communities, businesses, governments and environments, these changes represent ongoing challenges to the management of Australia's water resources. The future security of our food and energy supplies, and our ecosystems, depends on water availability, as the demand for water is also growing.

To ensure that future water needs are met, decision-makers need forward-looking datasets and methods to evaluate a range of conceivable futures while accounting for uncertainty. The National Hydrological Projections product suite supports the process of strategic decision-making processes for future water resource management, adaptation and water policy developments. It consists of nationally consistent hydrological projections datasets, information and guidance material on future changes in Australia's projected hydrological variables.

The National Hydrological (NHP) Projections service complements projections work that has been undertaken by many federal and state governments, universities, and other organisations across Australia. A broad overview of available projections for Australia is given in Table 1.1. It is important to understand the varying nature of these projections including NHP in selected global climate models and their generation, greenhouse gas emission pathways, downscaling methods, spatial resolution, output variables and anticipated purpose ahead of their use. Further details about the Australian projections landscape, guidance material and readily available projections datasets can be found here: https://www.climatechangeinaustralia.gov.au/en/overview/about-site/landscape/

Table 1.1. Projections landscape for Australia

Name	State	Link
Climate Change in Australia	National	https://www.climatechangeinaustralia.gov.au/en/
Electricity Sector Climate Information	National	https://www.energy.gov.au/government-priorities/energy-security/electricity-sector-climate-information-esci-project
NSW and Australian Regional Climate Modelling project	New South Wales/Australian Capital Territory	https://climatedata-beta.environment.nsw.gov.au/
Climate Change NT	Northern Territory	https://climatechange.nt.gov.au/
Long Paddock	Queensland	https://www.longpaddock.qld.gov.au/qld-future-climate/
SA Climate Ready	South Australia	https://environment.sa.gov.au
Climate Futures for Tasmania	Tasmania	https://climatefutures.org.au/projects/climate-futures-tasmania/
Victorian Climate Projections 2019 Victorian Water and Climate Initiative	Victoria	https://www.climatechangeinaustralia.gov.au/en/projects/victorian-climate-projections-19 https://www.water.vic.gov.au/climate-change/reserach/vicwaci
Western Australian climate projections	Western Australia	https://www.wa.gov.au/government/publications/western-australian-climate-projections-summary

1.1 Developing the National Hydrological Projections

Broadly, the National Hydrological Projections were produced by choosing representative emission pathways (RCPs) and using a number of global climate model (GCM) inputs to run with a hydrological landscape water balance model (Figure 1.1).

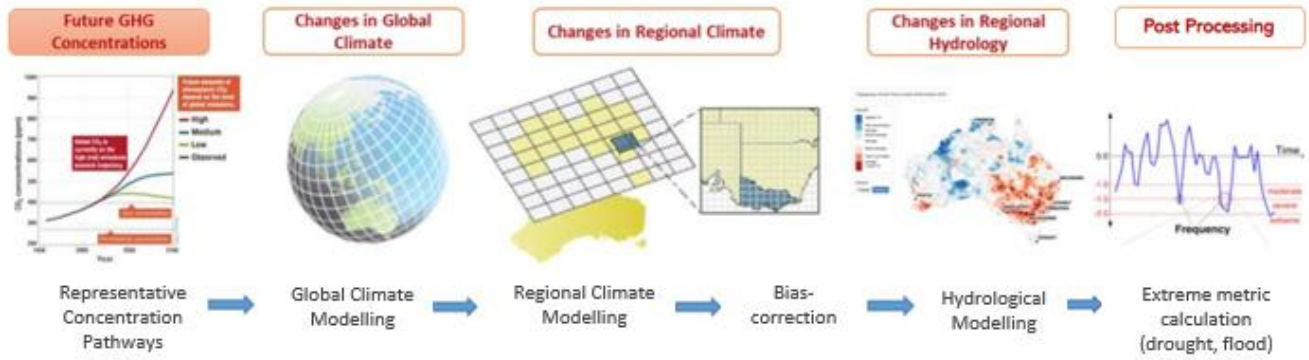

Figure 1.1. National Hydrological Projections workflow principles showing the processing steps: i) selecting representative concentration pathways, ii) running the 4 selected global climate models and also a regional climate model, iii) correcting the discrepancies between climate input and observation (bias correction) to produce the climate data, iv) running the climate data through a hydrological model to project hydrological changes and v) calculating projected hydrological extremes

State-of-the-art techniques were used to resolve the climate data to a finer geographic scale and correct for biases (to adjust for discrepancies between observations and the climate models). The resultant climate data was processed through a hydrological model to produce projections of future hydrological changes and extreme conditions.

Australian and international climate modelling groups simulate the world's weather and climate with global climate models under historical and future forcing from greenhouse gases as well as from atmospheric and solar forcing ('forcing' is the term used to describe the impacts of factors that affect Earth's climate). The models used for the National Hydrological Projections stem from the Coupled Model Intercomparison Project Phase 5 (CMIP5) (Taylor et al. 2012) undertaken by the World Climate Research Programme's Working Group on Coupled Modelling (WGCM) (PCMDI 2021).

First, 2 future scenarios were selected to represent potential future pathways of greenhouse gas concentrations, aerosols and other atmospheric chemical constituents: medium (RCP4.5) and high (RCP8.5) emissions of greenhouse gases (RCP stands for 'representative concentration pathway') (Figure 1.2). The medium RCP4.5 scenario sees emissions peak by mid-century at around 50% higher than the 2000 level then rapidly decline over 30 years before stabilising at half of the 2000 level. The high RCP8.5 greenhouse gas emission scenario simulates rapid emission increases through early and middle parts of the century to reach 950 ppm CO_2 by 2100. Both RCP4.5 and RCP8.5 were the only RCPs available for a dynamically downscaled regional climate model over Australia.

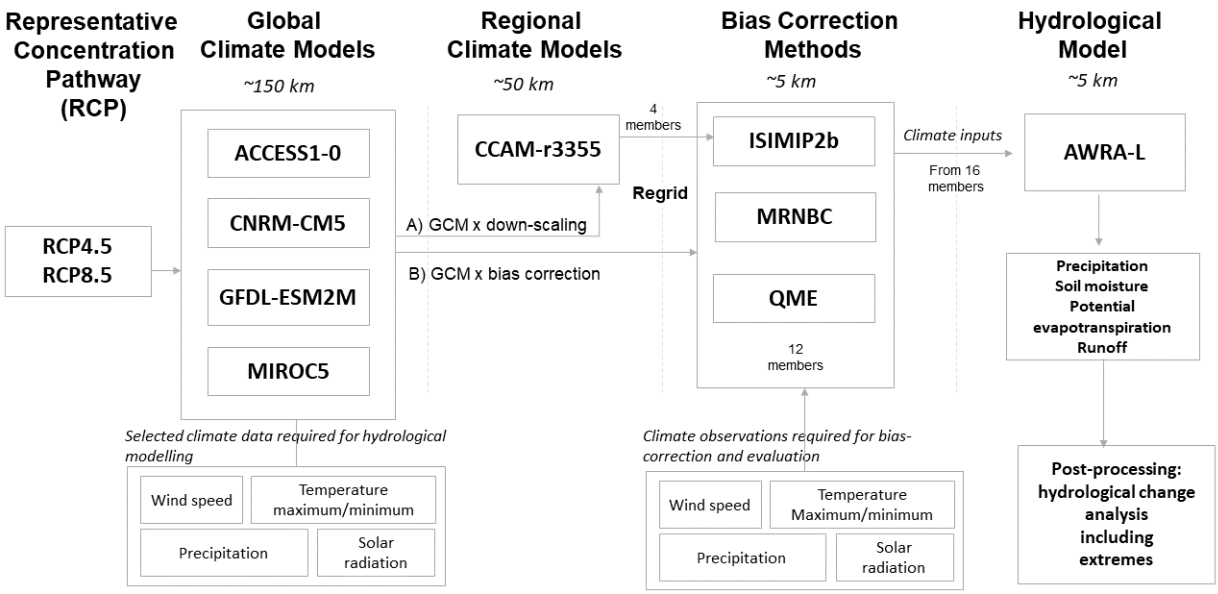

Figure 1.2. National Hydrological Projections showing details of the processing steps: i) 2 representative concentration pathways (RCP4.5 as medium and RCP8.5 as high) are selected, ii) 4 CMIP5 global climate models (GCMs) are selected, iii) path A – each GCM is downscaled by a regional climate model (RCM) to a 50km (0.5°) scale and then re-gridded to a 5 km (0.05°) scale. The RCM uses one bias-correction method (ISIMIP2b) that corrects the necessary climate inputs (precipitation, temperature, wind and solar radiation) against observations, iv) path B – each GCM is re-gridded to a 5 km (0.5°) scale and corrected directly using one of 3 bias-correction methods, and v) climate data from the 16-member ensemble is used to run the hydrological Australian Water Balance Model (AWRA-L) to produce hydroclimate change information for precipitation, soil moisture, runoff and evapotranspiration. These hydroclimatic variables are processed to understand future changes on the Australian water cycle components, including extremes

As shown in Figure 1.2, 4 CMIP5 GCMs were chosen, each with a spatial resolution of about 150 kilometres (km) (Srikanthan et al. 2022). These climate models were chosen as a subset of the models used in the Climate Change in Australia assessment (see Chapter 5 in CSIRO & Bureau of Meteorology 2015). The 4 global climate models were selected to represent a range (wet, medium and dry) of plausible future climates across Australia and for their ability to provide all the necessary climate inputs for the Australian Water Resources Assessment Landscape hydrological model (AWRA-L, version 6.1) (Frost & Wright 2018). In addition, a regional climate model (RCM) was used to bring each of the 4 selected GCMs to a finer resolution output of about 50 square kilometres (km^2) over Australia. These regional models better account for regional climatic influences, such as local topography.

Before using climate inputs from climate models, biases in the global and regional climate model forcing were corrected against observations in a process called bias correction. Three bias-correction methods were applied to the climate data from the models, resulting in the following 16-member ensemble (Figure 1.2):

- 12 members – comprising each of the 4 global climate models corrected with 3 different bias-correction methods
- 4 members – comprising each of 4 global climate models, downscaled and adjusted to a finer resolution as a regional climate model and corrected with one bias-correction method.

Each ensemble member reflects the chosen characteristics of its bias-correction method; the range of ensemble members lets decision-makers select the approach best suited to their needs.

To examine future impacts of climate change and to inform decisions on adaptation, outputs from the climate modelling process were re-gridded to a 5 km scale and used in our hydrological model to provide projections at that scale across Australia. Using bias-corrected climate inputs of precipitation, temperature, wind and solar radiation from the 16-member ensemble, the hydrological AWRA-L model produced daily model outputs over Australia of soil moisture, runoff and potential evapotranspiration (the amount of evaporation and transpiration that would occur at a particular location when water available for this process is non-limited).

To assess hydrological changes, temporal results are aggregated in 30-year periods centred around 2030, 2050, 2070 and 2085 on annual and seasonal timescales. These results are shown as maps demonstrating the spatial variability of the region's change or as graphs showing aggregated results across the regions.

Each step of the National Hydrological Projections modelling chain is carefully evaluated to understand the uncertainties associated with the modelling process. Uncertainties in hydroclimate change analysis can come from multiple sources, including:

- how greenhouse gas emissions will change into the future
- the processes represented in the climate models
- the effect of bias-correction and downscaling processes
- the hydrological modelling itself.

More details on how we address these uncertainties are discussed in Chapter 3. Further information on these models and the choices made in their selection as well as the evaluation process are detailed in our scientific publications and reports.

1.2 National Hydrological Projections hydrological assessment reports

Projection results feature many sources of uncertainty, including uncertainty over future trajectories of atmospheric greenhouse gas concentrations, how a warmer climate will lead to changes to hydroclimatic features and feedback loops, and the ability of climate models to represent those features. Acknowledging these uncertainties, the National Hydrological Projections ensemble provides a unique opportunity to examine impacts of plausible future changes on Australia's hydroclimate and its water resources.

To understand future impacts on Australia's water resources, region-specific assessment reports have been prepared on plausible future hydrological changes, including changes in precipitation, runoff, potential evapotranspiration, and soil moisture as well as changes in extremes including droughts and floods. These assessment reports are based on 8 regions, formed from clusters of natural resource management (NRM) regions of Australia, that can be affected differently by climate change. These regions broadly represent groups of similar climatic and biophysical settings in Australia and corresponding natural resources. The National Hydrological Projections build on these regions and the scientific work that was previously carried out by the Climate Change in Australia (CCiA) initiative (CCiA n.d. a). CCiA provided the most nationally comprehensive, robust and consistent scientific information on future climate changes for Australia. Projected climate change has been described in detail in the individual CCiA reports for the NRM clusters (CCiA n.d. b), with additional regional detail being provided through ongoing initiatives from Australian state and federal governments. This work builds a complementary picture in the context of the regional hydrological cycle, regional water assets and its future impacts.

These hydrological assessment reports are a demonstration case of the applicability of the National Hydrological Projections data and plausible future water resource impact analysis across Australia. They are intended to provide a high-level regional picture and raise awareness of plausible hydrological changes for a water-sensitive audience, including Australia's water, energy and environmental managers; emergency and recovery services; transport operators; farmers; and people generally interested in future changes to water resources. The reports present information in the form of 'storylines' of plausible future occurrences of hydrological extreme events (e.g.

floods) and long-term hydroclimatic changes. This information can be used to guide investment decisions and develop mitigation and adaptation strategies.

This report focuses on the East Coast region and is structured as follows:

- Chapter 1 introduces the National Hydrological Projections.
- Chapter 2 describes the assessment region, including its physiographic and hydroclimatic characteristics, recent conditions and long-term hydroclimatic trends.
- Chapter 3 evaluates our ability to simulate future hydrological changes, including the multiple levels of uncertainty, whether the climate models chosen can represent the region's climate and how well the hydrological AWRA-L model performs in the region. It also presents the results from the evaluation of the bias-correction methods. This information provides important context for the following chapter.
- Chapter 4 assesses the region's future hydroclimate conditions, which are presented as available National Hydrological Projections storylines. Changes are shown for precipitation, evapotranspiration, soil moisture and runoff assessed against the reference period (1976–2005). The chapter also provides insights into plausible future extremes of wet and dry periods.
- Chapter 5 demonstrates the applicability of storylines by exploring future water-sensitive impacts of selected case studies.

All foundational National Hydrological Projections datasets underpinning the assessment report analyses are also available as application-ready datasets via the National Computational Infrastructure (NCI) Data Catalogue (https://dx.doi.org/10.25914/6130680dc5a51).

For further detailed regional analysis, guidance on the use of National Hydrological Projections data or further general information, please contact us via water@bom.gov.au.

2 Regional description and hydroclimate of the East Coast region

The East Coast region (Figure 2.1) is defined on its western boundary by the Great Dividing Range and on its eastern boundary by the east Australian coastline. The region contains 5 of the 10 largest urban areas in Australia and is home to around 40% of Australia's population. Urban water security is therefore a key climate-sensitive management risk for the region.

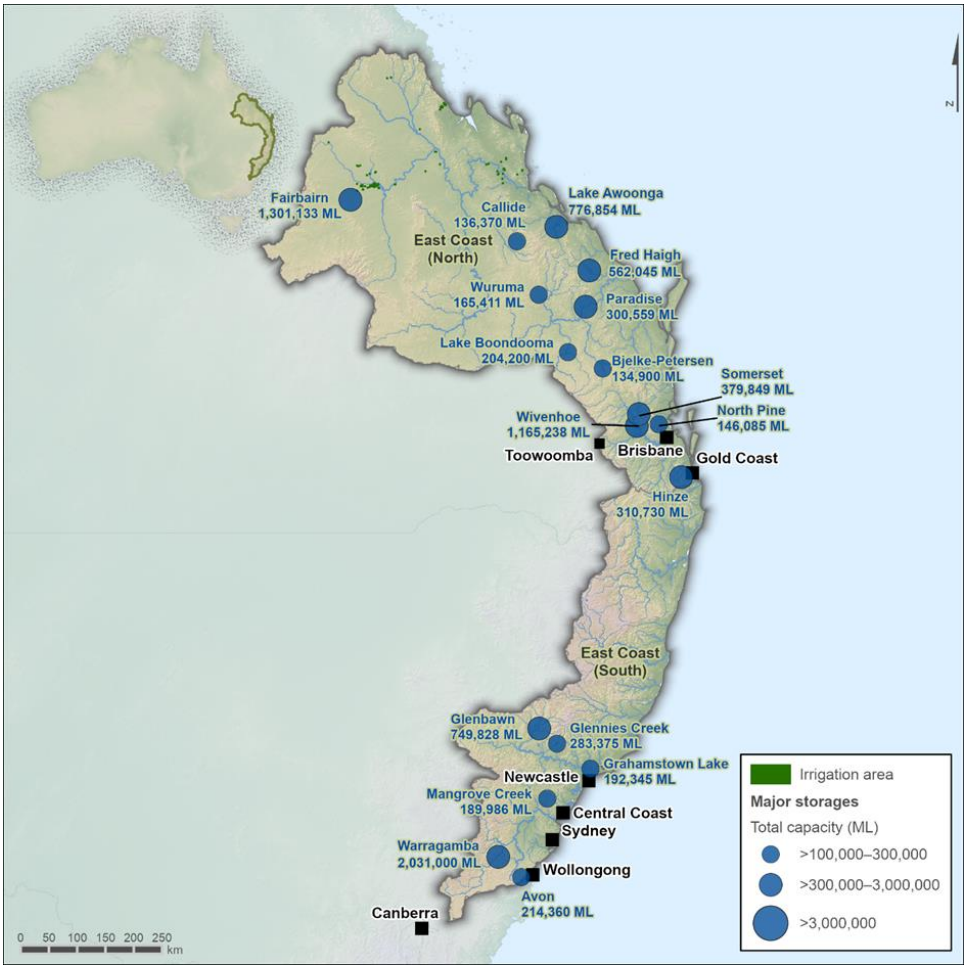

Figure 2.1. East Coast region showing major water storages

2.1 Climate

The East Coast region ranges from the tropical climate in the north to the temperate climates of the southern New South Wales coast near Wollongong. The coastal fringe along the east are the wettest parts of the region (Figure 2.2 and Figure 2.4). Most of the precipitation falls in the summer months across both the northern and southern subregions (Figures 2.3 and 2.5). The difference between winter and summer precipitation is more pronounced in the north than in the south. This difference is due to the northern subregion having larger tropical influences (such as the monsoon, tropical cyclones and tropical depressions) and receiving less precipitation associated with fronts during the cooler months. Those fronts are a more important feature of the southern region. Average annual precipitation is less in the northern subregion than in the southern subregion.

While the region's year-to-year variability matches that of many other parts of Australia, it has moderately reliable summer precipitation and unreliable cool-season precipitation. Across the region, more precipitation generally falls near the coast than further inland.

The seasonal precipitation characteristics in the East Coast region are determined by the complex interactions of several rain-bearing weather systems. Precipitation in the sub-tropical northern subregion can be enhanced by exposure to the summer trade winds, which bring moist, warm air masses to the northern part of the continent. Extreme precipitation in northern areas can also be associated with tropical cyclones during the warmer months of the year, typically from about November to April. During the cooler months, fronts and low pressure systems (such as east coast lows) can bring wet conditions to the region, particularly in southern areas. Throughout the year, precipitation is also brought by cloud bands associated with the formation of troughs at upper levels of the atmosphere.

A strong annual cycle of thunderstorm activity occurs throughout the East Coast region, with a maximum during the warmer months and a minimum during the cooler months (Dowdy & Kuleshov 2014). The East Coast region experiences thunderstorms on about 20 to 50 days a year, depending on location. This is higher than most other regions in other parts of Australia at similar latitudes (Kuleshov et al. 2006).

Year-to-year precipitation variability in the East Coast region is related to changes in sea-surface temperatures (SSTs) of adjacent ocean basins. Prominent influences include the oscillation between El Niño– and La Niña–type conditions in the eastern and central Pacific, and variability of SSTs in the Indian Ocean. Precipitation variations are also linked to a mode of variability known as the Southern Annular Mode (SAM), which affects the strength of the summer easterly circulation over Australia (Hendon et al. 2007).

2.1.1 East Coast north subregion

The East Coast north subregion is bounded to the south by the Queensland – New South Wales border, and it includes one of Australia's largest urban centres: the Brisbane – Gold Coast metropolitan area. To the north, the subregion is bounded by the Fitzroy River catchment, which is the largest cattle-producing region in Australia. The East Coast north subregion supports a diverse range of agricultural enterprises including broadacre cropping (cereals, pulses and cotton), sugar cane, citrus, avocados and other tropical fruit, vegetables and dairy.

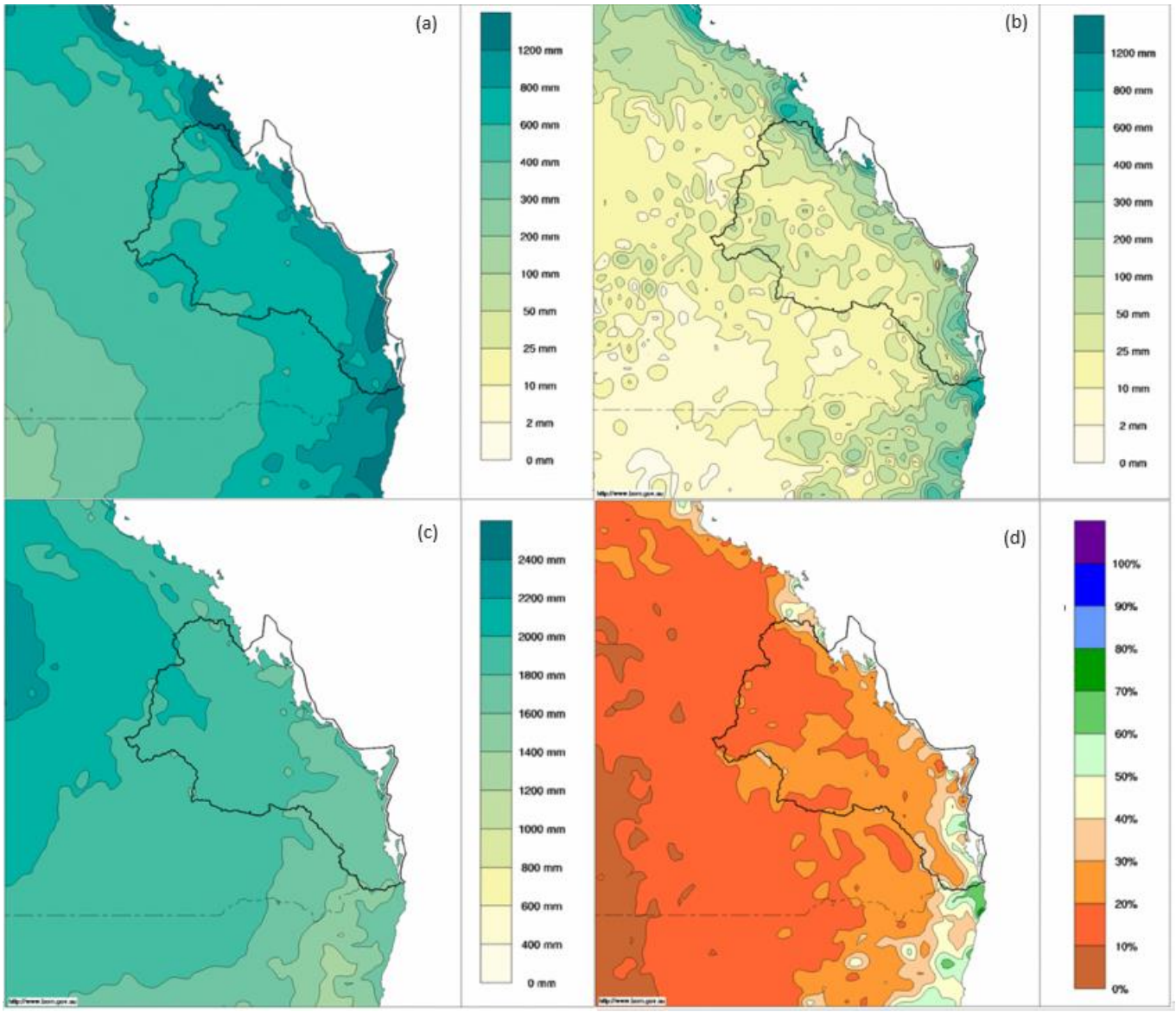

Figure 2.2. East Coast north subregion annual average hydroclimate (1976–2005) showing (a) observed precipitation and AWRA-L modelled values for (b) runoff, (c) potential evapotranspiration and (d) soil moisture

The Fitzroy River catchment is the furthest north and therefore experiences the most monsoonal weather. Soil moisture and streamflow in this area are driven by wet season precipitation, and streams often cease to flow in the dry season. The seasonality of the streamflow is also governed by the monsoon: a delayed monsoonal onset can delay streamflow until the middle of the wet season, as was observed in 2019–20. The northern parts of the East Coast north subregion are subject to tropical cyclones and associated impacts such as flooding. Tropical cyclone frequency has decreased in the region. At the southern end of the East Coast north subregion – the South East Queensland (SEQ) area – streamflow is similarly governed by the higher summer precipitation but is typically sustained through the winter months.

Mean monthly precipitation, runoff and soil moisture, and the mean potential evapotranspiration and maximum, minimum and mean temperatures for East Coast north are shown in Figure 2.3. While precipitation varies between the warm season (November–March) and the cool season (April–October), soil moisture is retained and shows comparable less seasonal variability. Due to lower temperatures, potential evaporation is comparable less during the cool season.

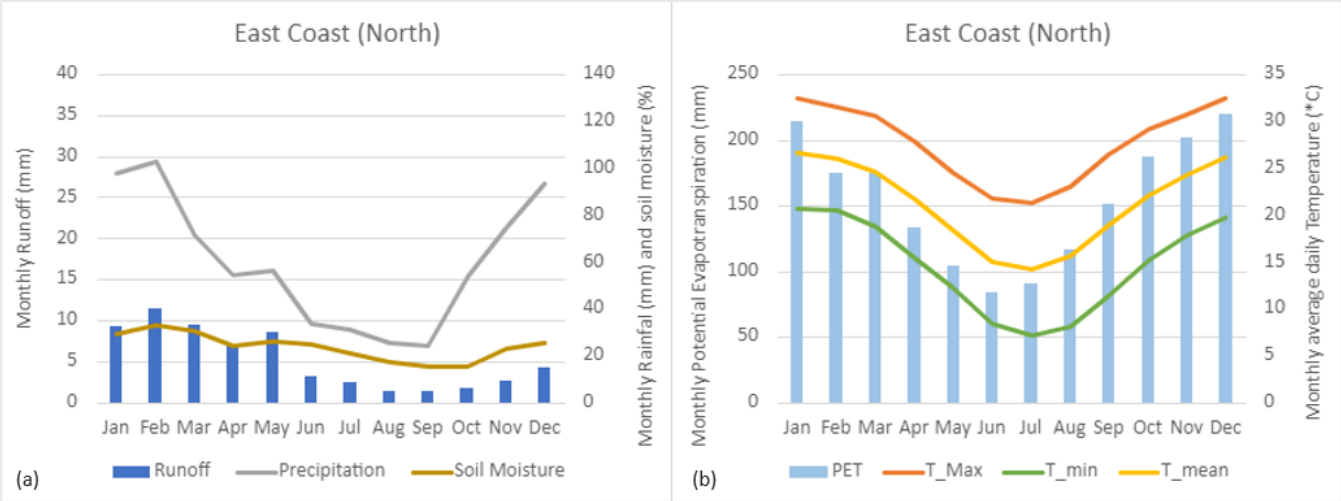

Figure 2.3. Monthly average observed (a) precipitation and AWRA-L modelled runoff and soil moisture and (b) temperature and AWRA-L modelled potential evapotranspiration for the East Coast north subregion for the reference period (1976–2005)

2.1.2 East Coast south subregion

The East Coast south subregion extends from the Queensland – New South Wales border to Wollongong (Figure 2.4). It is dominated by a sub-tropical climate, with temperate influences in the south and tropical influences in the north. This subregion features Sydney, which is Australia's largest urban centre. Precipitation is relatively high in the southern parts of the subregion, driven by frontal systems and east coast lows.

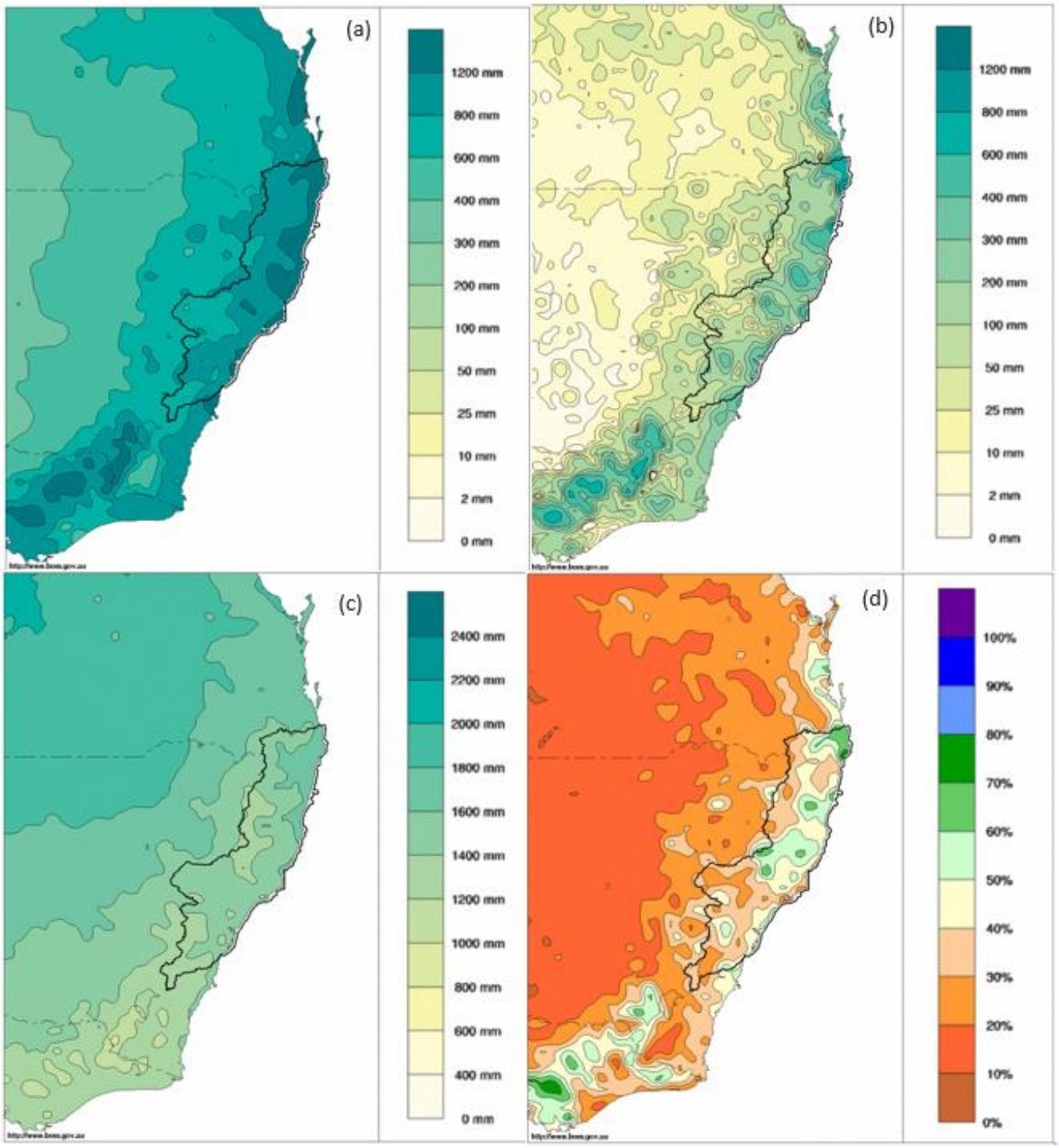

Figure 2.4. East Coast south subregion annual average hydroclimate (1976–2005) showing (a) observed precipitation and AWRA-L modelled values for (b) runoff, (c) potential evapotranspiration and (d) soil moisture

Mean monthly precipitation, runoff and soil moisture and mean potential evapotranspiration and maximum, minimum and mean temperatures for East Coast south are shown in Figure 2.5. Most precipitation occurs in the summer and autumn months from January to May. Despite precipitation and modelled runoff peaking in summer and autumn, most storage infilling in the southern subregion occurs during winter and spring (Pepler et al. 2021).

There is a general pattern of streamflow seasonality in the southern subregion: catchments nearer the coast have higher streamflow in the summer while inland areas are more likely to peak in winter, especially towards the south.

East coast low events (strong cyclonic systems off the east coast of New South Wales associated with prolonged high precipitation) were responsible for 66% of high-inflow days in the East Coast south subregion. These included the major dam-filling events since 1992 and 11 of the 13 largest precipitation events. These weather patterns are the most significant factor affecting dam levels in the Sydney region (Pepler & Rakich 2010).

For example, early February 2020 saw the highest daily precipitation on record for parts of Sydney. Warragamba Dam went from 42% to 82% full in less than a week – effectively gaining 2 years' water supply in a few days and ending a period where storage levels where below 50%. This event highlights the somewhat sporadic influence of high-intensity precipitation that significantly contributes to the region's water security.

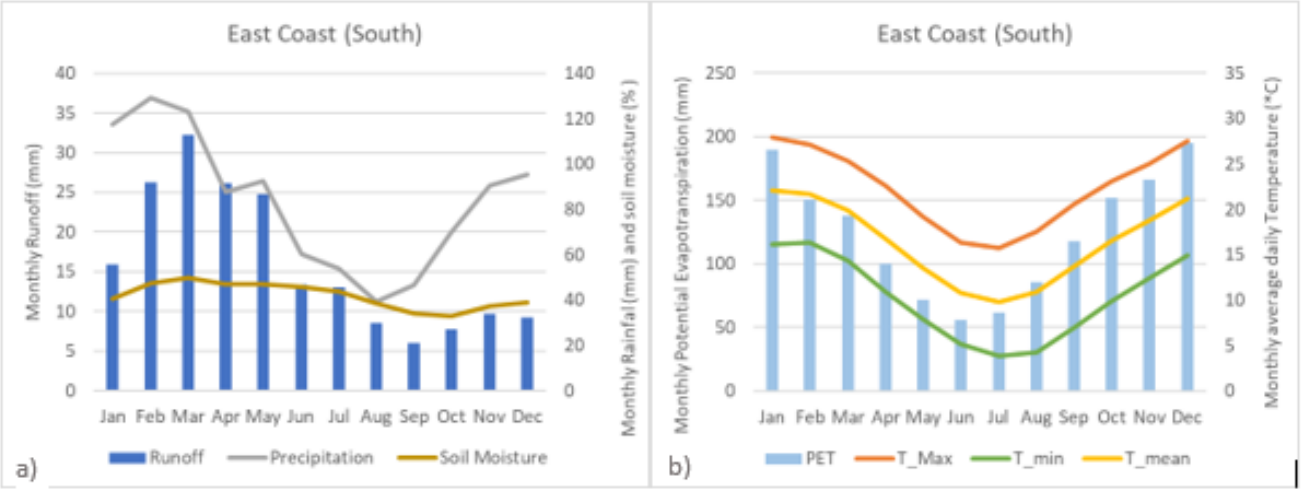

Figure 2.5. Monthly average observed (a) precipitation and AWRA-L modelled runoff and soil moisture and (b) temperature and AWRA-L modelled potential evapotranspiration for the East Coast south subregion for the reference period (1976–2005)

2.2 Recent hydroclimatic trends and condition

2.2.1 East Coast north subregion

In recent decades, this area has experienced severe droughts that have triggered serious water security thresholds in the SEQ water grid. This is due to the natural variability of the region, which has many multi-year dry spells in the historic record. However, temperature and evapotranspiration rates have increased in the historic record (1976–2005), which has resulted in a decreasing trend in soil moisture and exacerbated the natural dry conditions.

Figure 2.6 shows time series plots of precipitation, runoff, soil moisture and potential evapotranspiration anomalies for the East Coast north subregion. Precipitation has decreased over the past 30 years in some parts of the subregion: annual precipitation has decreased near Brisbane and summer precipitation has decreased in the north. However, the annual precipitation over the entire East Coast north subregion is considered stable with no significant trend. The regional precipitation trend in recent decades is still within natural variability, with high inter-annual precipitation being a characteristic of the region.

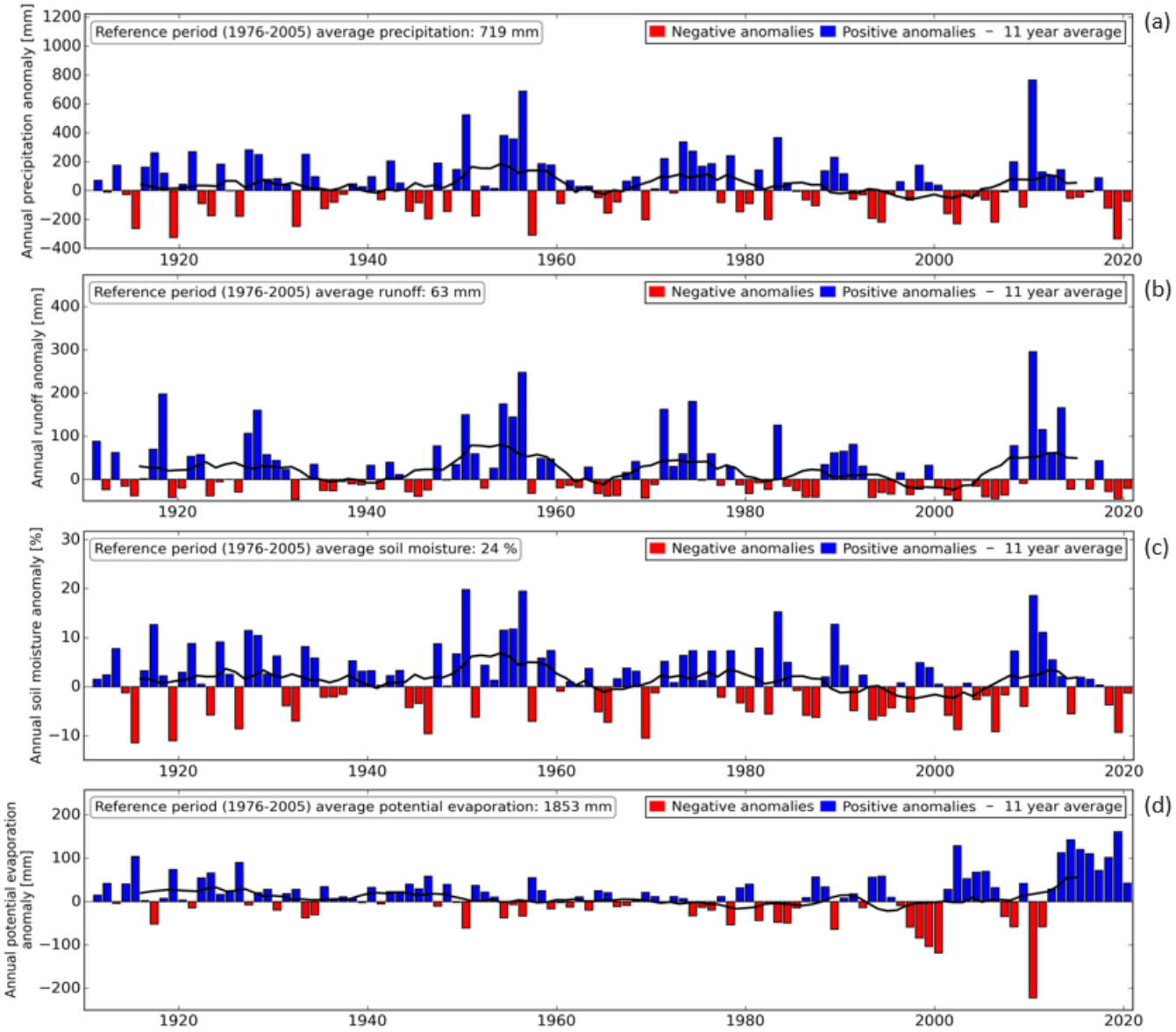

Figure 2.6. East Coast north subregion annual anomalies relative to the reference period (1976–2005) mean in (a) observed precipitation and AWRA-L modelled values for (b) runoff, (c) soil moisture and (d) potential evapotranspiration

2.2.2 East Coast south subregion

Figure 2.7 shows time series plots of annual precipitation, runoff, soil moisture and potential evapotranspiration anomalies for the East Coast south subregion. The precipitation, runoff, soil moisture and potential evapotranspiration potential do not show any significant trend. However, recent decades have seen a decline in cool-season precipitation in this southern subregion. Pepler et al. (2021) showed that most of the observed cool-season precipitation decline in south-eastern Australia is associated with a decrease in the frequency of fronts and cyclones that produce precipitation. Simultaneously, the frequency of cold fronts and thunderstorms that do not produce precipitation have increased in some areas.

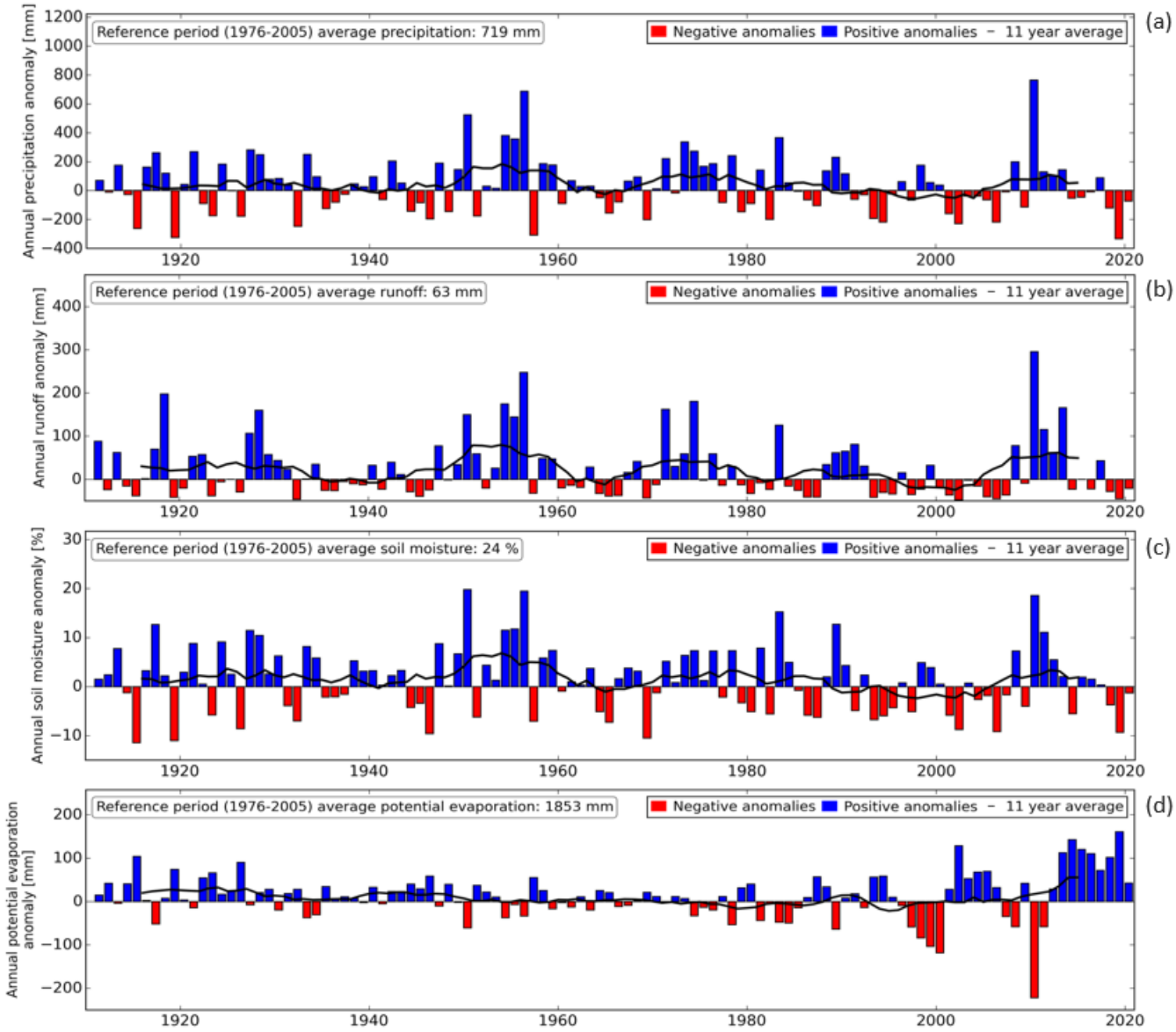

Figure 2.7. East Coast south subregion annual anomalies relative to the reference period (1976–2005) mean in (a) observed precipitation and AWRA-L modelled values for (b) runoff, (c) soil moisture and (d) potential evapotranspiration

Hydrological reference stations can be used to explore long-term trends in streamflow. These are monitoring stations that have long-term high-quality observations and that are unimpaired from storages or major land use change (station data available at the Bureau of Meteorology: http://www.bom.gov.au/water/hrs/). Most hydrological reference stations within the southern subregion show consistent trends of decrease in streamflow in all seasons. Wasko et al. (2021) found that of the 26 stream gauge sites in the subregion, all (100%) showed a decreasing trend in winter, 24 (92%) in autumn, 16 (62%) in spring and 12 (46%) in summer. These observed decreases in streamflow, despite annual precipitation that does not show a significant decrease, can potentially be explained by the impact of increased temperatures causing either catchments to dry or increased use of river water. Long-term drying can affect water availability by reducing groundwater recharge and therefore baseflow (sustained streamflow not generated by precipitation excess). This can have significant impacts on storage inflow volumes, particularly in dry periods where groundwater baseflow is the only water source. The degree to which these phenomena affect water security is catchment specific, but once a catchment is reaches a low-flow state, it takes many months of above-average precipitation to return the system back to average conditions. In the recent 2018 to 2019 dry period, this region experienced some of the lowest precipitation and soil moisture amounts on record, and the resulting reductions in runoff and inflows into storages were amplified due to high temperatures coinciding with

precipitation deficits. These recent conditions illustrate how compounding climate impacts can exacerbate water security risk. They provide an example of catchment conditions that may become more frequent in a warming climate.

2.3 Water availability and management

2.3.1 East Coast north subregion

Australia's third largest metropolitan area, South East Queensland, is found in the East Coast north subregion. The large population in this region obtains its water supply from an interconnected grid of large water storages. As an example of typical water use, in the financial year 2019–20, the total water supplied was sourced 93% from surface water, 6% from groundwater and 3% from desalination. In that year, around 84% of the water was used for urban consumption and 16% for agriculture.

The region has experienced prolonged periods of extreme dry, including during the Millennium drought and, more recently, in the 2017–19 dry period. These periods of multi-year below-average precipitation and surface water storage inflows resulted in serious water scarcity issues. The region mitigates threats to water scarcity by operating the system as a grid and making large transfers between storages to connect regions with an oversupply of water to others with an undersupply, and also by diversifying water sources for this important population centre.

To the north, in the predominantly agricultural catchments of the Fitzroy, Burnett and Mary rivers, most of the available water for use is sourced from surface water storages and some from groundwater. In the Fitzroy River catchment, the largest and furthest north catchment in the region, about 84% of water used is sourced from surface water and the 16% from groundwater. Most of this water is used for agriculture, including irrigation schemes (around 25% of total water use). Grazing makes up the majority of land use in these northerly catchments, and therefore soil moisture sustaining pasture growth is a key source of water for this industry. Precipitation in summer is a key driver for autumn and winter soil moisture as little rain falls in the cooler months to replenish soil moisture stores.

Streams in the northern catchments and their inflows into storages follow the pattern of seasonal precipitation, predominantly filling during February and March and then sustaining water uses through drier winters or for multiple years when summer rain fails to fill the dams. In wetter years, the warm-season inflows often occur in the form of large floodwater events. Most of this floodwater is not available for use; it flows out to the sea taking with it sediment and nutrients that can impact the Great Barrier Reef in the most northerly parts of the region.

2.3.2 East Coast south subregion

Sydney is the key water use for the southern subregion. A number of large storages in the metropolitan region are the key source of water, including Warragamba Dam, the largest storage in the East Coast region. Large catchments draining to these storages cover most of the southern portions of this subregion. In this region water can be sourced from desalination and to a small degree from groundwater.

All major storages in the southern subregion are within the Sydney metro area or the Hunter River area around Newcastle directly to Sydney’s north (Figure 2.1). There are no major storages between the Hunter River and the Queensland border, and water is sourced from smaller regional storages and stream offtake from largely unregulated rivers, such as the Bellinger and the Clarence rivers. The key uses of water from the rivers include forestry, irrigation (maize and sugar cane), beef and dairy, and fruit and nuts.

Soil moisture is a key source of available water in this region, it is particularly important from October to April for the extensive forests of the region. Periods of extreme dry are associated with catastrophic bush fires, as seen in

the January 2020 fires that affected environmental assets, forestry and public health. Soil moisture availability in all seasons is also important for sustaining pasture for cattle, which is a key commodity in these regions.

3 Ability to simulate hydroclimatic conditions of the East Coast region

Assessing how well climate and hydrological models simulate key elements of the hydroclimate for Australia and the East Coast region is an essential part of understanding the potential future impacts of climate change. Assessments of model performance against observations and the latest scientific understanding of hydroclimatic processes provide a basis for confidence, in the sense of enabling trust in sets of projections. Models are not expected to reproduce observations exactly but rather are assessed in terms of their ability to capture important aspects of variability and their representation of important processes. Bias correction is an important step in the process of hydrological impact modelling. It brings information simulated by global climate models about the impacts on our climate system of rising greenhouse gases together with our best representation of hydrological processes at local scales (in this case, the assessment region). Bias-corrected climate data and the simulated hydrological output data are compared against observations to assess the performance of the models and processes. For a detailed description of the modelling process and a technical assessment of performance, please see the National Hydrological Projections technical report (Srikanthan et al. 2022).

Climate and hydrological models are always an imperfect representation of the reality (and plausible future) and are therefore associated with various sources of uncertainties. These uncertainties are intrinsic to hydroclimatic modelling and arise from the selection of climate models and the differences in model responses in a warming climate. These differences include the representation of climate drivers and their expression through, for example, El Niño and La Niña events and can also include the uncertainty of future human behaviours affecting greenhouse gas emissions. Further sources of uncertainties stem from the influence of bias corrections as well as from the hydrological modelling and the representation of hydrological processes itself. Thus, we can never forecast the exact time series of Australian temperature, precipitation and other climate drivers, and the National Hydrological Projections will differ from observations over short to medium periods. These uncertainties influence our ability to simulate the hydroclimate in Australia. This section briefly introduces the models and methods used in these National Hydrological Projections and assesses our ability to simulate the hydroclimate of the East Coast region in the context of the uncertainties. More details on the methods used can be found in the technical report (Srikanthan et al. 2022).

A number of choices were made in developing the datasets used in these National Hydrological Projections. Four global climate models (GCMs) were selected: ACCESS1-0, CNRM-CM5, GFDL-ESM2M and MIROC5. These models were selected from the suite of 42 models in the international Coupled Model Intercomparison Project Phase 5 (CMIP5). These 4 were chosen because they fulfilled important requirements, including the following:

- GCM data was available for input into the hydrological models.
- The GCM had been used to force one or more dynamical downscaling models.
- The GCM represents the large-scale drivers of climate and weather variability well.
- The GCM simulates Australia's precipitation, temperature, wind and radiation relatively well.
- The 4 models together represent the range of future precipitation and temperature changes relative to the spread of the 42 models of the CMIP5 ensemble.

The range of climate responses from each GCM, in any particular year, derives from the particular state of the weather and large-scale variability occurring within that model in that year. Each GCM models its own weather, and the climate varies over the longer term of the simulation in response to changing atmospheric levels of greenhouse gases, aerosols and ozone in the upper atmosphere (and the Antarctic ozone hole).

In addition, one atmosphere-only climate model was used to 'downscale' the GCMs from their 150 km resolution to 50 km. CCAM, CSIRO's Conformal Cubic Atmospheric Model, is a global model in which the grid point spacing is stretched to have fine resolution over Australia. Additional dynamically downscaled data was available to the National Hydrological Projections under the Victorian Climate and Water Initiative (VicWACI) and other initiatives of

the Victorian Government. Another regional model known as WRF (Weather Research and Forecasting model) dynamically downscaled the GCMs to about 50 km through the New South Wales Government–led partnership NARCliM (NSW and ACT Regional Climate Modelling). NARCliM output was included in the historical era simulations using the hydrological model but was not available for projections at the time of the release. The aim is to include further downscaling models in future updates to the projections service.

Three bias-correction methods were implemented to improve the representation of local climate conditions and reduce biases relative to observed data. First, the output of the GCMs and downscaling model were scaled down from their original scale (about 150 × 150 km) to 5 × 5 km resolution using a conservative re-gridding method; then the bias correction was applied. Each of the bias-correction methods is designed to preserve various features of the climate signal such as trend, inter-annual variability or seasonality of a climate variable.

The ability of each ensemble member to simulate the future hydroclimate of the East Coast region was assessed by evaluating its ability to reproduce the observations and observation-based model results of the 1976 to 2005 reference period. This evaluation let us identify any biases in the models that were likely to be carried forward into future projections. A range of evaluation techniques and statistics were used to evaluate the ability of the ensemble to simulate the hydroclimate of each individual region.

The following 3 bias-correction methods were used:

- ISIMIP2b, a quantile-based method that preserves the trend in the data (Hempel et al. 2013)
- QME, a quantile-based method that models the extremes well (Dowdy 2020)
- MRNBC, a method that preserves the interdependence among the variables as well the low-frequency characteristics (Johnson & Sharma 2012; Mehrotra & Sharma 2016).

The bias-corrected data was evaluated to assess the effectiveness of the bias-correction methods. The AWRA-L model (see Section 3.2) was then run with the bias-corrected climate data as input.

3.1 Ability to simulate Australian key climate drivers

The skill of the 4 National Hydrological Projections GCMs (among other GCMs) to represent the key large-scale drivers of Australia's climate was assessed previously by the Climate Change in Australia initiative (Moise et al. 2015). This assessment provided a basis for placing confidence in the model's projection for Australia and identified individual ensemble members or ensemble groups that may have significant performance issues in simulating a key aspect of climate variability.

Many CMIP5 GCMs have a bias in the Pacific Ocean whereby the ENSO signal extends too far towards Australia along the equator (Grose et al. 2017). This bias is minimal in the 4 National Hydrological Projections models selected; thus they represent the processes influencing climate variability in northern and eastern Australia reasonably well (Brown et al. 2016). A common bias seen in the eastern Indian Ocean in the Australian spring is relatively small in 3 of the models. However, CNRM-CM5 has this bias, which might limit the expected increase in the frequency of extreme positive Indian Ocean Dipole events and their expression through dry conditions in south-east Australia (Wang et al. 2017).

The 4 GCMs chosen for these projections, ACCESS1-0, CNRM-CM5, MIROC5 and GFDL-ESM2M (Table 3.1), were found to represent the weather-scale features influencing northern Australia well, and their future changes should be considered reliable. However, CMIP5 GCMs in general do not capture the eastward propagating sub-seasonal monsoon activity, cloudiness and precipitation linked to the Madden–Julian Oscillation (Moise et al. 2015).

Table 3.1. Details of selected global climate models

Climate model	Type	Institute	Country of origin	Reference
ACCESS1-0	Global	CSIRO and Bureau of Meteorology	Australia	Collier and Uhe (2012)
CNRM-CM5	Global	Centre National de Recherches Météorologiques – Groupe d'études de l'Atmosphère Météorologique (CNRM-GAME) and Centre Européen de Recherche et de Formation Avancée	France	Voldoire et al. (2013)
GFDL-ESM2M	Global	Geophysical Fluid Dynamics Laboratory, National Oceanic and Atmospheric Administration (NOAA)	USA	Dunne et al. (2012)
MIROC5	Global	Japan Agency for Marine-Earth Science and Technology (JAMSTEC)	Japan	Watanabe et al. (2010)
CCAM r3355	Regional	CSIRO	Australia	Rafter et al. (2019)

For completion, MIROC5 fulfils the requirements for inclusion in our ensemble although it does not represent the weather features that are important for the southern Australian climate as well as some others and might be considered less reliable. However, its inclusion helps the National Hydrological Projections GCM ensemble embrace the range indicated by the full range of 42 CMIP5 models (Srikanthan et al. 2022).

3.2 Hydrological modelling: the Australian Water Resources Assessment Landscape model (AWRA-L)

The Bureau's operational Australian Water Resources Assessment Landscape model (hereafter AWRA-L) was used to project root zone soil moisture, potential evapotranspiration and runoff. AWRA-L is a daily semi-distributed water balance model based on a 5 × 5 km (0.05°) grid. It models hydrological processes separately for each spatial unit, called a hydrologic response unit (HRU). At each grid cell it simulates the flow of water through the landscape: precipitation entering the grid cell, passing through the vegetation and soil moisture stores, and leaving the grid cell through evapotranspiration, runoff or deep drainage to the groundwater (Figure 3.1). Each grid cell in AWRA-L is divided into 2 HRUs, these represent deep-rooted vegetation (trees) and shallow-rooted vegetation (grass). The spatial distribution of the HRUs remains static over time and does not reflect land use change.

The AWRA-L model is calibrated at the national scale to match streamflow, soil moisture and evapotranspiration observations from across the country. This calibration enables a nationally consistent dataset, but model evaluation results can vary between regions and landscape features (Frost & Wright 2018).

Model performance can be affected by the number of calibration catchments local to the region or representative of the landscape feature. AWRA-L better captures the runoff dynamics in wetter regions and periods, while discontinuous runoff regimes, consisting of long dry periods followed by short periods of extreme precipitation, are more difficult to characterise. A positive bias in runoff can result in areas with extended periods of no flows in central and northern Australia. Groundwater–surface water interactions are not well represented in AWRA-L, resulting in a drop in performance in areas where there is a high dependency on the contribution of baseflow to the generation of streamflow.

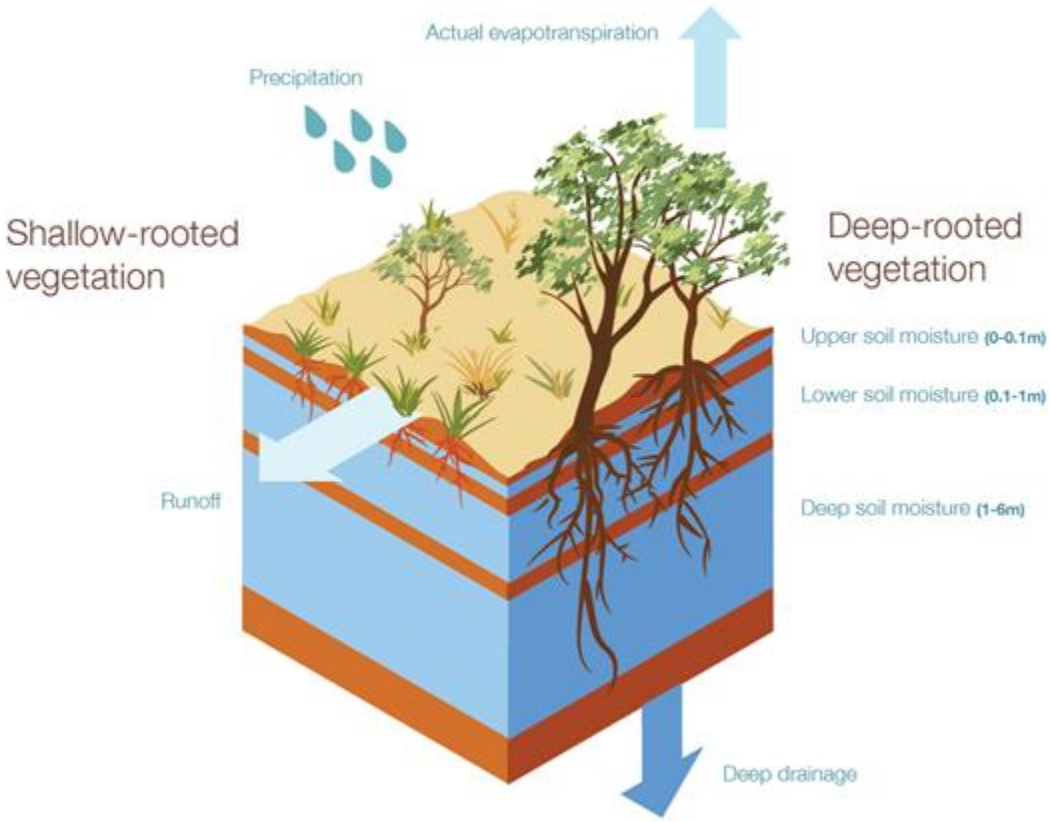

Figure 3.1. AWRA-L model grid cell with key water stores, fluxes and the hydrologic response units of deep- and shallow-rooted vegetation

The Bureau's operational AWRA-L was chosen as the hydrological model based on the evaluation and benchmarking of the available national models presented in Frost & Wright (2018). Importantly, this evaluation considered runoff, soil moisture and actual evapotranspiration in the assessment of the models. AWRA-L was run independently using the bias-corrected GCM climate data as input. The lack of feedback between the GCMs and AWRA-L means that the potential role of increased carbon dioxide levels on vegetation growth and evapotranspiration rates are not modelled (Greve et al. 2017; Yang et al. 2019). Future land use changes and vegetation changes resulting from future temperature and water availability changes are also not considered in AWRA-L or the GCMs. Together these factors will grow in importance over time, adding an extra facet of uncertainty to the soil moisture and runoff projections later in the century. A detailed description of the quantification of the AWRA-L model uncertainty can be found in Azarnivand et al. (2022).

3.3 Ability to simulate the hydroclimate of the East Coast region

The 4 GCMs were chosen to represent the range of future precipitation and temperature changes for Australia as described in the National Hydrological Projections technical report (Srikanthan et al. 2022). The 4 selected GCMs were compared to the entire ensemble of 42 CMIP5 Climate Change in Australia (CCiA) models to see how these models represent wet or dry futures (Figure 3.2). This provides an overview of how the selected GCMs rank relative to the full CMIP5 ensemble across Australia and respective climate variables.

The 4 global climate models chosen for these projections, ACCESS1-0, CNRM-CM5, MIROC5 and GFDL-ESM2M (Table 3.1), were found to represent Australia's weather-scale features well, and their future changes should be considered reliable (Grose et al. 2015). In the East Coast region, the 4 selected GCMs do not capture the full range of change in precipitation projected by the complete CMIP5 ensemble. The selected models all project a drying trend in the East Coast region for the 2030 time period. Most of the models (3 out of 4) project a drying trend in 2070 although one model (MIROC5) projects an increase in precipitation (Figure 3.2). The full CMIP5 ensemble of 42 models projects an increase in temperature in the East Coast region, and the selected 4 capture

the central to lower end of this range. Overall, the 4 GCMs are representative to some extent of the projected future climate in the East Coast region; however, they tend to project a drier climate and less warming than is projected by the full suite of CMIP5 GCMs.

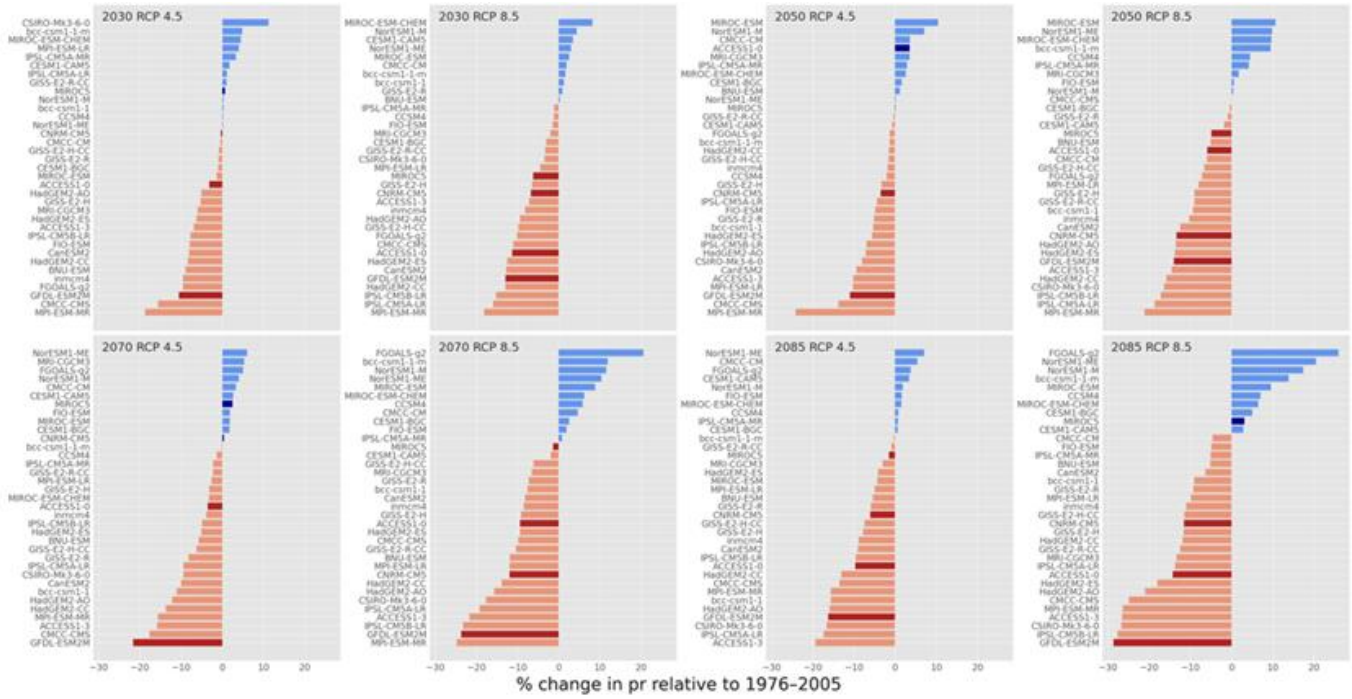

Figure 3.2. Ranking of the East Coast region precipitation projections for the GCMs used in this study (shown in darker colours) compared to the CCiA ensemble for RCP4.5 and RCP8.5 for 2030, 2050, 2070 and 2085. The horizontal bars indicate the change signal – the difference of the regional average quantity from the monthly pattern for the reference period (1976–2005)

Simulated hydroclimate data for the current climate (produced by the 16-member ensemble) is assessed by comparing it with observational datasets from the Australian Water Availability Project (AWAP) (Jones et al. 2009). In addition, 3 outputs (soil moisture, runoff and potential evapotranspiration) obtained by forcing the AWRA-L model with AWAP and bias-corrected data were also compared. Since the models are not perfect representations of the world, the simulated data will not exactly match the observed data. A certain tolerance level is used in assessing the model simulations. The precipitation and temperature observation network and the interpolated AWAP grids (Jones et al. 2009) provide a good representation of the spatial variability of precipitation (including extreme precipitation) in regions such as the central eastern seaboard of Australia where there is a high density of observations. Simulated hydroclimate data for the current climate (produced by the 16-member ensemble) is assessed by comparing it with observational data sets.

The evaluation of the ability of the ensemble members to replicate the reference period (1976–2005) observations and model runs revealed overall minimal bias in the East Coast region (Appendix Figures 8.1 to 8.10). Evaluation criteria, such as representing the seasonality of the climate variables, are found to be adequately preserved in all ensemble members.

Projections from all ensembles adequately reflected the monthly variability of the climate variables except for those with those using the QME bias-correction method. This finding is expected as QME corrects bias on a seasonal, rather than monthly, time scale. Some individual ensemble members or ensemble groups showed seasonal biases in precipitation projections, including a tendency for ensemble members corrected with the MRNBC bias-correction method to underestimate winter precipitation (represented by a bias of around −6%) (Appendix Figure 8.1). The mean annual and seasonal maximum temperature have a small negative bias (<2%) (Figure 8.3) while minimum temperature has a small positive bias (<4%) except for one case (ISIMIP2b-GFDL-ESM2M 13%) (Figure 8.5). For

the other bias-correction methods, the bias is very small (<1%). Solar radiation has a small negative bias (<3%) for most cases (Appendix Figure 8.7). The bias in surface wind is either zero or small (<1%) (Appendix Figure 8.9).

Biases in the hydrological variables, including potential evapotranspiration, soil moisture and runoff, are calculated by comparing the results produced by the ARWA-L model forced with observed climate inputs and those modelled by the ensemble for the 1976 to 2005 reference period (see Appendix Figures 8.11 to 8.16). While individual ensembles showed both positive and negative biases across the seasons for potential evapotranspiration, across the ensemble members overall there was a slight (<1%) negative bias. ISIMIP2b has the highest negative bias (that is, produces the greatest underestimation) in potential evapotranspiration, particularly in autumn and winter (Appendix Figure 8.13). Most ensembles have a bias of less than 10% for soil moisture, and that bias tends to be positive (Appendix Figure 8.15). QME has the largest bias in soil moisture – up to 15%.

The AWRA-L model simulates runoff relatively well in the East Coast region. Except for the urban and small irrigation areas which are not represented in AWRA-L, the vegetation and landscape of the East Coast region are well represented in the AWRA-L model. The forested areas of the alpine and foothill regions are well represented by the deep-rooted hydrological response unit and the cleared flatlands by the shallow-rooted (grass) vegetation. Of the 305 national calibration catchments, 53 of them are in the East Coast region, so the model is well calibrated to this area. The performance of the continentally calibrated AWRA-L model for the East Coast region is good based on the median of the monthly Nash–Sutcliffe coefficient of efficiency (NSE) (Nash & Sutcliffe 1970) greater than 0.6. Wasko et al. (2021) analysed streamflow trends post 1970 for both streamflow observations and modelled runoff from the AWRA-L model. They found a combination of positive and negative trends in the runoff at 26 streamflow sites across the region. The AWRA model was able to match the trend direction for 14 (54%) of sites for annual volumes, and 20 (77%) and 24 (96%) using historical observations for summer and winter flows, respectively.

In summary, there is confidence in the ability of the ensemble members to simulate the hydroclimate of the East Coast region. The evaluation shows that the selected ensemble members can replicate hydroclimatic observations in most cases. The AWRA-L simulated runoff, soil moisture, and potential evapotranspiration from the bias-corrected climate data are satisfactory for most of 16-member ensemble across the East Coast region.

4 Available National Hydrological Projections storylines for the East Coast region

Generally, projections provide a collection of plausible future 'storylines' rather than a forecast or likelihood of a specific outcome. Individually each ensemble member represents an internally consistent future storyline. Thus, while the ensemble members are based on slightly different physics, they all are built on plausible representations of physical processes. Individual ensemble members are the most appropriate method to represent this internal consistency and are a key element of establishing a storyline. No 2 ensemble members will follow the same changes in the many different climate features that can be considered.

The National Hydrological Projections used in this report allow for a unique region-wide assessment of projected hydroclimatic changes of the East Coast region. Results below are drawn from the assessment of the 16-member ensemble of hydroclimatic variables. The projected hydroclimate for the region is presented in this chapter as a set of available plausible future changes of key hydrological variables or storylines. It presents a set of key figures representing the change in the hydroclimate into the future under 2 different representative concentration pathways and showing how this change varies within the East Coast region.

In addition to the National Hydrological Projections, previous climate projections for the region are described in the East Coast Climate Change in Australia (CCiA) report (Dowdy et al. 2015a). Some state-based efforts further provide projections information in parts of this region. For NSW, NARCliM provides detailed downscaled information at 10 km resolution that is based on an older generation of GCMs (CMIP3) and the A2 projection scenario, which is similar to RCP8.5 (Adapt NSW n.d.). Queensland projections information can be found on the Long Paddock website (Syktus et al. 2020). Queensland projections use 10 climate models in total. Each of the GCM outputs used in Syktus et al. (2020) is downscaled using CCAM to 50 km resolution, as used in the National Hydrological Projections. Queensland projections then downscale projections data to 10 km. Basic climate variables are provided as well as wind and potential evapotranspiration, but Syktus et al. (2020) does not provide other hydrological variables.

4.1 Interpreting the National Hydrological Projections storylines

The projected future conditions are represented by the degree of change relative to the conditions of the reference period (1976–2005). Each of the 16-member ensemble is run for this reference period and for the future. As described in Chapter 3, each ensemble member is evaluated on the basis of the differences between the modelled reference period and the observations. These differences inform our assessment of the change in conditions projected by each ensemble member for the future. The change can be presented in absolute values (e.g. millimetres of precipitation) or as a relative proportion of the mean for the region (e.g. a 10% increase in precipitation). There is significant value in interpreting both absolute and relative values depending on the application.

Chapter 3 outlines how an ensemble of GCMs and bias-correction methods has been used to develop a range of plausible future conditions. This spread in the 16-member ensemble represents a range of plausible future conditions that decision-makers can use to explore impacts. The median of the 16-member ensemble represents a mid-range view of those plausible futures. The results are communicated against a series of future 30-year periods, which are referred to by their midpoint. For example, the results reported against 2050 represent the average of the 2036–2065 period. This allows us to identify general trends into the future beyond annual fluctuations. Results from other projections are discussed to contextualise where these storylines fit in a broader understanding of plausible futures.

Spatial variations in the projected conditions are represented by the differences in ensemble median and only presented for the futures, representative concentration pathways and units that are most relevant to the key finding in the region. Inter-annual variability is visually represented by a single ensemble member (ACCESS1-0_ISIMIP2b) in the time series graphs. This single ensemble member time series should not be interpreted as a forecast for

individual years; it is designed to model the extent to which the shorter-term climate drivers are likely to vary from the annual values.

Summary tables present key findings from multiple levels of evidence: projected results that describes the spread of the 16-member ensemble, concordance with historical trends reached by previous studies if available, and the assessment of the ability of the ensemble to simulate the hydroclimate in the region.

4.2 Precipitation

Projections for annual mean precipitation in the East Coast region project differ under the 2 representative concentration pathways and show small to larger decreases by the end of the century (Figure 4.1). The ensemble median projects little change but represents generally a large model spread, suggesting that both increases and decreases are plausible (Figure 4.2). This is for both representative concentration pathways and for all future time periods, except for the time periods centred in 2050 and 2070, where RCP8.5 projects only decreases.

A large year-to-year variability in annual precipitation is projected for the next few decades in the East Coast region as illustrated by the ACCESS1-0_ISIMIP2b ensemble example (Figure 4.1) with some periods in mid-century that project larger variability. Inter-annual variability is likely to remain significantly greater than the projected long-term change, meaning that wet and dry years will still occur, but the base from where these year-to-year peaks and troughs occur could change.

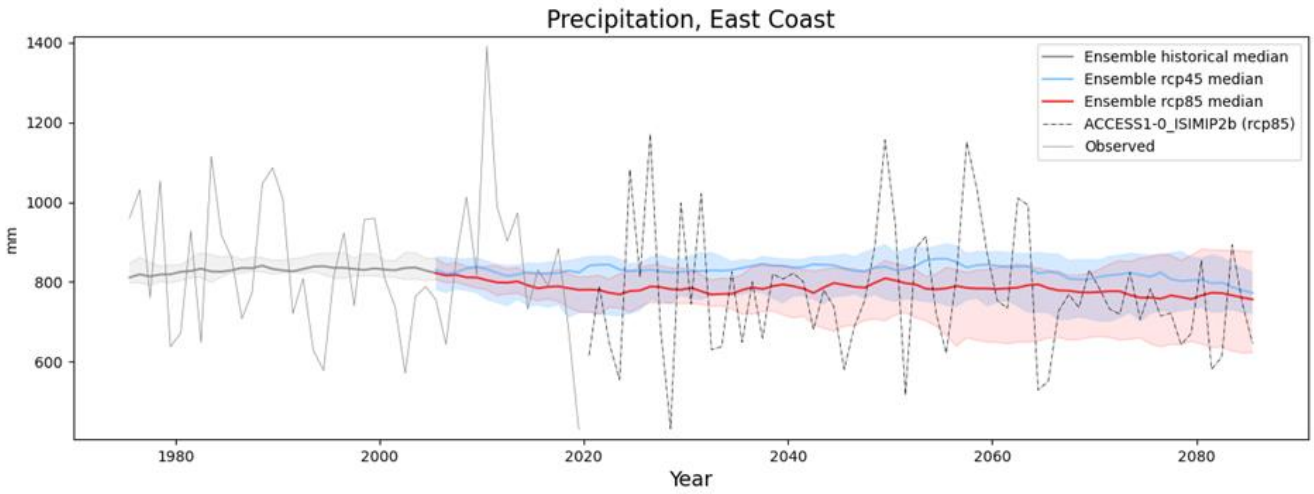

Figure 4.1. Annual modelled precipitation projected to 2099 by the 16-member ensemble for RCP4.5 (blue) and RCP8.5 (red) in the East Coast region. The shaded areas represent the 10th to 90th percentile range for all ensemble members in the historical and future time periods. The time series for ACCESS1-0_ISIMIP2b (RCP8.5) is included (dotted line) to show the variability projected for an individual ensemble member. The grey line represents the observed historical median precipitation based on AWAP data

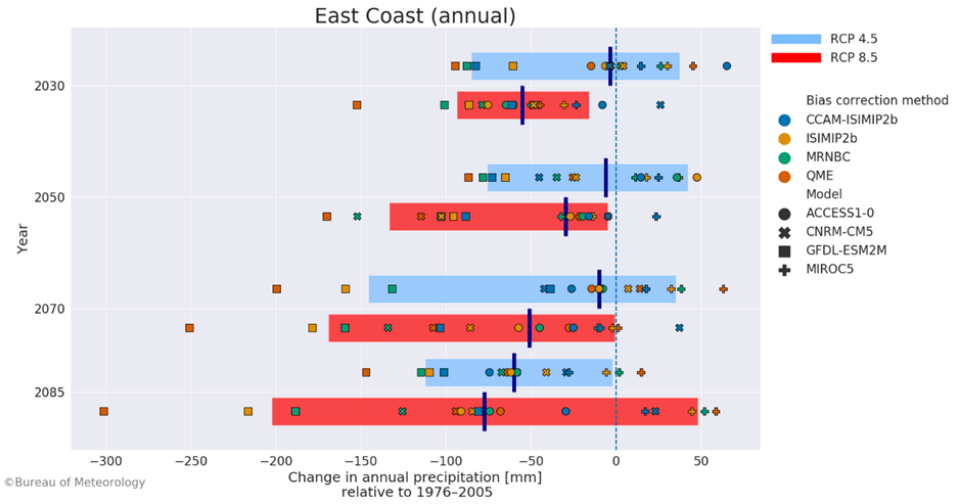

Figure 4.2. Change in annual precipitation (mm) projected by each ensemble member for 2030, 2050, 2070 and 2085 in the East Coast region. The red bar shows the 10th to 90th percentiles for RCP8.5. The blue bar shows the 10th to 90th percentiles for RCP4.5. The dark blue line shows the ensemble median. The change is relative to the reference period (1976–2005)

Average spring precipitation is projected to range from large decreases to little change (Figure 4.3d). The spring ensemble member median projects a region-wide decrease in spring average precipitation, with large decreases in the north of the region. Thunderstorms, east coast lows and fronts are important springtime rain-bearing weather in this region. In the northern regions, the spring rain is correlated with the El Niño–Southern Oscillation (ENSO), monsoon and the Southern Annular Mode. In the south there is only a weak ENSO correlation but a strong correlation with the dynamics of the sub-tropical ridge. There is evidence that springtime thunderstorms are increasing in this region (while decreasing in other parts of the country) and that the intensity of the events is increasing (Pepler et al. 2021). In addition, thunderstorms are known to have a role in causing spring precipitation but are generally not simulated well by climate models (Dowdy 2020).

The strong signal for decreases in spring precipitation is suggested to be an important result from this project, and it may provide added value from the processing methods, which produce a signal not evident in other projection sets. However, the inclusion of only one regional climate model (CCAM) is limiting. Future research could include multiple RCMs to better understand future weather system processes relevant to this region.

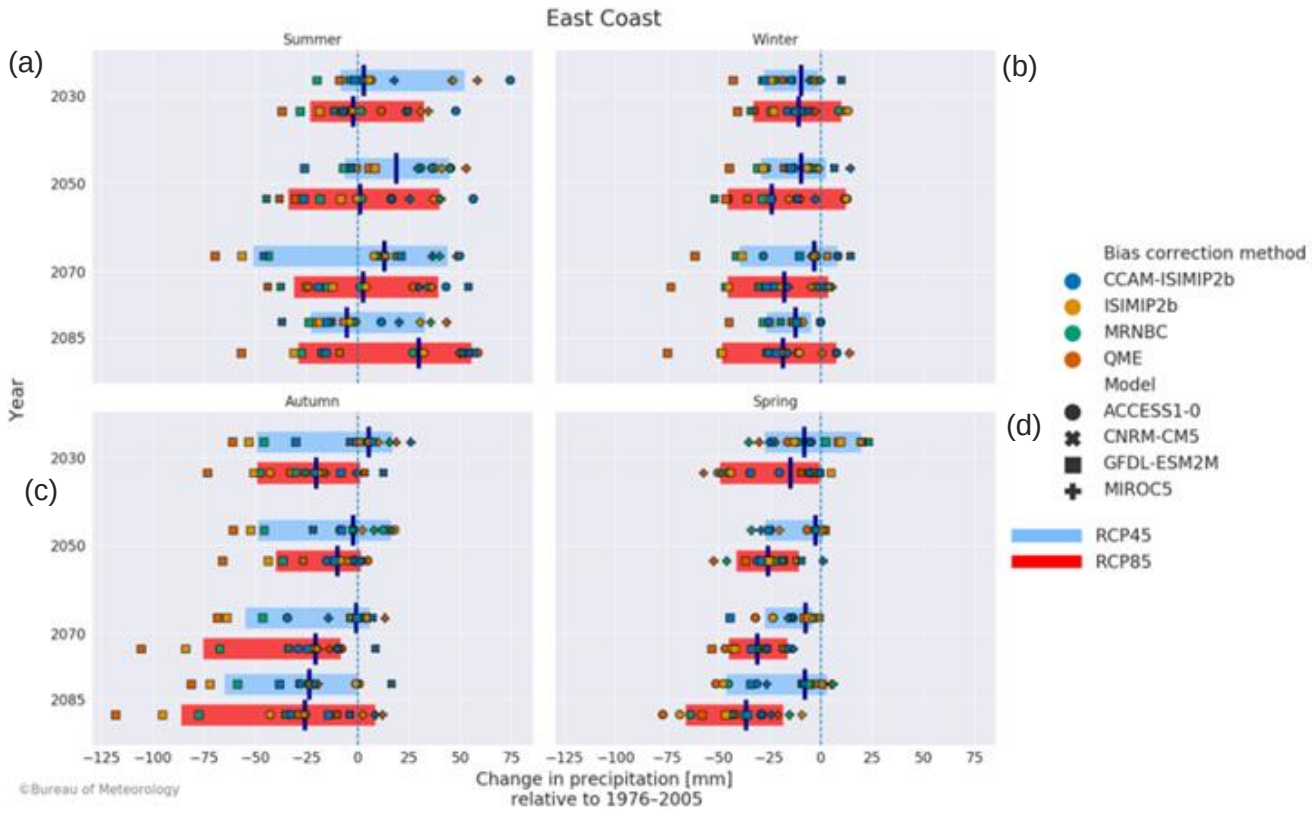

Figure 4.3. Absolute change (mm) (median) in seasonal modelled precipitation projected across the East Coast region for (a) summer (December–February), (b) winter (June–August), (c) autumn (March–May) and (d) spring (September–November) for 2030, 2050, 2070 and 2085 in the East Coast region. The red bar shows the 10th to 90th percentiles for RCP8.5. The blue bar shows the 10th to 90th percentile for RCP4.5. The dark blue line shows the ensemble median. The change is relative to the 1976–2005 reference period

The largest precipitation decreases in absolute terms are projected for autumn (Figure 4.3c), with projections ranging from −118 to 12 mm/season (−50% to 5%). Projected autumn precipitation decreases under greenhouse gas emission scenario RCP8.5 are larger than decreases in any other season due to uncertainties associated with representing the ENSO, thunderstorms, tropical cyclones and the monsoon (Dowdy et al. 2015a).

The region features projections for an increase (15%) and a decrease (−18%) in summer precipitation. Projections show a trend of increasing summer average precipitation towards the south of the region (Figure 4.4b). The East Coast region has both an observed and projected increase in the number and intensity of thunderstorms in summer (Dowdy 2020). Our understanding of the processes causing this trend is growing – it appears to relate to changes in the southeast Australian current – and this provides some medium to high confidence in these projections (Pepler et al. 2021).

Projections for winter precipitation range from increases (13%) to decreases (−57%). Projections show a trend of decreases towards the south, and a decrease in winter precipitation has already been observed in the historic record. Additionally, we have a good understanding, particularly in southern subregion, of the influence of the intensity of the sub-tropical ridge (Hope et al. 2015, Lucas et al. 2021) in reducing the number of rain-bearing cool-season storms, including from east coast lows (Catto et al. 2013; Dowdy et al. 2019; Pepler et al. 2021).

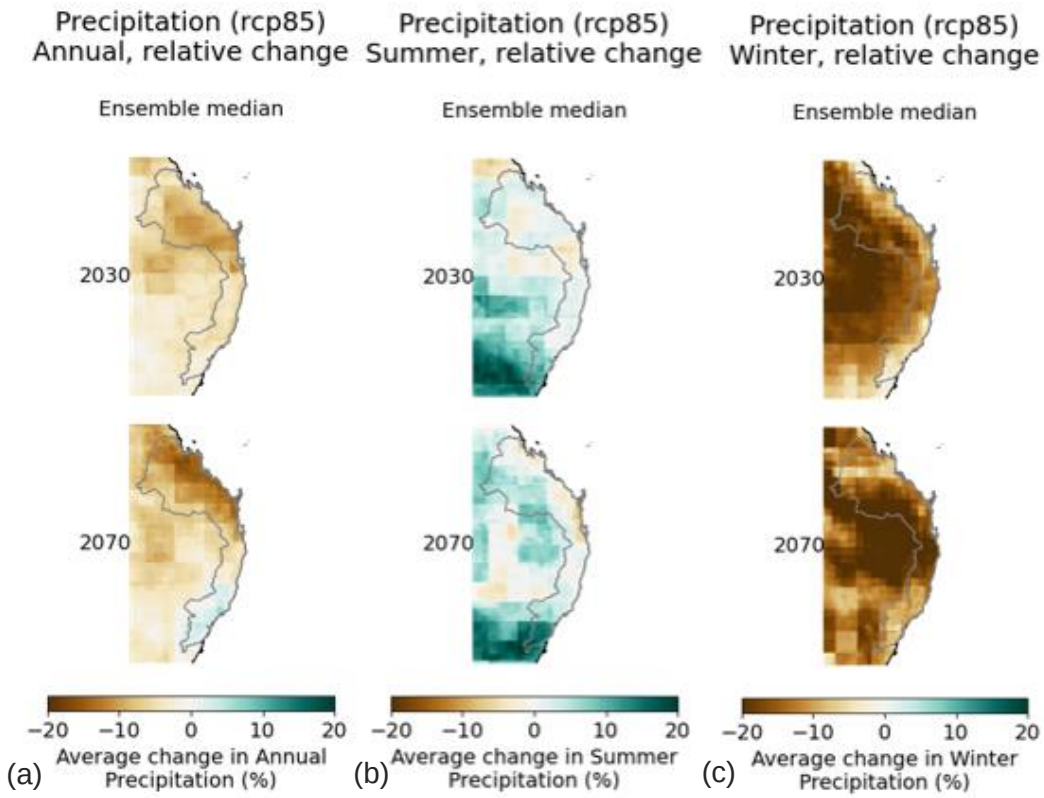

Figure 4.4. Relative change (%) (mean) in (a) annual, (b) summer (December–February) and (c) winter (June–August) precipitation across the East Coast region projected for the 2030 and 2070 periods under RCP8.5. The change is relative to the reference period (1976–2005)

The assessment summary for precipitation in the East Coast region is presented in Table 4.1.

Table 4.1. Assessment summary for precipitation for the East Coast region

Feature	Largest plausible range of change	Additional evidence: plausible process	Additional evidence: ability to simulate	Summary statement
Cool-season precipitation (May–October)	RCP4.5 −-121 to 26 mm/season (−40% to 9%) RCP8.5 −160 to 24 mm/season (−52% to 9%)	Precipitation decreases have been observed in recent decades during the cool season, mainly autumn and spring. Expanding sub-tropical ridge is blocking winter rain-bearing storms; cool-season decrease has been observed for the region, especially in the south.	Most GCMs do not simulate the position of the sub-tropical ridge well, introducing uncertainty.	Increases and decreases are possible. Evidence such as observed precipitation decreases, and a good understanding of the process mean that a drier future is more plausible than a wetter one.
Warm-season precipitation (November–April)	RCP4.5 −97 to 99 mm/season (−16% to 18%) RCP8.5 −149 to 72 mm/season −24% to 13%)	Poor understanding of how warm-season weather will respond to a changing climate. Increase in thunderstorm activity observed.	Thunderstorms require high spatial and temporal resolution not achieved in any projection data.	Changes to warm-weather precipitation are uncertain due to uncertainty in the ability to simulate summer weather. Very large increases and decreases are both plausible. Natural inter-annual variability will continue to be important climate feature.

4.3 Runoff

Both increases and decreases are projected for changes to mean annual runoff, but the ensemble median shows little change. The median mean annual runoff from the 16-member ensemble shows a small decrease under RCP8.5, while RCP4.5 projects a small increase in runoff by mid-century (Figure 4.5).

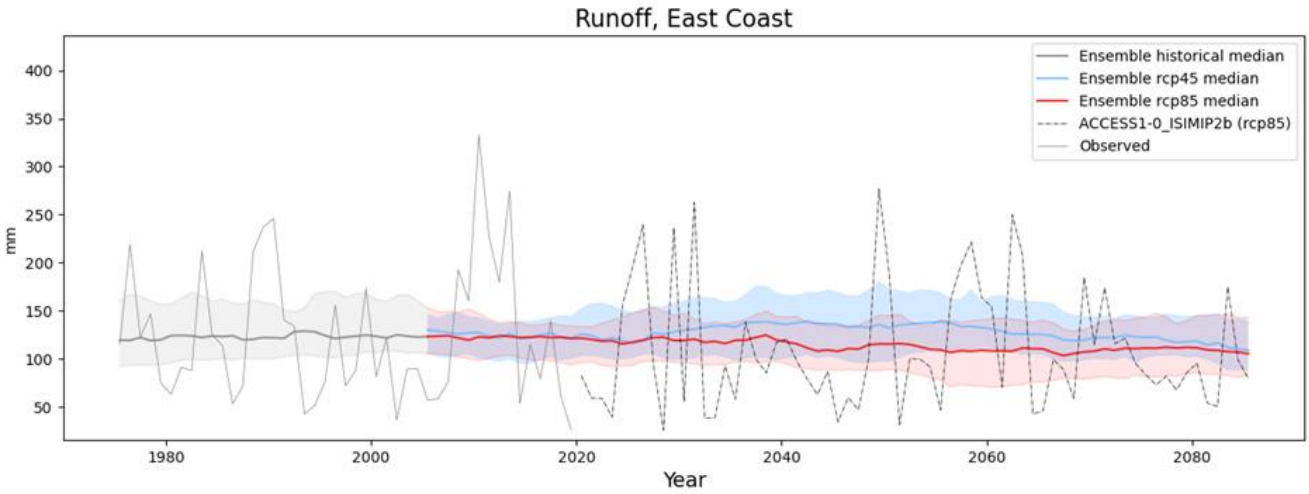

Figure 4.5. Annual modelled runoff (mm) projected to 2099 by ensemble members for RCP4.5 (blue) and RCP8.5 (red) greenhouse gas emission scenarios in the East Coast region. The shaded areas represent the 10th to 90th percentile range for all ensemble members in the historical and future time periods. The time series for ACCESS1-0_ISIMIP2b (RCP8.5) is included (dotted line) to show the variability projected for an individual ensemble member. The grey line represents the modelled historical median runoff

The large model spread in these results means that both increases and decreases are plausible (Figure 4.6). However, the annual median runoff for each of the representative concentration pathway is projected to become drier with each of the time periods. Previous downscaled projections for the East Coast region (that is, NARCliM downscaling projections based on CMIP3 GCMs) indicate a reduction in the number of east coast lows that usually occur during the cooler months of the year, and little change in their number during summer (Ji et al. 2015). Although fewer east coast lows are projected to occur, those that do occur could potentially produce heavier precipitation in some cases (based on increased moisture availability as temperatures increase). These projections suggest that it is plausible that the types of weather that generate runoff in winter that is important for filling storages in the southern regions will decrease. Conversely, the potential increase in precipitation intensity produced by some east coast lows, combined with projections of little change in the frequency of east coast lows during summer and the potential for increased precipitation from thunderstorms, provides some indication of a potential increase in precipitation during summer (Dowdy et al. 2015b; Dowdy 2020).

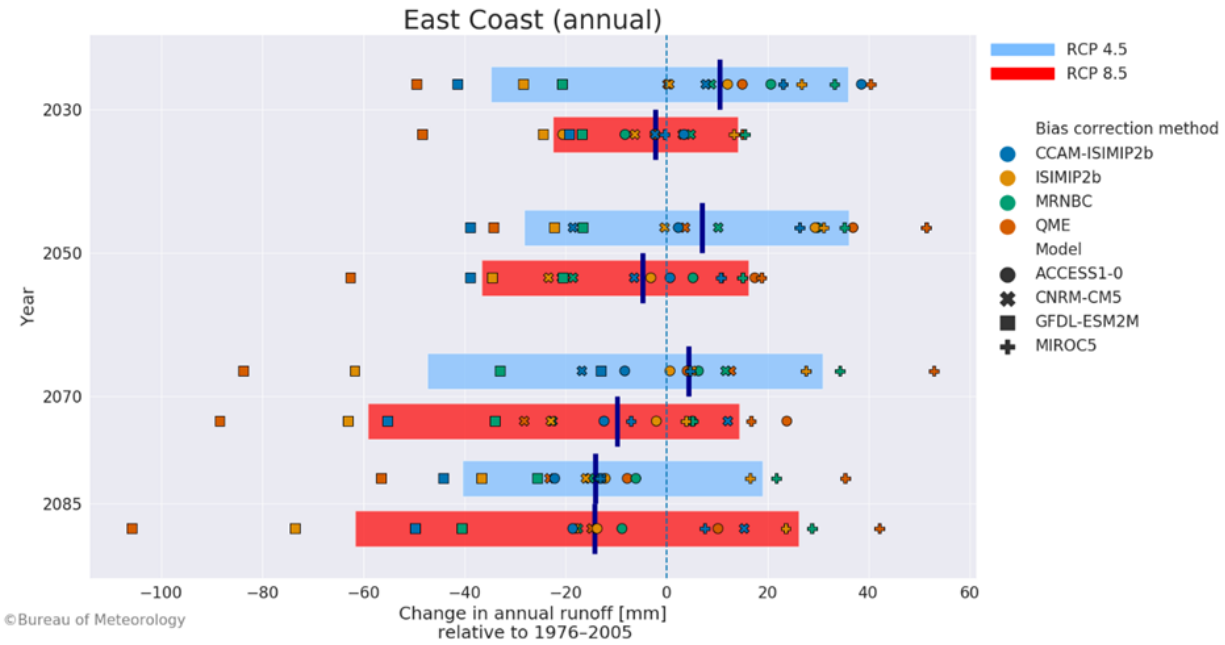

Figure 4.6. Absolute change in annual runoff (mm) projected by each ensemble member for 2030, 2050, 2070 and 2085 in the East Coast region. The red bar shows the 10th to 90th percentiles for RCP8.5. The blue bar shows the 10th to 90th percentile for RCP4.5. The dark blue line shows the ensemble median. The change is relative to the reference period (1976–2005)

Summer runoff projections for the East Coast region show little change to increases until mid-century and then increases and decreases to late century (Figure 4.7a). Autumn runoff projections show both increases and decreases (Figure 4.7c). Autumn and winter also feature large model spread with both increases and decreases plausible, with a larger trend towards decreases in the south following the spatial and seasonal trends of projected changes to precipitation.

Spring precipitation projections range from little change to moderate decreases, and the ensemble medians runoff project small decreases from late century (Figure 4.7d). Projections for changes to winter also show increases and decreases, and with an ensemble median projecting decreases from late century (Figure 4.7b).

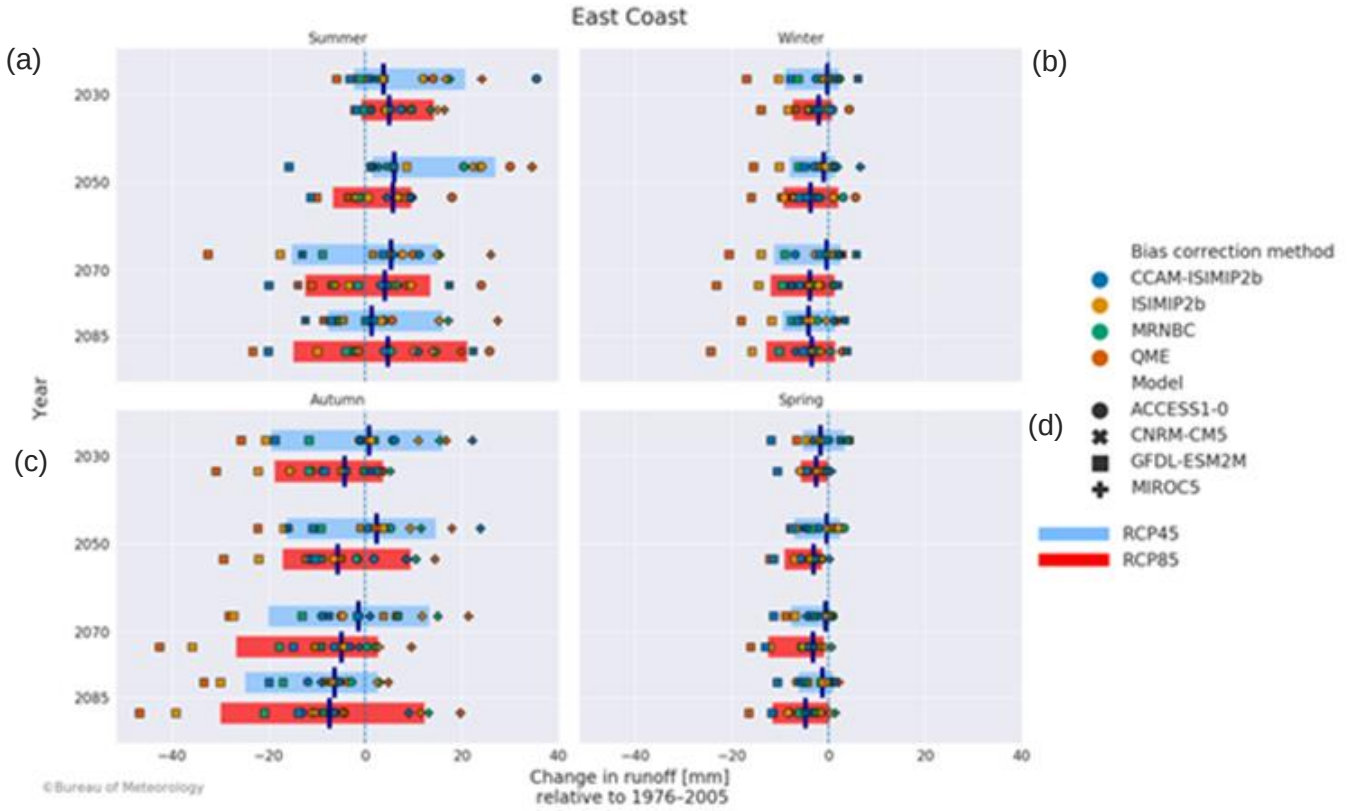

Figure 4.7. Absolute change (mm) in modelled seasonal runoff projected by each ensemble member for (a) summer (December–February), (b) winter (June–August), (c) autumn (March–May) and (d) spring (September–November) for 2030, 2050, 2070 and 2085 in the East Coast region. The red bar shows the 10th to 90th percentiles for RCP8.5. The blue bar shows the 10th to 90th percentile for RCP4.5. The dark blue line shows the ensemble median. This change is relative to the reference period (1976–2005)

Decreases in winter and spring precipitation are projected in the south and are potentially significant in terms of future impacts to water security for the major population centre of Greater Sydney (Figure 4.8). While the modelled runoff shows increased runoff in summer, most inflows to Sydney's storage catchments would occur in winter and spring. These large inflows around the cooler months of the year are typically associated with high-intensity storm events produced by east coast low weather systems. The high intensity of the storms, as well as occurring in cooler seasons with wetter catchments, leads to high runoff volumes being generated, which translate to storage inflows. However, modelled runoff does not correspond to seasonality of inflows. Given the uncertainty about the ability of the climate models to represent the small temporal and spatial scale of some weather systems, there is considerable uncertainty in relating these results to changes in water resource impacts, particularly for the southern part of this region.

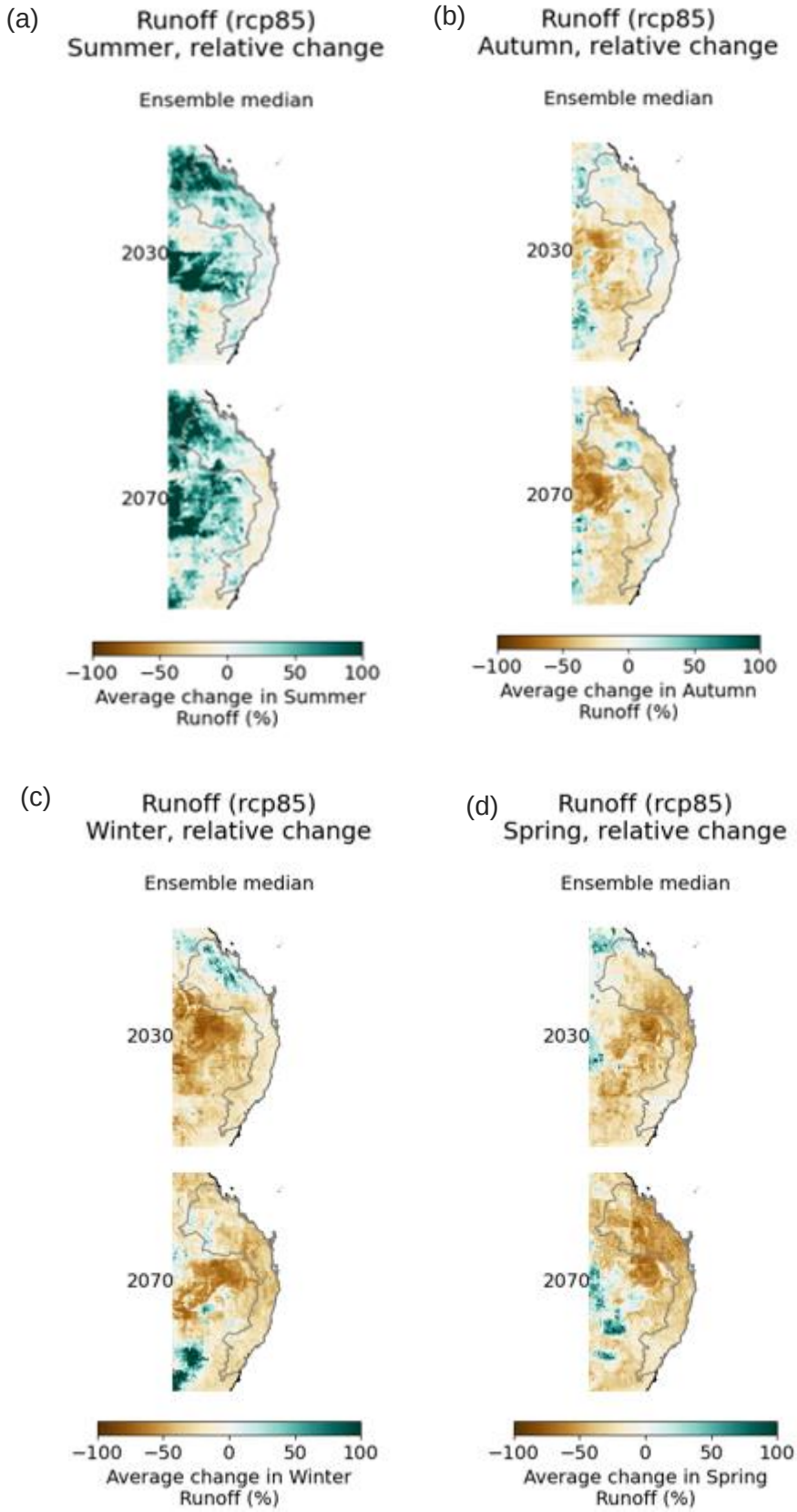

Figure 4.8. Relative change (%) (median) in modelled (a) summer, (b) autumn, (c) winter and (d) spring runoff across the East Coast region projected for 2030 and 2070 under RCP8.5. This change is relative to the reference period (1976–2005)

The assessment summary for runoff for the East Coast region is presented in Table 4.2.

Table 4.2. Assessment summary for runoff for the East Coast region

Feature	Largest plausible range of change	Observed trends	Additional evidence: plausible process/ model reliability	Summary statement
Cool-season runoff (May–October)	RCP4.5 −48 to 17 mm/season (−71% to 42%) RCP8.5 −56 to 4 mm/season (−82% to 10%)	Both increases and decreases to historical streamflow have been observed. 96% of streamflow gauge sites matched the trend direction in winter.	Ensembles that are bias-corrected with QME show largest positive bias and those that are bias-corrected with MRNBC show smallest bias, which is mostly negative.	Very large increases and decreases are projected for cool-season runoff. There is a trend for decreases towards the southern portion of the region. RCP8.5 projections range from little change to very large decreases.
Warm-season runoff (November–April)	RCP4.5 −47 to 54 mm/season (−32% to 60%) RCP8.5 −56 to 42 mm/season (−42% to 47%)	Both increases and decreases to historical streamflow have been observed. 77% of streamflow gauge sites matched the trend direction in summer.		Very large increases and decreases are projected for warm-season runoff. Large inter-annual variability is expected to remain a key feature of warm-season runoff.

4.4 Soil moisture

Plausible changes to mean annual soil moisture under both representative concentration pathways and for all future time periods vary from little change to very large decreases (Figure 4.9). The large variability in year-to-year average soil moisture content is expected to continue, associated with variability in the annual precipitation total for the next few decades in the East Coast region, as illustrated by the ACCESS1-0_ISIMIP2b ensemble example (Figure 4.9).

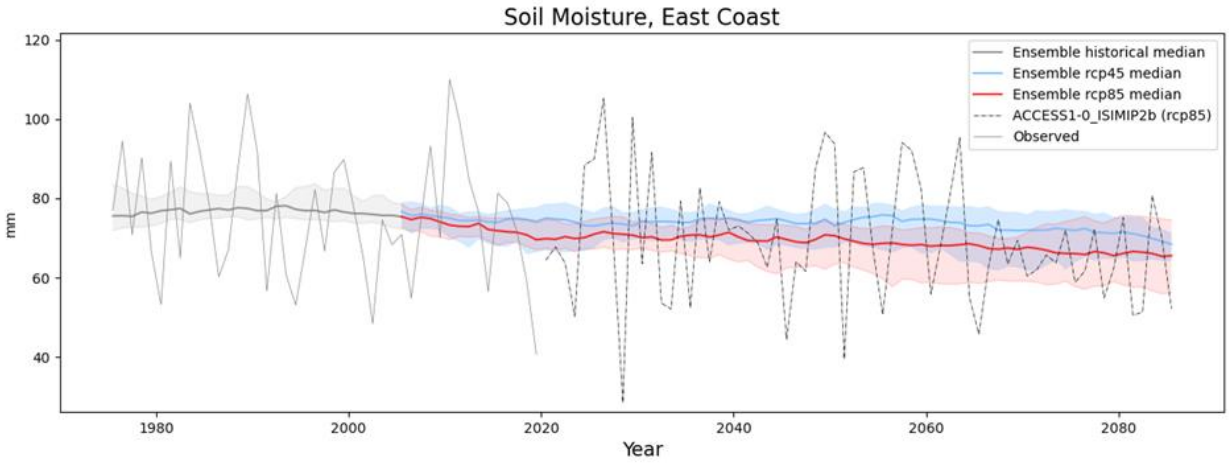

Figure 4.9. Annual modelled root zone soil moisture projected to 2099 by ensemble members for RCP4.5 (blue) and RCP8.5 (red) in the East Coast region. The shaded areas represent the 10th to 90th percentile range for all ensemble members in the historical and future time periods. The time series for ACCESS1-0_ISIMIP2b (RCP8.5) is included (dotted line) to show the variability projected for an individual ensemble member. The grey line represents the modelled historical median soil moisture

However, most of the 16-member ensemble project decreases in soil moisture (Figure 4.10) and there is good understanding of the processes by which increased potential evapotranspiration, and to some degree projected decreases in precipitation, contribute to drying of soil moisture stores. Larger decreases later into the century are projected, which aligns with the projected increases in temperature and potential evapotranspiration.

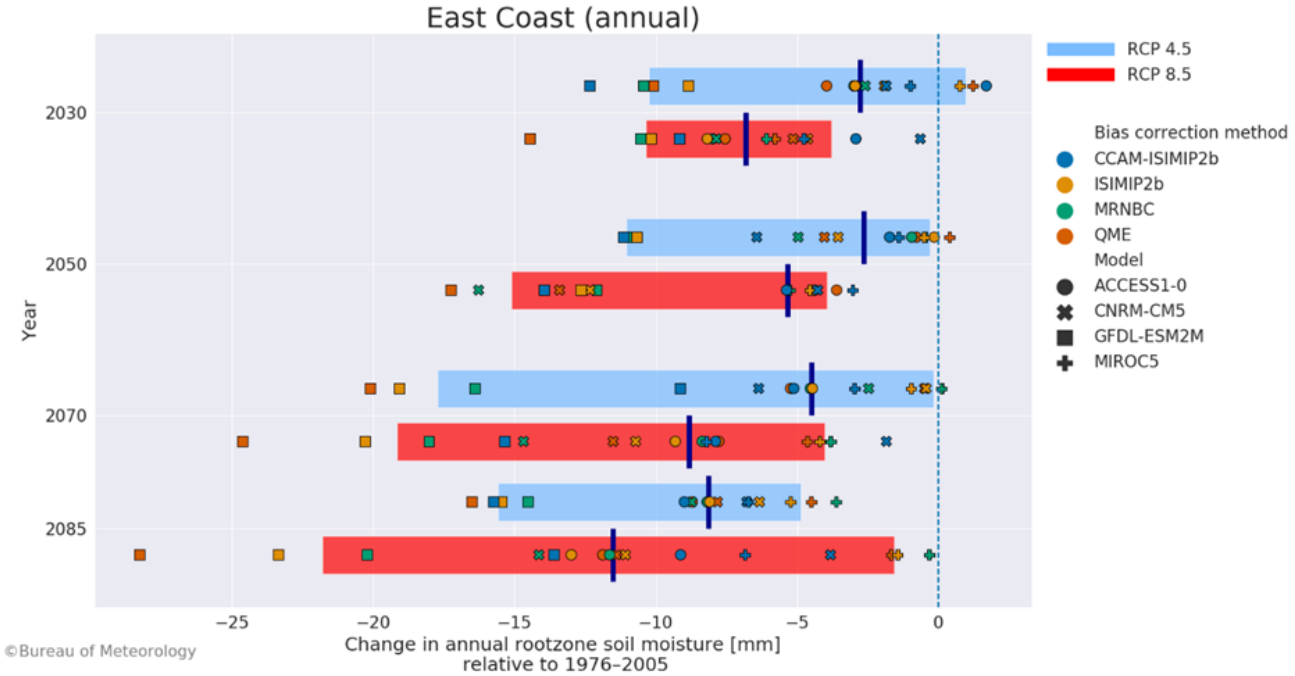

Figure 4.10. Absolute change (mm) in annual root zone soil moisture projected by each ensemble member for 2030, 2050, 2070 and 2085 in the East Coast region. The red bar shows the 10th to 90th percentiles for RCP8.5. The blue bar shows the 10th to 90th percentiles for RCP4.5. The dark blue line shows the ensemble median. The change is relative to the reference period (1976–2005)

Winter and spring soil moisture are projected to range from little change to very large decreases under both representative concentration pathways for both mid-century and late century (Figure 4.11). Most of the ensembles project a decrease in winter soil moisture and all the ensembles project a decrease in spring soil moisture,

corresponding to projections of increases in potential evapotranspiration and decreases in precipitation for this season. Summer and autumn projections show mostly decreases with some increases.

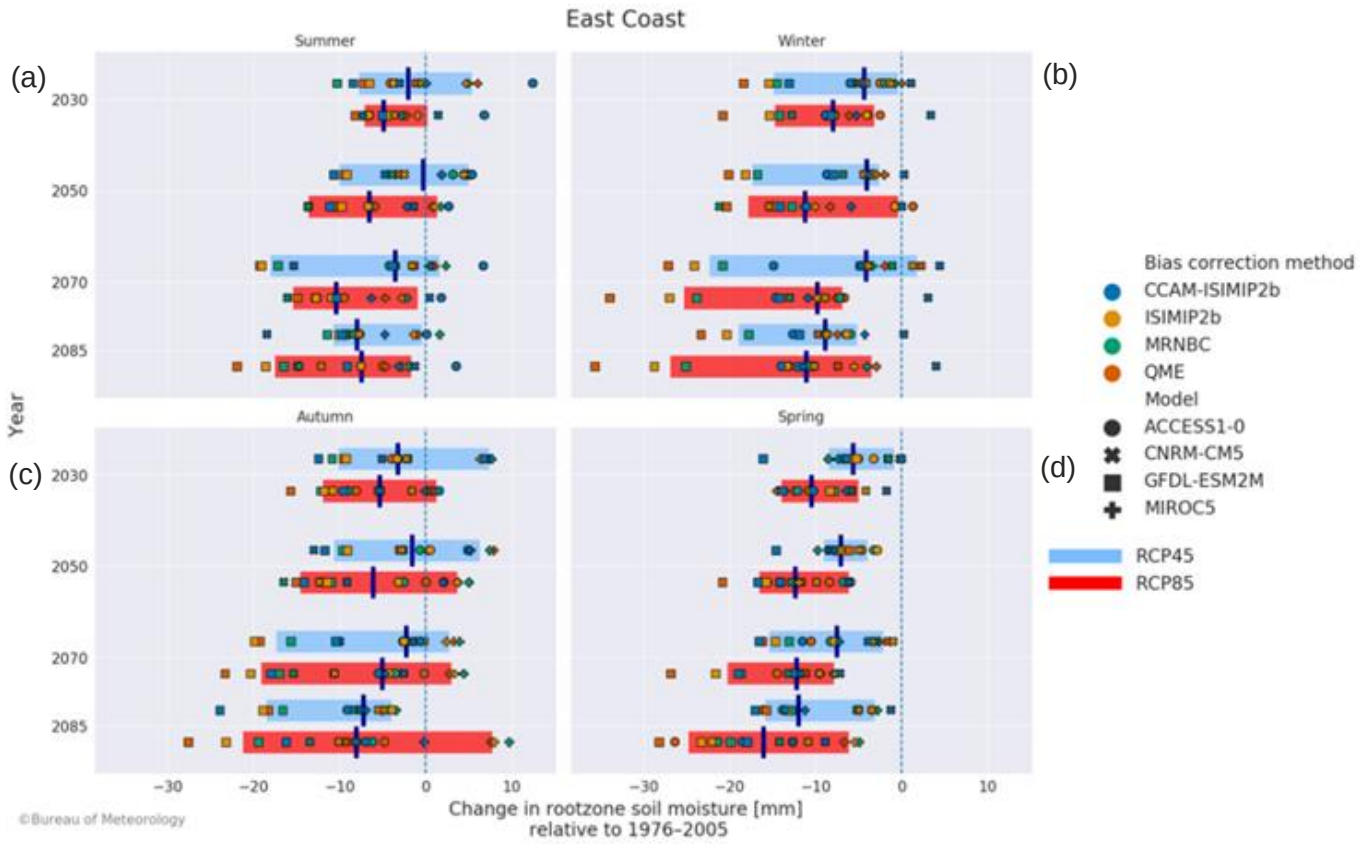

Figure 4.11. Absolute change (mm) in seasonal modelled soil moisture projected by each ensemble member for (a) summer (December–February), (b) winter (June–August), (c) autumn (March–May) and (d) spring (September–November) for 2030, 2050, 2070 and 2085 in the East Coast region. The red bar shows the 10th to 90th percentiles for RCP8.5. The blue bar shows the 10th to 90th percentile for RCP4.5. The dark blue line shows the ensemble median. The change is relative to the reference period (1976–2005)

The spatial distribution of the relative change in annual root zone soil moisture is shown in Figure 4.12. There are slightly larger decreases in soil moisture in the northern subregion than in the southern subregion, which relates to spatial patterns of projected decreases in precipitation.

The strong decreases in soil moisture would have wide impacts on many sectors within the region. Winter and spring soil moisture are important for generating runoff to fill storages from rain-bearing storms, particularly in the south. Springtime soil moisture is critical for nourishing rain-fed agriculture when summer crops are sowed. Also, for the large population centres of Greater Sydney and Greater Brisbane, decreases in soil moisture could be expected to increase demand for residential garden watering and industry water uses, which would further strain depleted water resources.

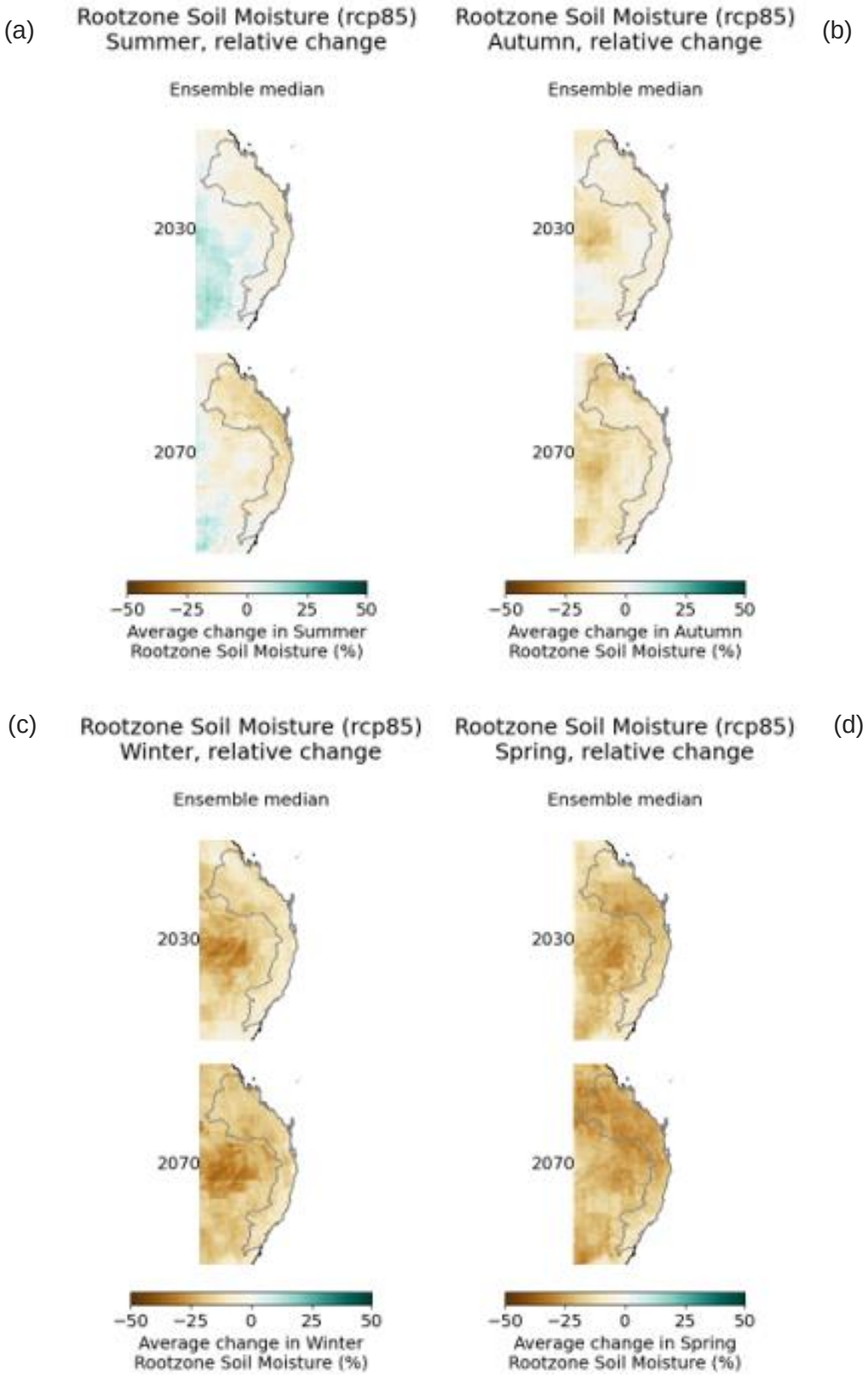

Figure 4.12. Relative change (%) (median) in (a) summer (December–February), (b) winter (June–August), (c) autumn (March–May) and (d) spring (September–November) soil moisture projected across the East Coast region for 2030 and 2070 under RCP8.5 . The change is relative to the reference period (1976–2005)

The assessment summary for soil moisture in the East Coast region is presented in Table 4.3.

Table 4.3. Assessment summary for soil moisture for the East Coast region

Feature	Largest plausible range of change	Additional evidence: process understanding	Additional evidence: plausible process/ model reliability	Summary statement
Cool-season soil moisture (May–October)	RCP4.5 −10 to 0.5 mm/season (−33% to 1%) RCP8.5 −14 to 0.5 mm/season (−45% to 2%)	Changes in soil moisture are driven by changes in seasonal average potential evapotranspiration and precipitation changes.	General 3% to 5% underestimation of soil moisture in all seasons. Very large positive and negative soil moisture bias from QME.	Soil moisture ranges from little change to very large decreases. These changes are related to increases in potential evapotranspiration and also decreases in precipitation, with larger decreases towards the south.
Warm-season soil moisture (November–April)	RCP4.5 −7 to 4 mm/season (−19% to 11%) RCP8.5 −9 to 2 mm/season (−26% to 5%)			Very large decreases in soil moisture are plausible under both representative concentration pathways. RCP4.5 projects increases while RCP8.5 has an upper range of little change.

4.5 Potential evapotranspiration

In the hydrological cycle, evapotranspiration plays an important role, particularly in soil evaporation and crop transpiration. While precipitation is the key driver of water availability, potential evapotranspiration is an indicator of potential losses in the total water balance for a system, and a limiting factor in the amount of water available for use. While these trends in potential evapotranspiration do not tell us what the projected changes to the actual evapotranspiration rate are, the signal indicates that the region could see impacts including:

- an increase in crop water demand (through higher transpiration of plants)
- increased evaporation from soils following a higher depletion rate of soil moisture
- the potential for greater losses from surface water storages through evaporation.

Annual potential evapotranspiration for the East Coast region is projected to increase in the future with higher increases under RCP8.5 than RCP4.5 and later in the century (Figures 4.13 and 4.14). The increase in potential evapotranspiration is understood be associated with increases in temperature.

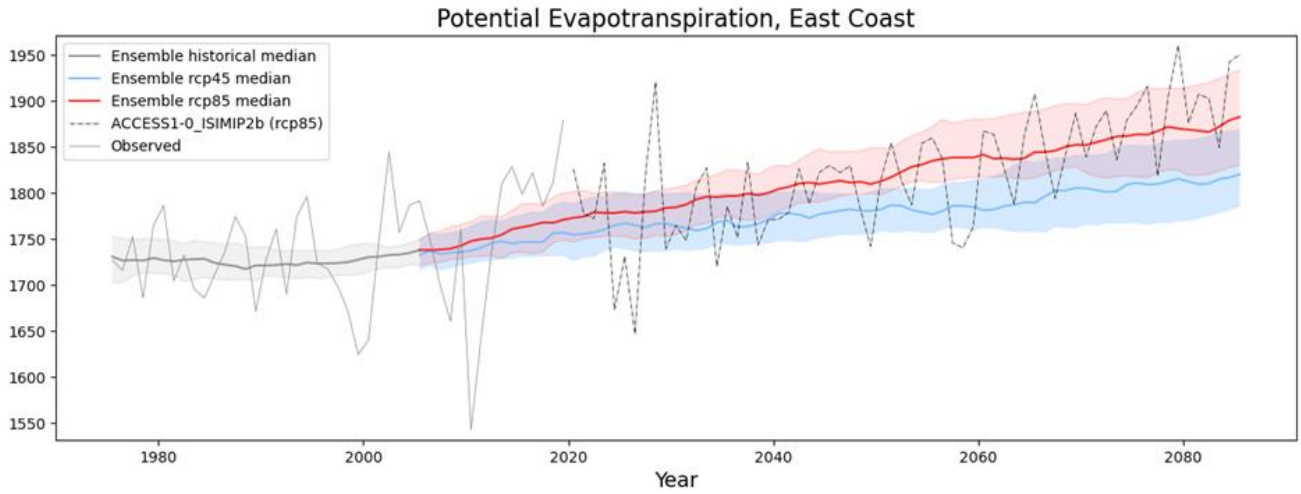

Figure 4.13. Annual modelled potential evapotranspiration (mm) projected to 2099 by ensemble members for RCP4.5 (blue) and RCP8.5 (red) in the East Coast region. The shaded areas represent the 10th to 90th percentile range for all ensemble members in the historical and future time periods. The time series for ACCESS1-0_ISIMIP2b (RCP8.5) is included (dotted line) to show the variability projected for an individual ensemble member. The grey line represents the modelled historical median potential evapotranspiration

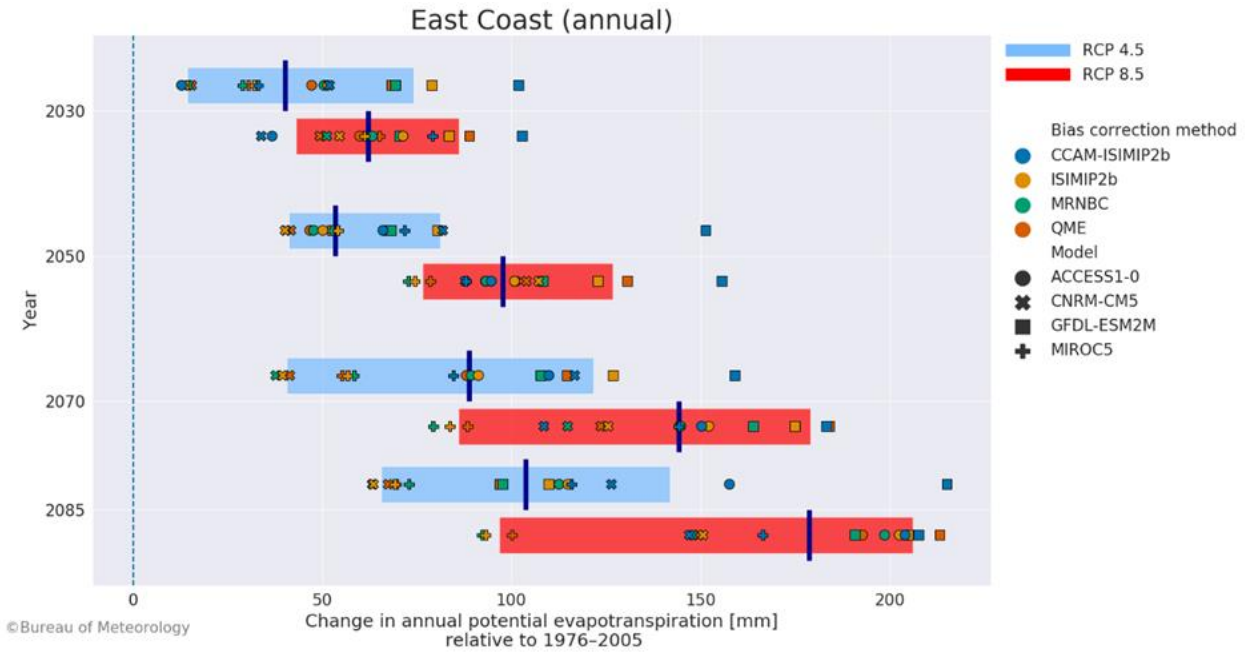

Figure 4.14. Absolute change (mm) in annual potential evapotranspiration projected by each ensemble member for 2030, 2050, 2070 and 2085 in the East Coast region. The red bar shows the 10th to 90th percentiles for RCP8.5. The blue bar shows the 10th to 90th percentile for RCP4.5. The dark blue line shows the ensemble median. The change is relative to the reference period (1976–2005)

An increase in potential evaporation is projected for all seasons for both representative concentration pathways and all time periods (Figure 4.15). The largest absolute changes in potential evapotranspiration compared to the reference period are projected for spring.

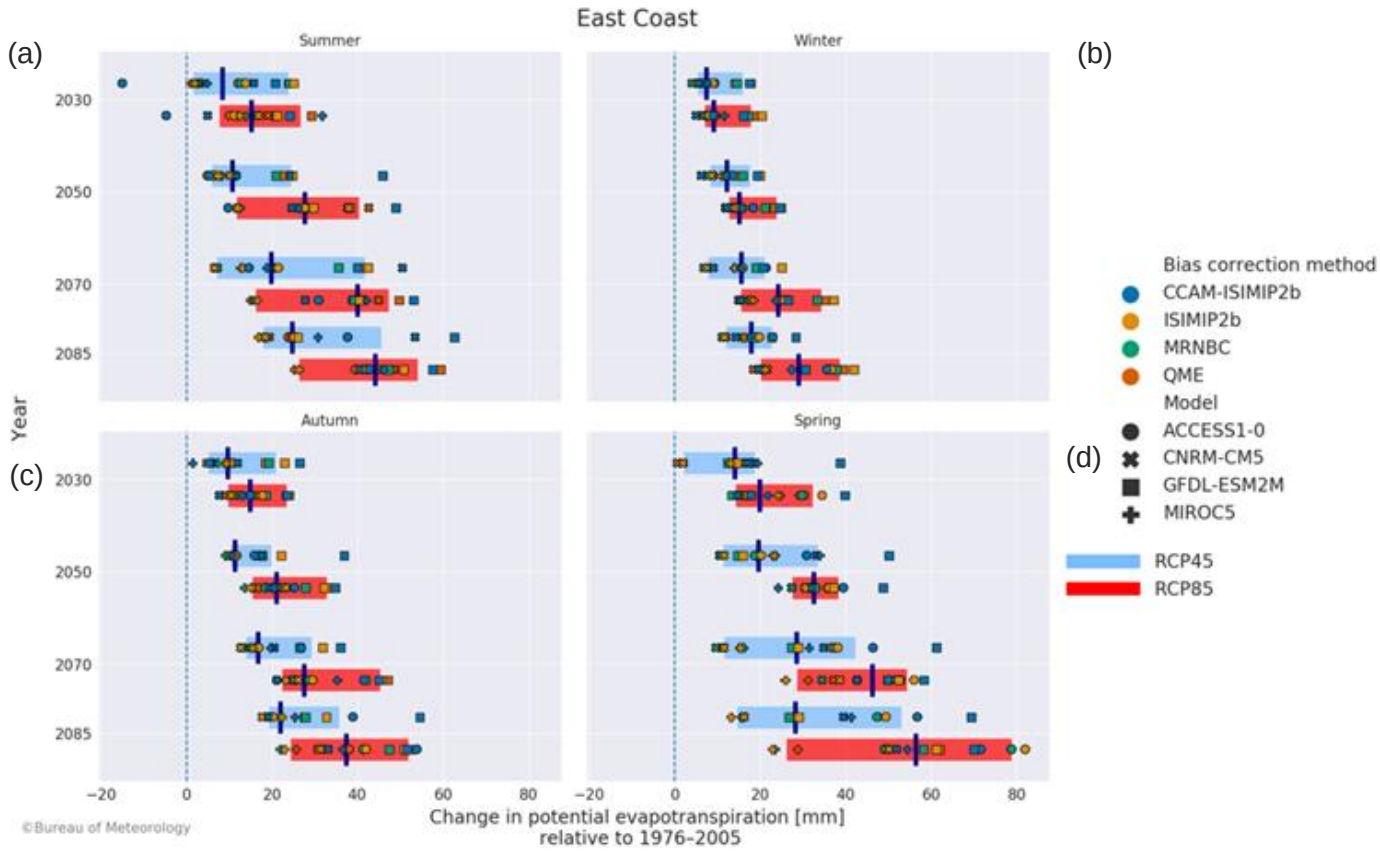

Figure 4.15. Absolute change (mm) in potential evapotranspiration projected by each ensemble member for (a) summer (December–February), (b) winter (June–August), (c) autumn (March–May) and (d) spring (September–November) for 2030, 2050, 2070 and 2085 in the East Coast region. The red bar shows the 10th to 90th percentiles for RCP8.5. The blue bar shows the 10th to 90th percentile for RCP4.5. The dark blue line shows the ensemble median. The change is relative to the reference period (1976–2005)

The increase in potential evapotranspiration is projected to occur uniformly across the entire region (Figure 4.16).

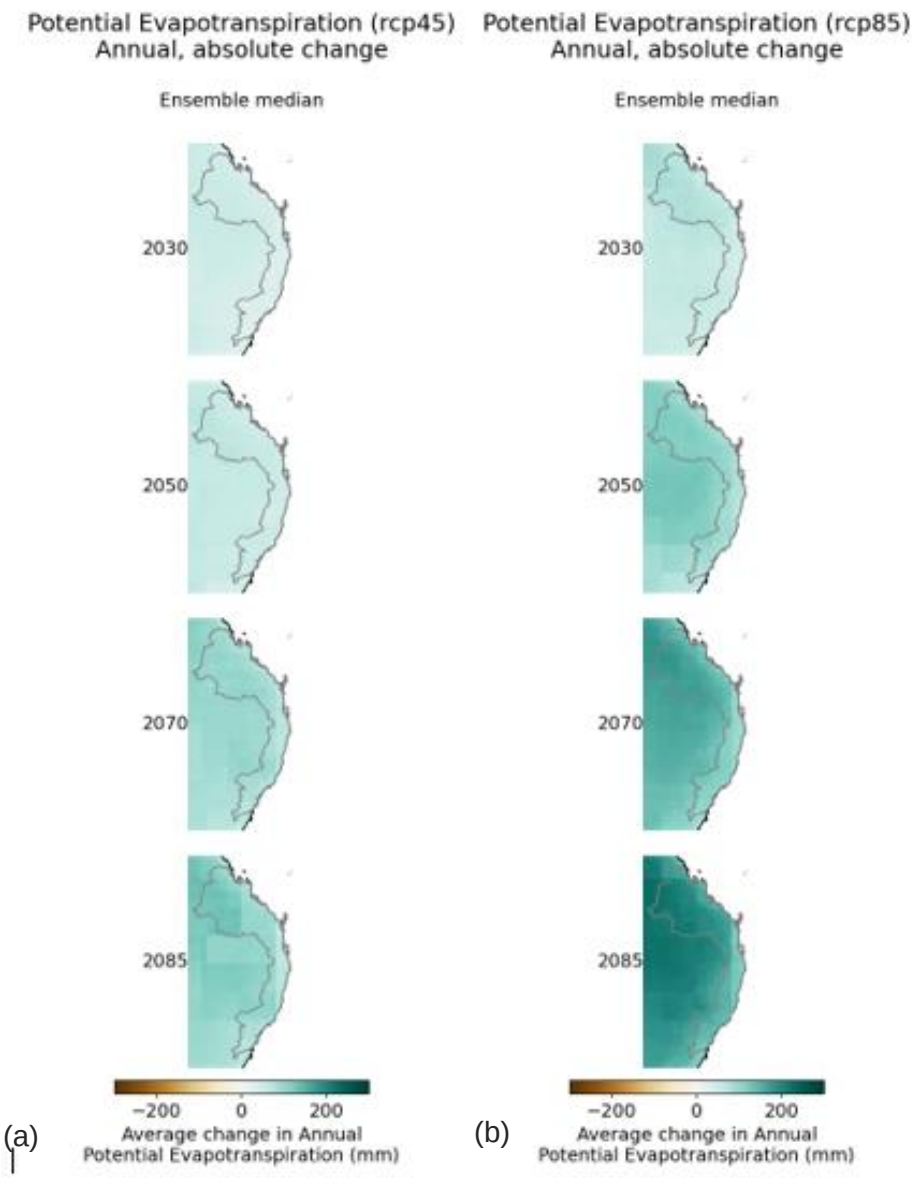

Figure 4.16. Absolute change (mm) (ensemble median) in annual potential evapotranspiration projected across the East Coast region under (a) RCP4.5 and (b) RCP8.5 for 2030, 2050, 2070 and 2085. The change is relative to the reference period (1976–2005)

The assessment summary for potential evapotranspiration in the East Coast region is presented in Table 4.4.

Table 4.4. Assessment summary for potential evapotranspiration for the East Coast region

Feature	Largest plausible range of change	Additional evidence: process understanding	Additional evidence: plausible process/ model reliability	Summary statement
Annual potential evapotranspiration	RCP4.5 −13 to 215 mm/year (1% to 13%) RCP8.5 −34 to 213 mm/year (−2% to 22%)	Small increase observed in the recent past. Aligned with the understanding that a warmer climate results in higher potential evapotranspiration.	Low bias in potential evapotranspiration simulation.	Increase in annual and seasonal potential evapotranspiration for both representative concentration pathways and in all seasons. Magnitude is proportionate to greenhouse gas emission concentration.

4.6 Extreme events

Hydrological extremes, including floods and droughts, are among the costliest natural disasters in the world (Wasko & Nathan 2019). They pose risks to life, food security, infrastructure and energy supply. Future climate change is expected to bring a more variable precipitation pattern with longer dry spells and more frequent extreme events, such as flood-producing rain and cyclones (Easterling et al. 2000; Johnson & Murray 2004; Milly et al. 2002; Palmer & Räisänen 2002; Walsh & Ryan 2000). On the extreme dry end of the spectrum, prolonged absence of precipitation, for example, through a failure of the monsoon, may result in increasing dry spells. On the extreme wet end of the spectrum, an increase in extreme rains can exacerbate flooding events. Changes in the frequency, amount and duration of precipitation have serious impacts on sectors such as agriculture, water management and flood control (Alam et al. 2018). The ability to project future climate can help improve irrigation planning, flood planning, and design and management of hydraulic structures such as dams and stormwater drainage systems. This knowledge will also help us identify Australia's vulnerability to future droughts and improve resilience through mitigation actions.

4.6.1 Extreme precipitation and runoff

Earlier studies using observations and projections have shown an increase in the frequency of extreme precipitation events in the Australian region (Alexander & Arblaster 2009; Rafter & Abbs 2009). In a warming climate, heavy precipitation events are likely to increase in magnitude due to the increased moisture-holding capacity of a warmer atmosphere (Sherwood et al. 2010; Yin et al. 2020). Such excessive precipitation events may enhance the potential risk of flooding, depending on antecedent conditions. However, Wasko & Nathan (2019) found that, in Australia as in many other parts of the world, soil moisture deficits that are first re-filled during precipitation events commonly reduce flood magnitudes, despite increasing precipitation extremes. Therefore, in this project, we estimated projected future flood scenarios based on both precipitation and runoff.

Characterising changes in flood frequency and intensity at a large spatial and temporal scale is challenging; flood risk often depends on local topography, sub-daily precipitation intensity and antecedent conditions. We calculated a set of threshold-based indicators using precipitation and runoff to capture changes in flood risk on a broad scale. The changes on the extreme wet end of the spectrum are determined using 3 indicators: the projected annual mean and maximum daily precipitation and runoff, and the 20-year return period precipitation and runoff estimated using the generalised extreme value (GEV) distribution. The GEV distribution is generally used to represent the rare events (Bali 2003), which are indicative of floods.

Both precipitation (Figure 4.17) and runoff (Figure 4.18) analyses show a substantial increase in the maximum 1-day and 20-year return period for two 30-year periods (2030 and 2070) and both greenhouse gas emission scenarios (RCP4.5 and RCP8.5) (Figures 4.17 and 4.18). In comparison, the trends in the annual mean precipitation and runoff clearly show that the median of the 16-member ensemble for mean precipitation and runoff is tending towards little change or decrease, and precipitation is tending towards a decrease across both representative concentration pathways. This pattern (little change or decrease in annual mean relative to increase in extremes) is found in almost all other National Hydrological Projections regions and is supported by the results from other studies (Alexander & Arblaster 2009; Rafter & Abbs 2009; Wasko & Sharma 2017) and reflects a shift in larger portions of precipitation occurring in the form of high-intensity events. The magnitudes of the simulated changes in extreme precipitation indicators depend heavily on the representative concentration pathways, the given ensemble member and the time period in question. Therefore, the magnitude of change is uncertain. This could be because smaller-scale systems that generate extreme precipitation are not well represented by GCMs (Fowler & Ekström 2009). In the East Coast region, the RCP4.5 scenario has a slightly larger ensemble spread than in the RCP8.5 greenhouse gas emission scenario; in the latter, the spread in the runoff indicators is slightly larger than the spread in the precipitation indicators.

In summary, the results suggest that the intensity of extreme events is going to increase in the East Coast region, possibly via an increase in intensity of east coast lows (Pepler et al. 2021). However, the magnitude and timing of the future change in intensity of wet extremes from natural climate variability of the region cannot be projected with certainty.

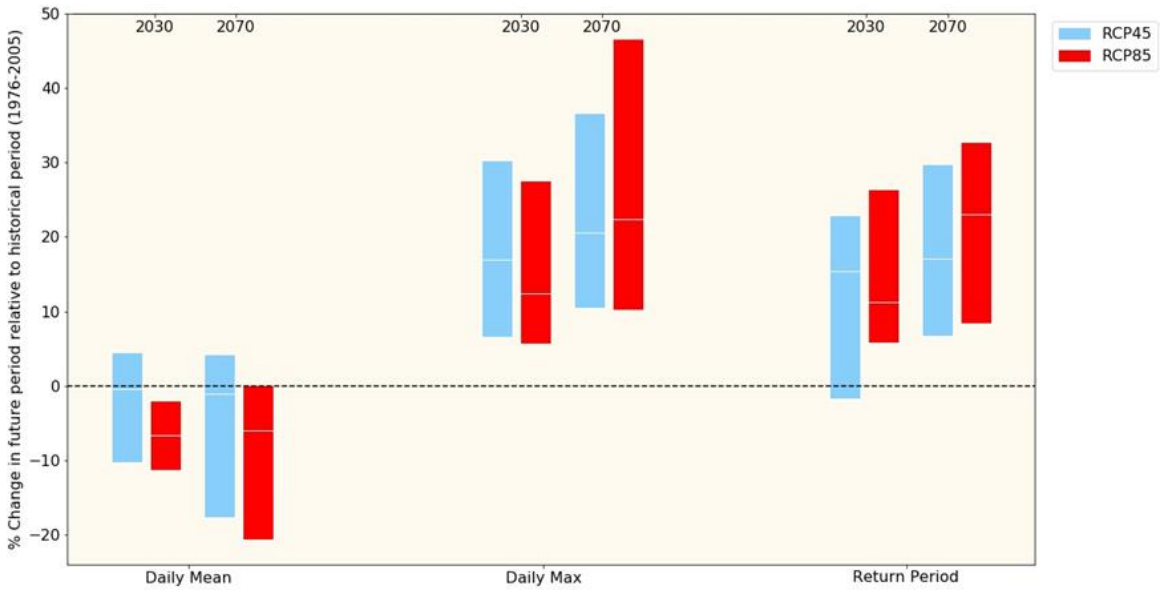

Figure 4.17. Future extreme wet analysis based on modelled precipitation shown by changes (%) in mean daily precipitation, maximum daily precipitation and 20-year return period of the annual maximum precipitation for 2030 and 2070 in the East Coast region. The red bar shows the 10th to 90th percentiles for RCP8.5. The blue bar shows the 10th to 90th percentiles for RCP4.5. The white lines show the ensemble median. The change is relative to the reference period (1976–2005)

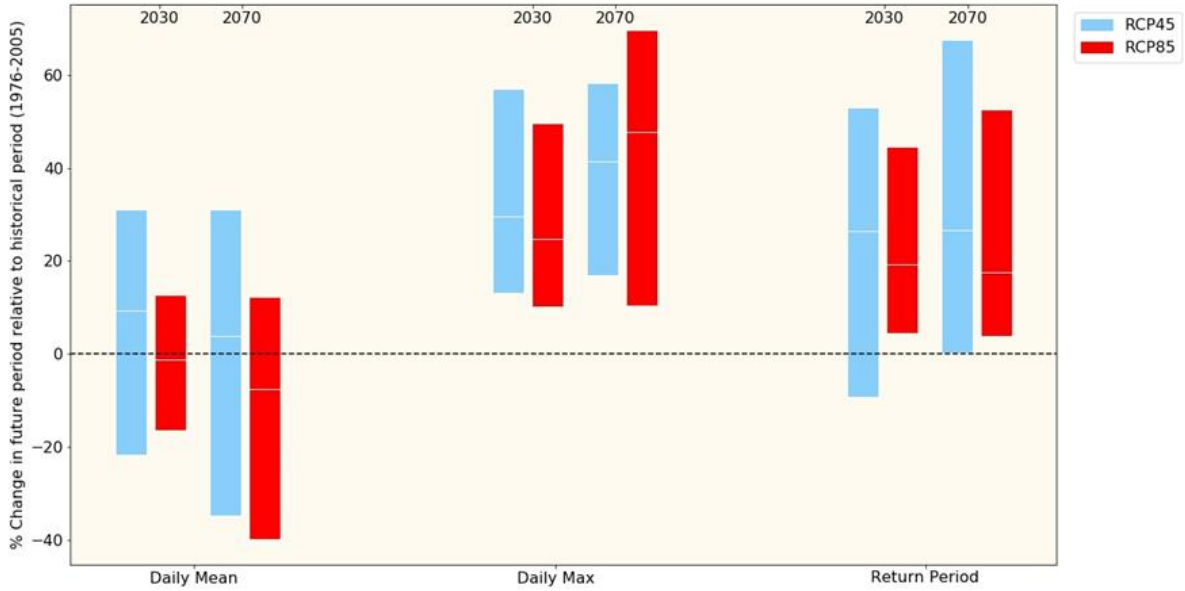

Figure 4.18. Future extreme wet analysis based on modelled runoff shown by changes (%) in mean daily runoff, maximum daily runoff and 20-year return period of the annual maximum runoff for 2030 and 2070 in the East Coast region. The red bar shows the 10th to 90th percentiles for RCP8.5. The blue bar shows the 10th to 90th percentiles for RCP4.5. The white lines show the ensemble median. The change is relative to the reference period (1976–2005)

4.6.2 Dry landscape conditions

To gain a greater understanding of future extreme dry conditions or droughts and the range of socioeconomic impacts, it is important to combine multiple lines of evidence encompassing climatological and hydrological extreme dry states. Projected extreme meteorological, hydrological and agricultural dry conditions were investigated using 3 separate indicators. A meteorological extreme dry state refers to when an area is subject to below-average precipitation that results in dry landscape conditions. A hydrological extreme dry state refers to when water resources are insufficient, for example, in rivers and water storages. An agricultural extreme dry state is determined through the impacts of soil moisture deficits on crops and vegetation and its subsequent effect on livestock. Analysis of future conditions must also take into account different time frames, as hydrological dry states arise over a longer time period than meteorological and agricultural extreme dry periods (which can include ‘flash droughts’). Hydrological dry states result from prolonged spells of below-average precipitation and the subsequent below-average runoff. However, a reduction in precipitation may result in a decrease in water available for stock or a depletion of topsoil moisture needed to grow crops. This will impact agriculturalists sooner than it will cause disruption to the whole hydrological system.

In this study, projected precipitation, runoff and soil moisture data was used to represent these 3 types of droughts: meteorological, hydrological and agricultural. This lets us capture the potential impacts on key sectors of agricultural and water-sensitive industries. The indicators are used as a proxy for drought, noting that they should be taken as an indicative estimate of drought conditions because many other factors involved in determining whether a region is in drought have not been included in this analysis.

As the various types of extreme dry conditions or droughts arise over different time frames, our analysis addresses short-term to long-term durations by calculating the median extreme dry condition duration (short, moderate, long or prolonged). An extreme dry condition is defined by applying a threshold quantile of 15% of the historical period to future projections. We use percentile thresholds to determine drought periods as this method involves no assumptions about the data distribution. Using the 15th percentile as the drought threshold means that any month

below this threshold is classified as being in drought. The 15th percentile corresponds approximately to a threshold of −1 for the widely used Standardised Precipitation Index (SPI) (McKee et al. 1993) and is commonly used to characterise ‘moderate’ droughts (McKee et al. 1993). We use this threshold to ensure we have a sufficient number of drought events to infer trends in drought metrics reliably. Previous work has shown that while simulated drought characteristics can be somewhat sensitive to the choice of threshold, inter-model differences represent a much greater source of uncertainty (Ukkola et al. 2018). The 15% threshold definition is applied separately for each indicator and for each different time period. Figure 4.19 and Table 4.5 show that various characteristics of the extreme dry condition were evaluated, namely, the future change in the cumulative duration of the short, moderate, long and prolonged extreme dry spells and the change in the spatial extent of the area undergoing short, moderate, long, and prolonged extreme dry conditions compared to the historical reference period (1976–2005). Using the defined drought metrics, the average percentage of time spent in drought in the future was also calculated and is presented below in Table 4.5.

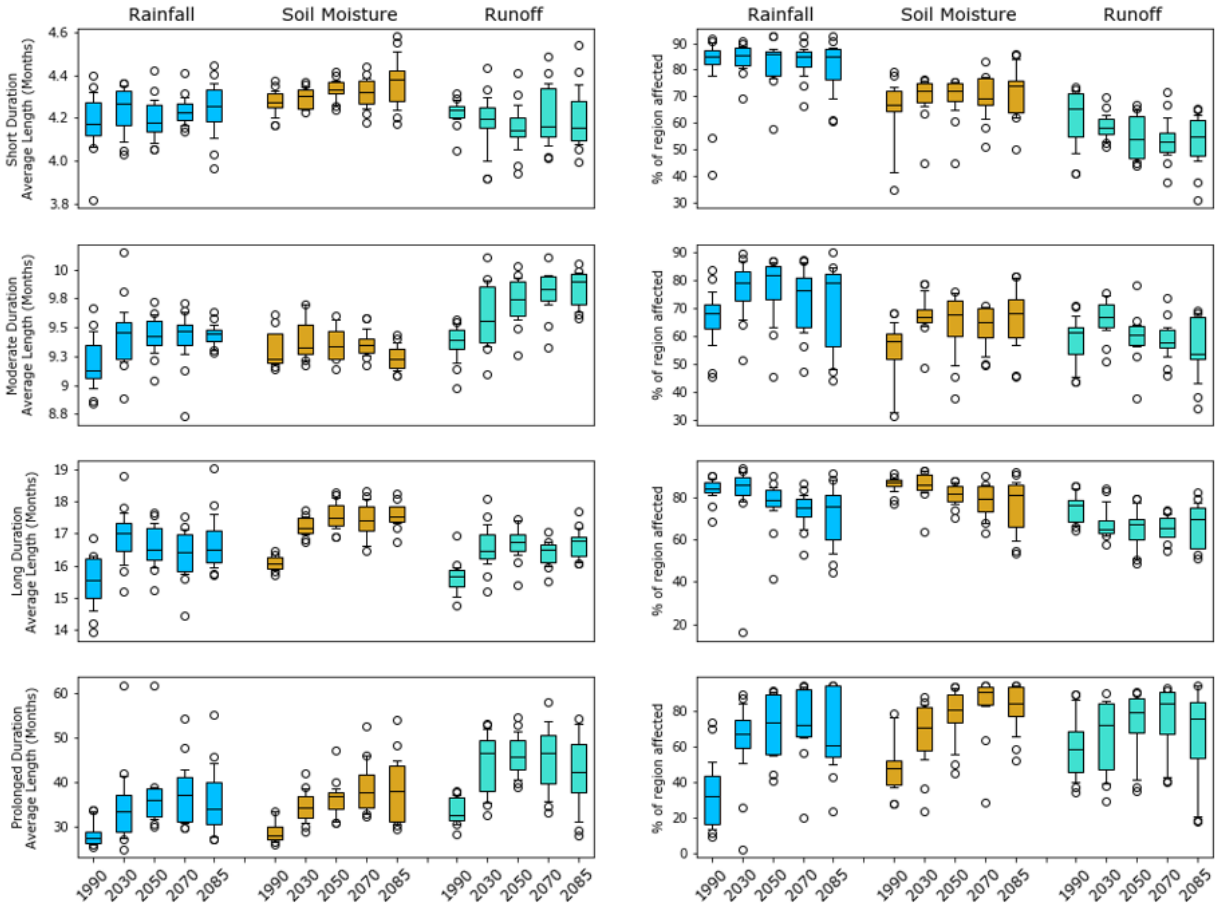

Figure 4.19. Change in projected median drought lengths (left) and percentage of total area affected by extreme dry conditions (right) for modelled precipitation (meteorological drought indicator), modelled soil moisture (agricultural drought indicator) and modelled runoff (hydrological drought indicator) in the East Coast region. The box plots show the median, 10th and 90th percentiles and outliers. They are presented for short-term, moderate, long-term and prolonged drought durations. The change is relative to the reference period (1976–2005)

Table 4.5. Summary of the primary results shown in Figure 4.19

Duration	Drought type	Projected result	Impact
Short (3–6 months)	All types	Little change on average projected for all drought types in terms of duration and a slight decrease on average in spatial extent of drought but a wider ensemble spread is shown in the change in spatial extent.	Projected flash droughts (as represented by 3–6 months duration), remain similar on average compared to the historical reference period. Higher variability is plausible for the drought-affected regions.
Moderate (7–11 months)	All types	Little change on average projected for all drought types in terms of duration and a slight decrease on average in spatial extent of drought, but a wider ensemble spread is shown in the change in spatial extent.	Projected moderate droughts remain similar to the historical reference period with higher variability plausible for the drought-affected regions.
Long term (12–23 months)	All types	Increases projected to varying degrees across the future time periods, where the maximum increase is seen in agricultural long-term drought conditions (>12%). Areas under drought are projected to decrease by as much as 10%, varying over the future time periods for all types of droughts.	Projected long-term droughts to increase, which could have negative implications for river health, water-dependent industries and agricultural systems in the future.
Prolonged (>24 months)	Meteorological dry conditions	Projected increase in time in drought by up to ~15%, varying across the future time periods. Projected increase in area under meteorological by up to ~40%, varying across future time periods.	Projected increases in prolonged periods of low precipitation are plausible with an intensification of precipitation-deficient areas in the future.
	Hydrological dry conditions	Projected increase in time in drought by up to ~30%, varying across the future time periods. Projected increase in area under meteorological by up to ~20%, varying across future time periods.	Projected increase in prolonged periods of low-runoff states, which can lead to water supply shortages and insufficient environmental flows in the future (see Chapter 5).
	Agricultural dry conditions	Projected increase in time in drought by up to ~25%, varying across the future time periods. Projected increase in area under meteorological by up to ~45%, varying across future time periods.	Projected increase in prolonged soil moisture deficits and states are plausible, with an increase in drought-affected areas towards the end of the century. This could lead to impacts on crop and pasture growth and natural vegetation growth in the future.

In summary, the East Coast region is projected to have increased periods in multi-year extreme dry conditions towards the mid and latter part of the century. This is accompanied by an increase in the spatial extent of areas affected by multi-year extreme dry conditions across all indicators. There is larger uncertainty towards the end of the century (Figure 4.19 left) as indicated by the large spread in the ensemble. The area of the region undergoing prolonged dry conditions is projected to increase for all drought types, except for the latest period in the century. However, there is an increasing large spread in results (Figure 4.19 right).

The socioeconomic implications of the increase in long-term to prolonged dry spells mean that water-sensitive industries, agriculture and urban water supply and water management in general in this region would need to prepare for drier conditions and an unreliable year-to-year water supply. In particular, the increase in areas affected by prolonged agricultural drought means that this drier landscape could have implications for bushfire fuel, worsening bushfires in the future. The environmental implications for ecosystems and river health could be significant as these results project reduced availability of water for plants and less surface water, meaning more

variable environmental flows. Impacts associated with large areas of prolonged drought in this region include a lower capacity to rely on measures such inter-catchment transfers to mitigate water security impacts of unreliable water supplies.

5 Exploring future water resource impacts: applying selected storylines to the East Coast region

Projection results feature many sources of uncertainty, including uncertainty over future trajectories of atmospheric greenhouse gas concentrations, how a warmer climate will lead to changes in hydroclimatic features and feedback loops, and how well climate models will represent those features. Acknowledging these uncertainties, the National Hydrological Projections 16-member ensemble provides a unique opportunity to examine the impacts of plausible future changes on Australia's hydroclimate and its water resources. Projections provide a collection of possible future storylines rather than a forecast or likelihood of a specific outcome.

While the National Hydrological Projections 16-member ensemble does not represent every possible future outcome (e.g. of the CMIP5 climate models) for every possible future emissions profile, the ensemble members do represent a selection of internally consistent plausible hydroclimatic futures, or storylines, that let us investigate hydrological responses and inform adaptation planning. Storylines can be used to tie the projections results to a specific impact (Shepherd et al. 2018). We have selected a single ensemble member that represents changes to hydrological features that define a selection of storylines for the East Coast region.

5.1 Representing water-sensitive impacts on water security for Brisbane

These storylines explore changes to water security for the Brisbane metropolitan area for 2050. Wivenhoe Dam is the largest surface water storage in the South East Queensland water grid system. Wivenhoe Dam, together with Somerset, Hinze, North Pine, and Wyaralong dams, accounts for around 80% of the South East Queensland's surface water storage. Projected changes to warm-season (November–April) runoff for the Wivenhoe Dam catchment is used an indicator of changes to water supply. Cool-season (May–October) soil moisture for the Brisbane River catchment is an indicator of changes to demand in the region.

5.1.1 Establishing representative storylines

To determine plausible storylines reflecting range of changes to water availability, changes to warm-season (November–April) runoff for each ensemble member are plotted against changes to cool-season (May–October) soil moisture (Figure 5.1).

Key features of the results are that no storylines project increases to soil moisture, and only 2 of the ensemble set project decreases less than 5% (little change). The remainder project either decreases (−5% to −15%) or large decreases (decreases more than −15%). A number of storylines can be established that represent the extreme conditions from the perspective of changes in water supply and drivers of demand.

Table 5.1. Storylines for exploring changes in water supply and drivers of demand for 2050 for Brisbane

Storyline	Impacts to be explored
Very large decreases in cool-season (May–October) soil moisture and very large decreases in warm-season (November–April) runoff (GFDL-ESM2M_QME RCP8.5)	What are the impacts of large increases in consumptive use demands during the cool (dry) season (May–October) and very large decreases in storage inflows during the typical storage infilling season?
Increase in warm-season (November–April) runoff (52%) and decrease in cool-season (May–October) soil moisture (−13%) (MIROC5_QME RCP8.5)	What are the impacts when there are very large increases in storage infilling, but decreases in the cool (dry) season consumptive use demands?
Little change in cool-season (May–October) soil moisture and little change in warm-season (November–April) runoff (GFDL-ESM2M_CCAM_ISIMIP2 RCP8.5)	What are the impacts on water security under the 'best case' storylines and emission pathway RCP8.5 with little change to runoff and soil moisture?
Increase in warm-season (November–April) runoff (50%) and little change in cool-season (May–October) soil moisture (−4%) (MIROC5_ISIMIP2 RCP4.5)	What are the impacts to water security under increased runoff but little change to soil moisture?

The first 2 storylines are discussed in more detail below as they represent the most extreme combinations of the water security indicators.

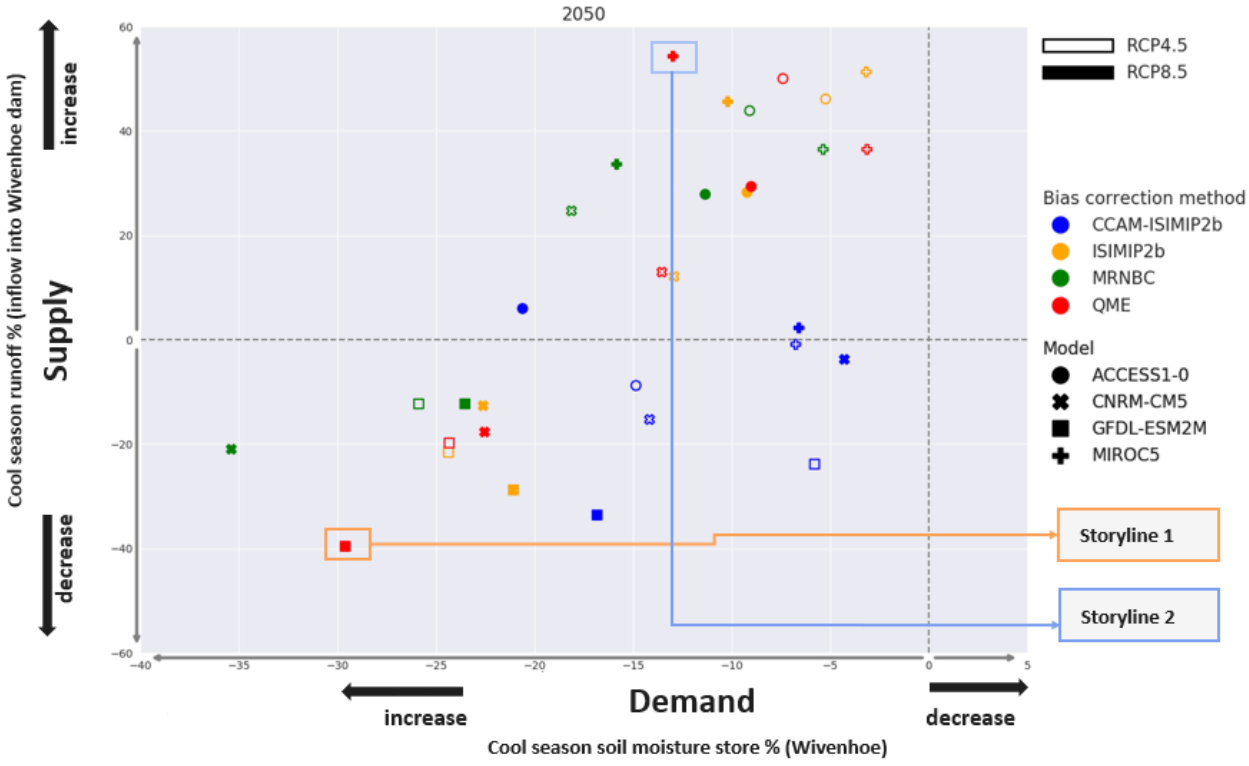

Figure 5.1. Projected changes for 2050 to projected changes to warm-season (November–April) soil moisture vs cool-season (May–October) runoff for the Wivenhoe Dam catchment. Cool-season runoff is used as a proxy for changes to water supply and warm-season soil moisture for changes to demand

5.1.2 Storyline 1: Very large decreases in cool-season (May–October) soil moisture and very large decreases in warm-season (November–April) runoff (GFDL-ESM2M_QME RCP8.5)

This storyline represents the largest decreases in November to April runoff (−40%), and the second largest decrease in May to October soil moisture (−30%). It projects the largest impact for water security in the region.

This storyline projects some of the largest increases in potential evapotranspiration in both seasons. Precipitation projections are for large decreases (−10%) during the filling (warm) season (November–April) and very large decreases (−38%) in the cool season (May–October). The combination of large increases in potential evapotranspiration and reductions in precipitation drives the projected reductions in runoff and soil moisture.

Both wet and dry years are plausible under this storyline, despite the average annual conditions represented by the storyline featuring large decreases compared to current conditions. With significant decreases in water availability and increases in demand, these projections describe a storyline where water scarcity risk is significantly higher in an average year. Under this storyline, alternative water supplies and permanent demand management measures should be considered.

5.1.3 Storyline 2: Increase in warm-season (November–April) runoff (40%) and decrease in cool-season (May–October) soil moisture (−13%) (MIROC5–QME RCP8.5)

This storyline features the largest projected increases in November–April (52%) runoff, but also significant projected decreases in soil moisture (−13%) that indicate increases to demand in average years.

This storyline projects increases to the runoff during the typical filling (warm) season for Wivenhoe Dam, meaning that average years would receive larger volumes of warm-season inflows than is received under current climate conditions. The increase in runoff is driven by projected increases in precipitation, and there is almost no change projected in soil moisture in the season. Projections suggest that future precipitation would more frequently occur in the form of extreme precipitation, leading to extreme runoff. Therefore, managing and operating the water grid to mitigate the impacts of extreme inflows while optimising water availability may become more challenging in the future.

Projected decreases in soil moisture and also decreases in runoff during the cool season (May–October) suggest increased demand under this storyline. This means stored water could be depleted faster in average years and less runoff could be generated in these months to replenish the water stores.

This storyline describes a system with a more pronounced seasonality of infilling and depletion of water than current conditions, making operating the water grid to balance the seasonal dynamics more challenging in average years.

5.2 Conclusions

National Hydrological Projections for changes to precipitation, soil moisture, runoff and evapotranspiration can be useful indicators for a range of water-sensitive impacts, such as water availability for the environment and human consumption, inflows and demands on water storages, and soil moisture for rain-fed agriculture or as a risk factor for bushfires. Using a storylines approach, we have used the National Hydrological Projections to interrogate potential changes to water security as an example of how impact risks can be assessed with these data. Each of the 16 ensemble members represents a plausible future storyline with respect to future changes to water security. Results from other projections are discussed to contextualise where these storylines fit in a broader understanding of plausible futures.

6 Acknowledgements

We acknowledge the work and support of the CSIRO CCAM model development team, including CSIRO Oceans and Atmospheres and CSIRO High Performance Computing along with partners, for their work producing, coordinating and making available the CCAM 50 km datasets required for this project. We thank Marcus Thatcher from the CCAM development team for their useful discussions around accessing, using, and interpreting these data.

We acknowledge the work and support of Dr Fiona Johnson, Dr Raj Mehrotra and Professor Ashish Sharma from the University of New South Wales School of Civil and Environmental Engineering for their roles in producing the MRNBC bias-correction methodology and for their useful discussion around implementing and interpreting this method.

For their roles in producing, coordinating and making available the ISIMIP2b input data and impact model output, we acknowledge the modelling groups, the ISIMIP2b sector coordinators and the ISIMIP cross-sectoral science for the useful discussions around implementing the ISIMIP2b bias-correction methodology. We acknowledge the work and support of Dr Andrew Dowdy from the Australian Bureau of Meteorology for producing and making available the QME bias-correction methodology and bias-corrected model input data.

We acknowledge the World Climate Research Programme's Working Group on Coupled Modelling, which is responsible for CMIP, and we thank the climate modelling groups (listed in Table 3.1 of this report) for producing and making available their model output. For CMIP, the US Department of Energy's Program for Climate Model Diagnosis and Intercomparison provides coordinating support and led development of software infrastructure in partnership with the Global Organization for Earth System Science Portals. This research project was undertaken with the assistance of resources and services from the National Computational Infrastructure (NCI), which is supported by the Australian Government. We thank Dr Kelsey Druken and Dr Yiling Liu for their support in providing the National Hydrological Projections foundational dataset as part of the NCI Data Collection.

The National Hydrological Project has been realised through the hard work and effort of the project team and the support of many individuals from the Australian Bureau of Meteorology, who we would like to thank: for project sponsorship and general project guidance, Dr Robert Argent, Jeff Perkins, Matt Coulton and Dr Elisabetta Carrara; for project management, Zeina Assouad and Anastasia Li; for her leadership while transitioning the product into a service, Elizabeth McDonald; for scientific leadership, Dr Pandora Hope and Dr Justin Peter on climate trends and modelling, and Dr Sugata Narsey on the storylines approach; for support in data processing and software development Dr Justin Peter, Dr Wendy Sharples, Vi Co Duong, Dr Greg Kociuba, Jake Roussis and others; James Devonshire for plotting maps; the Australian Water Outlook team that built the user interface to access National Hydrological Projections data, Khadiza Tahera, Subash Sharma, Ross Lillis, Kieran Lomas and Mark Menzel; for general guidance on the AWRA-L hydrological impact model, Dr Andrew Frost, Dr Ashkan Shokri and Stuart Barron-Hay; and for their general support, Katy Bahramian, Dr Ali Azarnivand and Dr Chris Ruediger. A special thanks to Dr Chantal Donnelly and Dr Louise Wilson who initiated and initially led the project.

We thank deeply all the lead and contributing authors named in the hydrological assessment reports for their large and continuous efforts in producing the hydrological assessment reports. We would like to acknowledge the tireless efforts of Dr Ulrike Bende-Michl who led the National Hydrological Project, developed, and directed the scientific content of the hydrological assessment reports and coordinated the report writing and reviews as well as being a lead contributing author. We would like to thank Dr Alison Oke greatly for her huge efforts in managing the hydrological assessment report writing, developing the report structure and scientific content as well as being lead contributing author. Thanks also to Dr Justin Peter and Dr Greg Kociuba who have developed and operationalised the graphs and plots underpinning the reports. We acknowledge Dr Sri Srikanthan for strengthening and fortifying the reports and Dr Vjekoslav Matic for developing the storylines.

This report benefited from the comments provided by several reviewers, including Drs Chiara Holgate, Ian Watterson, Mark Kennard, Masoud Edraki, Mitchell Black, Mohammed Bari, Murray Peel, Sugata Narsey, Andrew

Dowdy, Sunny Yu, Surendra Rauniyar as well as Artemis Kitsios, Jacqueline Schopf, Jacquie Bellhouse, Jacqui Russel, Susannah Clement and Timothy Willian Bond.

We also acknowledge the useful discussions with Dr Ramona Dalla Pozza and Geoff Steendam and teams from the Victorian State Government Department of Environment, Land, Water and Planning, and the useful discussions with Matthew Reilly from the New South Wales Department of Planning, Industry and Environment.

We acknowledge and are grateful for the participation of the Western Australian Department of Water and Environmental Regulation and Water Corporation WA in demonstration cases, including Artemis Kitsios, Jacquie Bellhouse and Jacqueline Schopf, and the useful discussions with Dr Francis Chew, Dr Steve Charles and Dr Nick Potter from CSIRO Land and Water.

We thank Dr Margot Turner for developing the National Hydrological Projections demonstration use cases in collaboration with state departments that also helped to inform the hydrological assessment reports.

We acknowledge PaperGiant for their consulting effort in the user centred design of the Australian Water Outlook portal and all the contributing participants from multiple organisations.

We thank Margie Beilharz from The Open Desk greatly for her editorial support.

7 References

Abbs, DJ & Rafter, AS 2009, *Impact of climate variability and climate change on rainfall extremes in Western Sydney and surrounding areas: Component 4 – dynamical downscaling*, Report to the Sydney Metro Catchment Management Authority and Partners, CSIRO, Aspendale.

Alam, MA, Emura, K, Farnham, C & Yuan, J 2018, 'Best-fit probability distributions and return periods for maximum monthly rainfall in Bangladesh', *Climate*, vol. 6, no. 1.

Alexander, LV & Arblaster, JM 2009, 'Assessing trends in observed and modelled climate extremes over Australia in relation to future projections', *International Journal of Climatology*, vol. 29, no. 3, pp. 417–435.

Alexander, LV & Arblaster, JM 2017, 'Historical and projected trends in temperature and precipitation extremes in Australia in observations and CMIP5', *Weather and Climate Extremes*,vol. 15, pp. 34–56.

Azarnivand, A, Sharples, W, Bende-Michl, U, Shokri, A, Srikanthan, S, Frost, AJ & Baron-Hay, S 2022, *Analysing the uncertainty of modelling hydrologic states of AWRA-L – understanding impacts from parameter uncertainty for the National Hydrological Projections*. Bureau of Meteorology, Bureau Research Report 060, Melbourne, <http://www.bom.gov.au/research/publications/researchreports/BRR-060.pdf>

Bali, TG 2003, 'The generalized extreme value distribution', *Economics Letters*, vol. 79, no. 3, pp. 423–427.

Brown, JR, Moise, AF, Colman, R & Zhang, H 2016, 'Will a warmer world mean a wetter or drier Australian monsoon?', *Journal of Climate*, vol. 29, no. 12, pp. 4577–4596.

Catto, JL, Jakob, C & Nicholls, N 2013, 'A global evaluation of fronts and precipitation in the ACCESS model', *Australian Meteorological and Oceanographic Journal*, vol. 63, pp. 191–203.

CCiA (Climate Change in Australia) n.d. a, *Climate change in Australia: climate information, projections, tools and data*, CCiA website, accessed 28 October 2021, <www.climatechangeinaustralia.gov.au>.

CCiA (Climate Change in Australia) n.d. b, *Clusters*, CCiA website, accessed 4 November 2021, <https://www.climatechangeinaustralia.gov.au/en/projections-tools/regional-climate-change-explorer/clusters/>.

Chiew, FHS 2006, 'Estimation of rainfall elasticity of streamflow in Australia', *Hydrological Sciences Journal*, vol. 51, no. 4, pp. 613–625.

Collier, M & Uhe, P 2012, *CMIP5 datasets from the ACCESS1.0 and ACCESS1.3 coupled climate models*, Centre for Australian Weather and Climate Research (CAWCR) Technical Report no. 059. CSIRO and Bureau of Meteorology, Australia.

CSIRO & Bureau of Meteorology 2015, *Climate change in Australia projections for Australia's natural resource management regions: technical report*. CSIRO and Bureau of Meteorology, Australia.

CSIRO & Bureau of Meteorology 2020, *State of the climate 2020*, Commonwealth of Australia.

Dowdy, A, Abbs, D, Bhend, J et al. 2015a, *East Coast cluster report*, Climate Change in Australia projections for Australia's natural resource management regions: cluster reports, M Ekström, P Whetton, C Gerbing, M Grose, L Webb & J Risbey (eds), CSIRO and Bureau of Meteorology, Australia.

Dowdy, A, Grose, M, Timbal, B, Moise, A, Ekström, M, Bhend, J & Wilson, L 2015b, 'Rainfall in Australia's eastern seaboard: a review of confidence in projections based on observations and physical processes', *Australian Meteorological and Oceaonographic Journal*, vol. 65, pp. 107–126.

Dowdy, AJ & Kuleshov, Y 2014, 'Climatology of lightning activity in Australia: spatial and seasonal variability', *Australian Meteorological and Oceanographic Journal*, vol. 64, no. 2, pp. 103–108.

Dowdy, AJ 2020, 'Seamless climate change projections and seasonal predictions for bushfires in Australia', *Journal of Southern Hemisphere Earth Systems Science*, vol. 70, no. 1, pp. 120–138.

Dowdy, AJ 2020. 'Climatology of thunderstorms, convective rainfall and dry lightning environments in Australia', *Climate Dynamics,* vol 54, no. 5, pp. 3041–3052.

Dowdy, AJ, Pepler, A, Di Luca, A et al. 2019, 'Review of Australian east coast low pressure systems and associated extremes', *Climate Dynamics*, vol. 53, no. 7, pp. 4887-4910.

Dunne, JP, John, JG, Adcroft, AJ et al. 2012, 'GFDL's ESM2 global coupled climate-carbon earth system models. Part I: Physical formulation and baseline simulation characteristics', *Journal of Climate*, vol. 25, no. 19, pp. 6646–6665.

Easterling, DR, Meehl, GA, Parmesan, C, Changnon, SA, Karl, TR & Mearns, LO 2000, 'Climate extremes: observations, modeling, and impacts', *Science*, vol. 289, no. 5487, pp. 2068–2074.

Fowler, HJ & Ekström, M 2009, 'Multi-model ensemble estimates of climate change impacts on UK seasonal precipitation extremes', *International Journal of Climatology*, vol. 29, no. 3, pp. 385–416.

Frost, AJ & Wright, DP 2018, *Evaluation of the Australian Landscape Water Balance model: AWRA-L v6*. Bureau of Meteorology Technical Report, Commonwealth of Australia.

Greve, P, Roderick, ML & Seneviratne, SI 2017, 'Simulated changes in aridity from the last glacial maximum to 4xCO_2', *Environmental Research Letters*, vol. 12, no. 11, p. 114021.

Grose, MR, Moise, AF, Timbal, B, Katzfey, JJ, Ekström, M & Whetton, PH 2015, 'Climate projections for southern Australian cool-season rainfall: insights from a downscaling comparison', *Climate Research*, vol. 62, no. 3, pp. 251–265.

Grose, MR, Risbey JS, Moise AF, Osbrough S, Heady C, Wilson L & Erwin, T 2017, 'Constraints on southern Australian precipitation change based on atmospheric circulation in CMIP5 simulations', *Journal of Climate*, vol. 30, no. 1, pp. 225–242, doi:10.1175/JCLI-D-16-0142.1

Hempel, S, Frieler, K, Warszawski, L, Schewe, J & Piontek, F 2013, 'A trend-preserving bias correction – the ISI-MIP approach', *Earth System Dynamics*, vol. 4, no. 2, pp. 219–236.

Hendon, HH, Thompson, DWJ & Wheeler, MC 2007, 'Australian rainfall and surface temperature variations associated with the Southern Hemisphere annular mode', *Journal of Climate*, vol. 20, no. 11, pp. 2452–2467.

Hope, P, Grose, MR, Timbal, B et al. 2015, 'Seasonal and regional signature of the projected southern Australian rainfall reduction', *Australian Meteorological and Oceanographic Journal*, vol. 65, no. 1, pp. 54–71.

Johnson, AKL & Murray, AE 2004, 'Modelling the spatial and temporal distribution of rainfall: a case study in the wet and dry tropics of North East Australia', *Australian Geographer*, vol. 35, no. 1, pp. 39–57.

Johnson, F & Sharma, A 2012, 'A nesting model for bias correction of variability at multiple time scales in general circulation model precipitation simulations', *Water Resources Research*, vol. 48, no. 1.

Jones, DA, Wang, W & Fawcett, R 2009, 'High-quality spatial climate data-sets for Australia', *Australian Meteorological and Oceanographic Journal*, vol. 58, no. 4, pp. 233–248.

Kuleshov, Y, Mackerras, D & Darveniza, M 2006, 'Spatial distribution and frequency of lightning activity and lightning flash density maps for Australia', *Journal of Geophysical Research: Atmospheres*, vol 111, no. D19.

Lucas, C, Rudeva, I, Nguyen, H, Boschat, G & Hope, P 2021, 'Variability and changes to the mean meridional circulation in isentropic coordinates', *Climate Dynamics*, vol. 58, no. 1, pp. 1–20.

McKee, TB, Doesken, NJ & Kleist, J 1993, 'The relationship of drought frequency and duration of time scales.' *Proceedings of the Eighth Conference on Applied Climatology*, American Meteorological Society, Boston, pp. 179–184.

Mehrotra, R & Sharma, A 2016, 'A multivariate quantile-matching bias correction approach with auto- and cross-dependence across multiple time scales: implications for downscaling', *Journal of Climate*, vol. 29, no. 10, pp. 3519–3539.

Milly, PCD, Wetherald, RT, Dunne, KA & Delworth, TL 2002, 'Increasing risk of great floods in a changing climate', *Nature*, vol. 415, no. 6871, pp. 514–517.

Moise, A, Wilson, L, Grose, M et al. 2015, 'Evaluation of CMIP3 and CMIP5 models over the Australian region to inform confidence in projections', *Australian Meteorological and Oceanographic Journal*, vol. 65, no. 1, pp. 19–53.

Nash, JE & Sutcliffe, JV 1970, 'River flow forecasting through conceptual models part I – A discussion of principles', *Journal of Hydrology*, vol. 10, no. 3, pp. 282–290.

Palmer, TN & Räisänen, J 2002, 'Quantifying the risk of extreme seasonal precipitation events in a changing climate', *Nature*, vol. 415, no. 6871, pp. 512–514.

PCMDI (Program for Climate Model Diagnosis & Intercomparison) 2021, *CMIP5 – Coupled Model Intercomparison Project Phase 5 -– Overview*, PCMDI website, accessed 10 November 2021, <https://pcmdi.llnl.gov/mips/cmip5/>.

Pepler, AS & Rakich, CS 2010, Extreme inflow events and synoptic forcing in Sydney catchments, *IOP Conference Series: Earth and Environmental Science*, vol. 11, no. 1, p. 012010.

Pepler, AS, Dowdy, AJ & Hope, P 2021, 'The differing role of weather systems in southern Australian rainfall between 1979–1996 and 1997–2015', *Climate Dynamics*, vol. 56, no. 7–8, pp. 2289–2302.

Rafter, AS & Abbs, DJ 2009, 'An analysis of future changes in extreme rainfall over Australian regions based on GCM simulations and Extreme Value Analysis', *CAWCR Research Letters*, vol. 3, pp. 43–48.

Rafter, T, Trenham, C, Thatcher, M, Remenyi, T, Wilson, L, Heady, C & Love, P 2019, *CCAM Climate Downscaling Data for Victoria 2019*,CSIRO Data Access Portal website, accessed 10 November 2021, <https://data.csiro.au/collection/38583>.

Shepherd, TG, Boyd, E, Calel, RA et al. 2018, 'Storylines: an alternative approach to representing uncertainty in physical aspects of climate change', *Climatic Change*, vol. 151, no. 3–4, pp. 555–571.

Sherwood, SC, Roca, R, Weckwerth, TM & Andronova, NG 2010, 'Tropospheric water vapor, convection, and climate', *Reviews of Geophysics*, vol. 48, no. 2.

Srikanthan, S., Bende-Michl, U, Sharples, W et al. 2022, *Introduction to the National Hydrological Projections Project*, Bureau of Meteorology, Bureau Research Report 061, Melbourne.

Syktus, J, Trancoso, R, Ahrens, D, Toombs, N & Wong, K 2020, *Queensland Future Climate Dashboard: downscaled CMIP5 climate projections for Queensland*, The Long Paddock website, accessed 4 November 2021, <https://www.longpaddock.qld.gov.au/qld-future-climate/dashboard/>.

Taylor, KE, Stouffer, RJ & Meehl, GA 2012, 'An overview of CMIP5 and the experiment design', *Bulletin of the American Meteorological Society*, vol. 93, no. 4, pp. 485–498.

Ukkola, AM, Pitman, AJ, De Kauwe, MG, Abramowitz, G, Herger, N, Evans, JP & Decker, M 2018, 'Evaluating CMIP5 model agreement for multiple drought metrics', *Journal of Hydrometeorology*, vol. 19, no. 6, pp. 969–988.

Voldoire, A, Sanchez-Gomez, E, Salas y Mélia, D et al. 2013, 'The CNRM-CM5.1 global climate model: description and basic evaluation', *Climate Dynamics*, vol. 40, no. 9–10, pp. 2091–2121.

Walsh, KJE & Ryan, BF 2000, 'Tropical cyclone intensity increase near Australia as a result of climate change', *Journal of Climate*, vol. 13, no. 16, pp. 3029–3036.

Wang, G, Cai, W & Santoso, A 2017, 'Assessing the impact of model biases on the projected increase in frequency of extreme positive Indian Ocean Dipole events', *Journal of Climate*, vol. 30, no. 8, pp. 2757–2767.

Wang, GQ, Zhang, JY, Xu, YP, Bao, ZX & Yang, XY 2017, 'Estimation of future water resources of Xiangjiang River Basin with VIC model under multiple climate scenarios', *Water Science and Engineering,* vol. 10, no. 2, pp. 87–96.

Wasko, C & Nathan, R 2019, 'Influence of changes in rainfall and soil moisture on trends in flooding', *Journal of Hydrology*, vol. 575, pp. 432–441.

Wasko, C & Sharma, A 2017, 'Global assessment of flood and storm extremes with increased temperatures', *Scientific Reports*, vol. 7, no. 1, 7945.

Wasko, C, Shao, Y, Vogel, E, Wilson, L, Wang, QJ, Frost, A & Donnelly, C 2021, 'Understanding trends in hydrologic extremes across Australia', *Journal of Hydrology*, vol. 593, p. 125877.

Watanabe, M, Suzuki, T, O'ishi, R, et al. 2010, 'Improved climate simulation by MIROC5: mean states, variability, and climate sensitivity', *Journal of Climate*, vol. 23, no. 23, pp. 6312–6335.

Yang, Y, Roderick, ML, Zhang, S, McVicar, TR & Donohue, RJ 2019, 'Hydrologic implications of vegetation response to elevated CO_2 in climate projections', *Nature Climate Change*, vol. 9, no. 1, pp. 44–48.

Yin, J, Guo, S, Gu, L, He, S, Ba, H, Tian, J, Li, Q & Chen, J 2020, 'Projected changes of bivariate flood quantiles and estimation uncertainty based on multi-model ensembles over China', *Journal of Hydrology*, vol. 585, p. 124760.

Zhang, XS, Amirthanathan, GE, Bari, MA et al. 2016, 'How streamflow has changed across Australia since the 1950s: evidence from the network of hydrologic reference stations', *Hydrology and Earth System Sciences*, vol. 20, no. 9, pp. 3947–3965.

8 Appendix: Evaluation of bias-correction methods

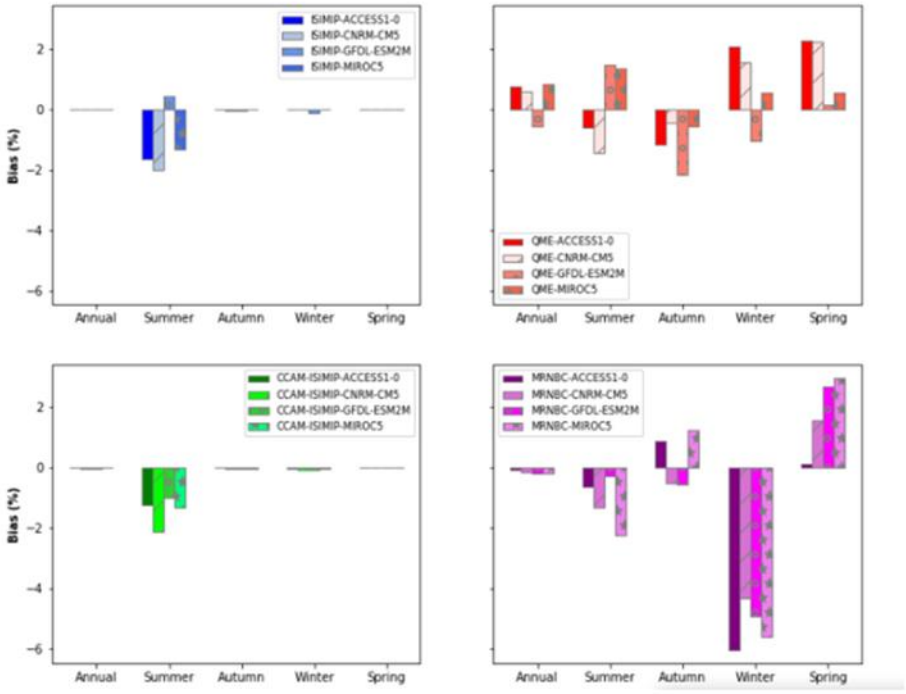

Figure 8.1. Bias (%) in mean annual and seasonal precipitation for the East Coast region

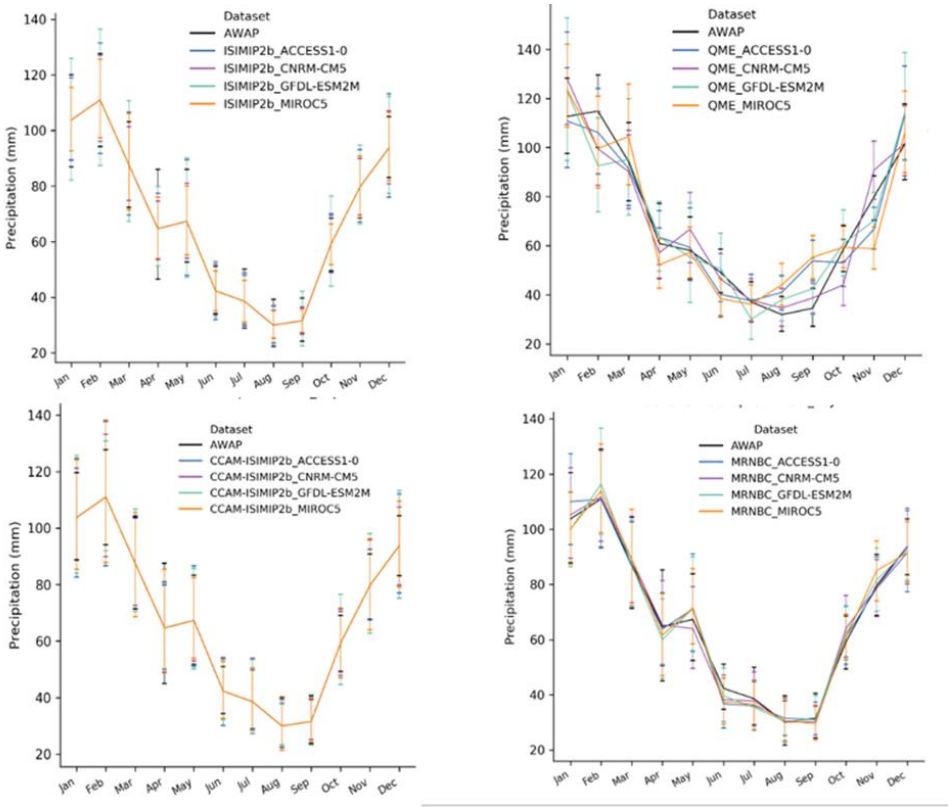

Figure 8.2. Comparison of the mean monthly precipitation (mm) for the 16-member ensemble and observed (AWAP) data for the East Coast region (1976–2005

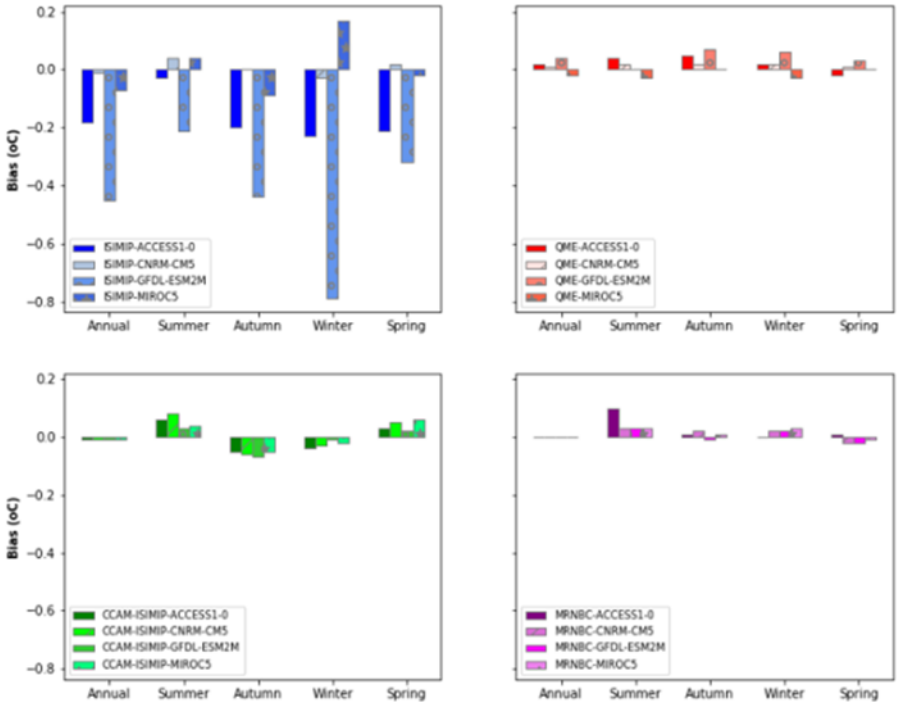

Figure 8.3. Bias (°C) in mean annual and seasonal maximum temperature for the East Coast region

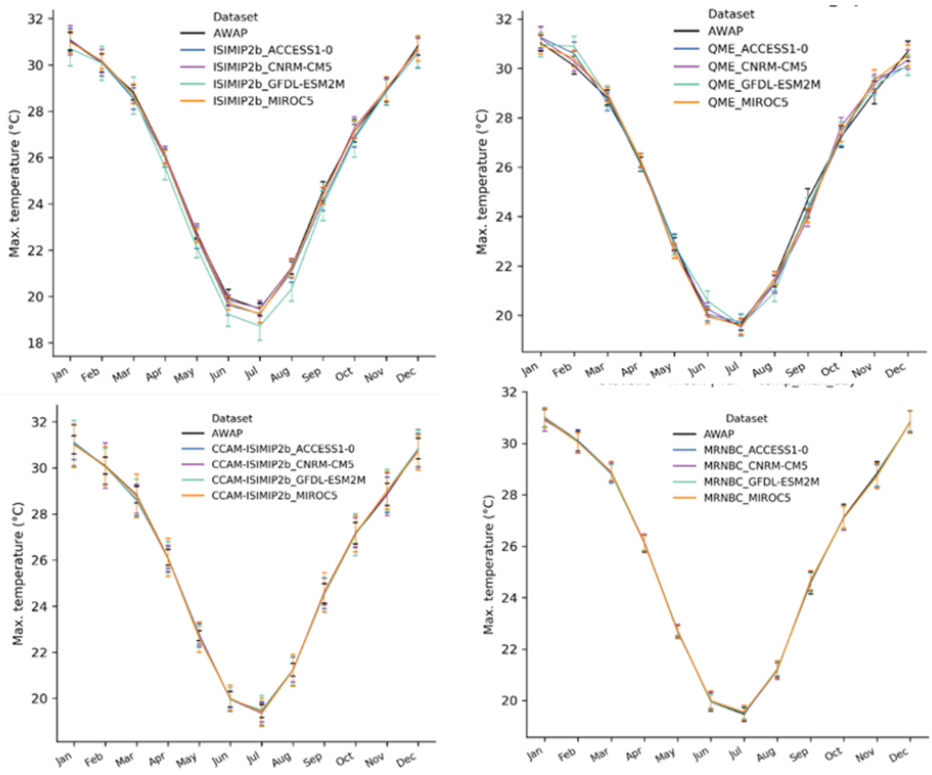

Figure 8.4. Comparison of the mean monthly maximum temperature (°C) for the 16-member ensemble and observed (AWAP) data for the East Coast region (1976–2005)

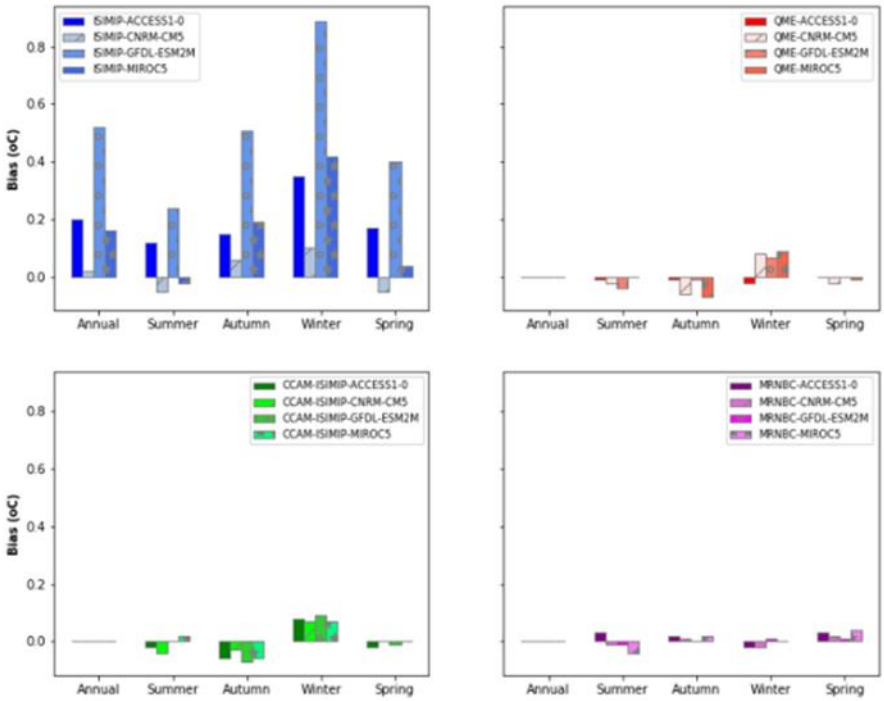

Figure 8.5. Bias (°C) in mean annual and seasonal minimum temperature for the East Coast region

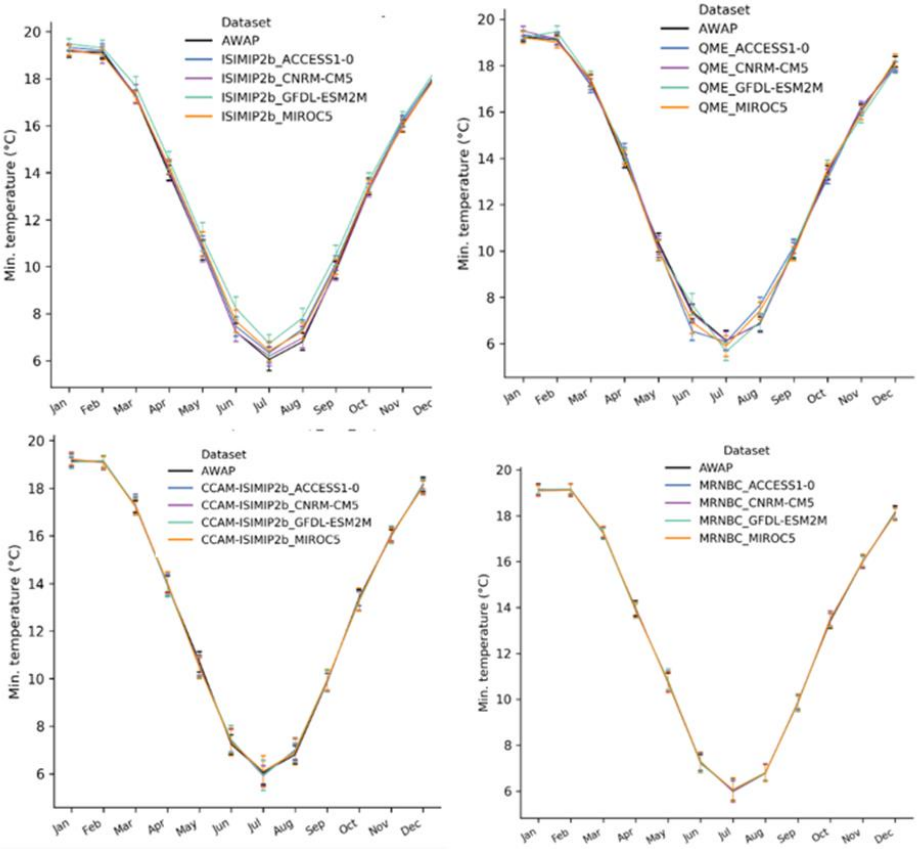

Figure 8.6. Comparison of the mean monthly minimum temperature (°C) for the 16-member ensemble and observed (AWAP) data for the East Coast region (1976–2005)

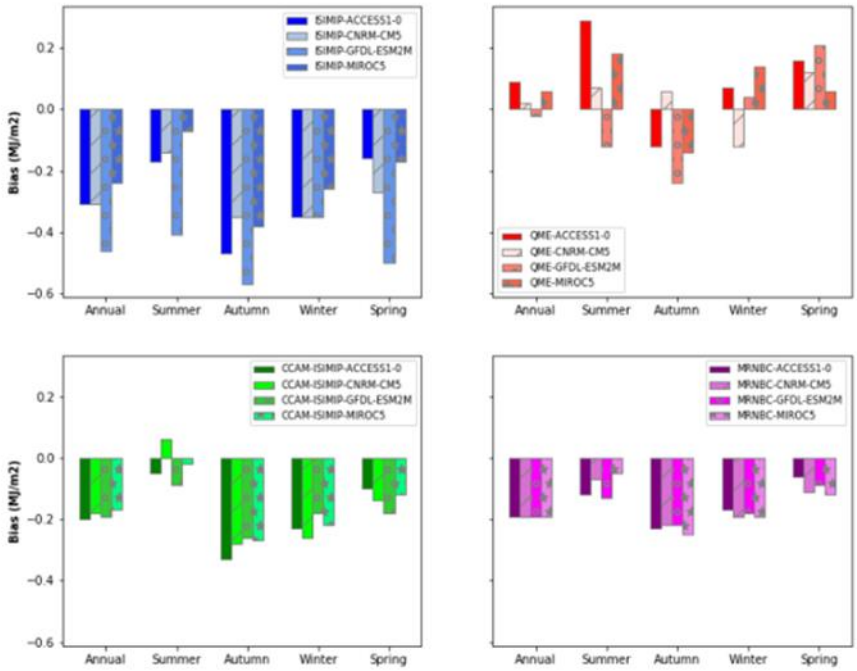

Figure 8.7. Bias (megajoules per square metre, MJ/m^2) in mean annual and seasonal solar radiation for the East Coast region

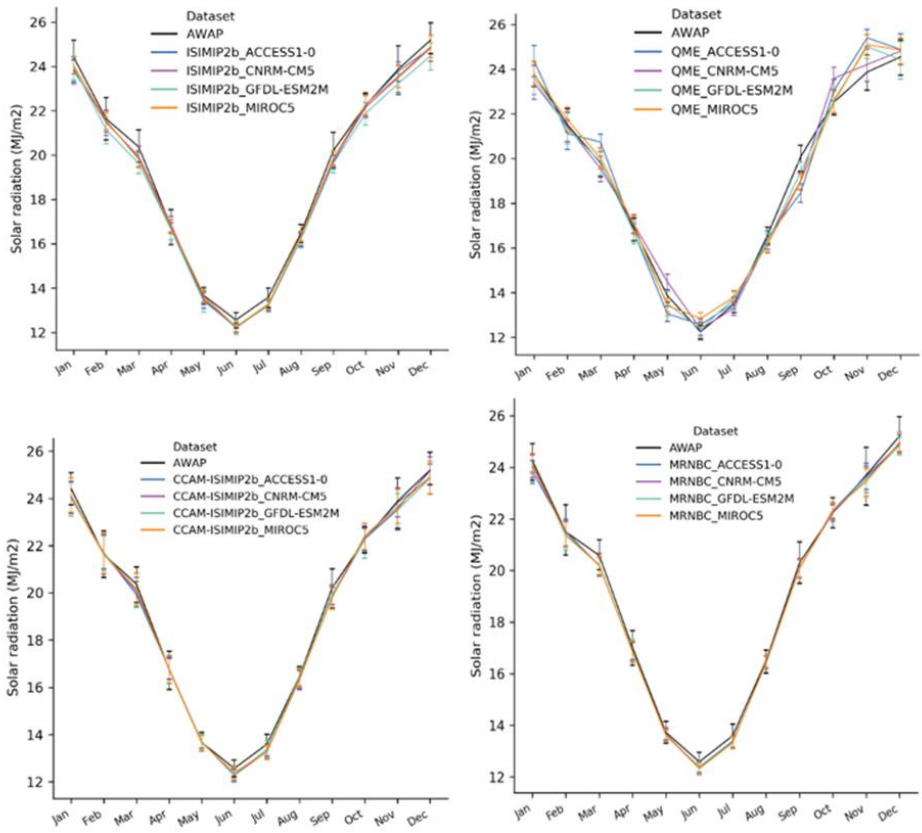

Figure 8.8. Comparison of the mean monthly solar radiation (MJ/m^2) for the 16-member ensemble and observed (AWAP) data for the East Coast region (1976–2005)

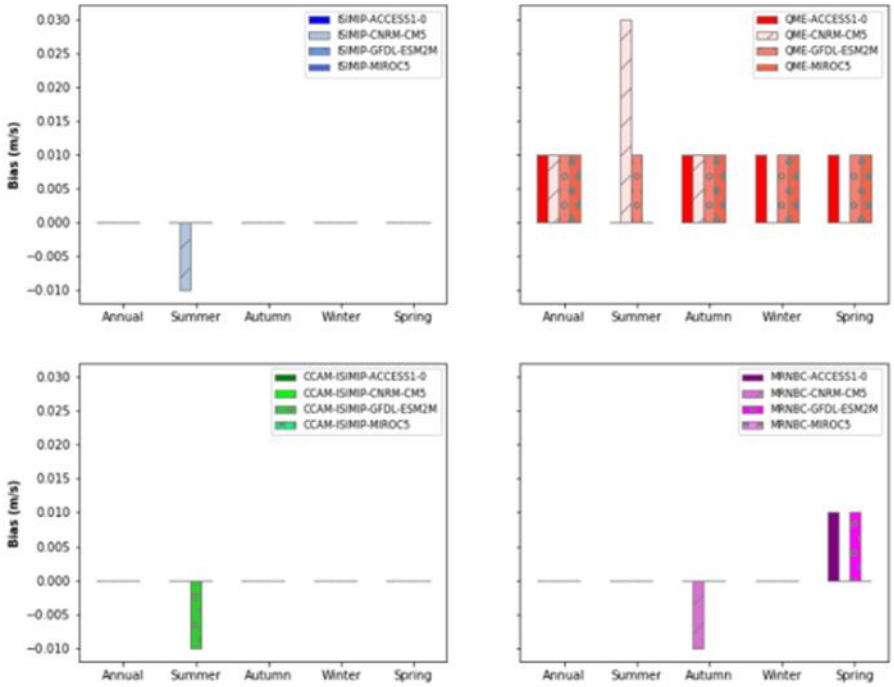

Figure 8.9. Bias (m/s) in mean annual and seasonal wind speed for the East Coast region

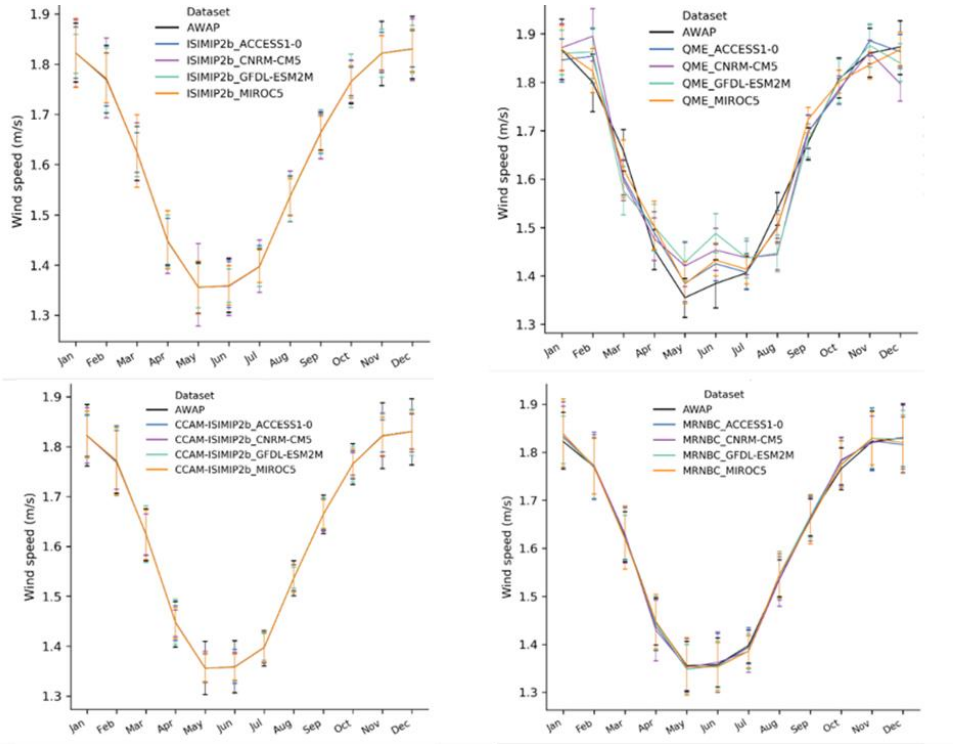

Figure 8.10. Comparison of the mean monthly wind speed (m/s) for the 16-member ensemble and observed (AWAP) data for the East Coast region (1976–2005)

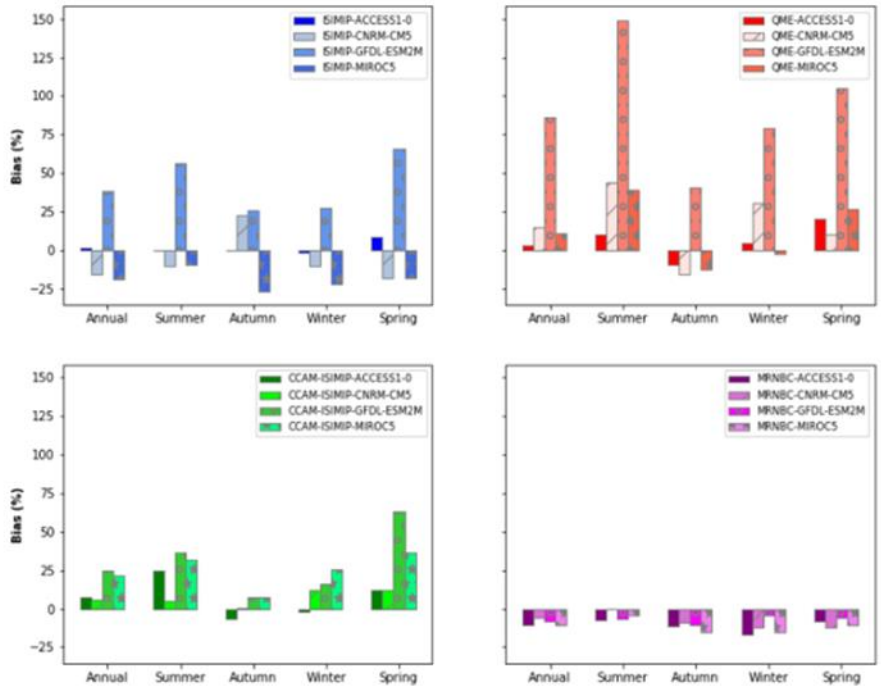

Figure 8.11. Bias (%) in mean annual and seasonal runoff for the East Coast region

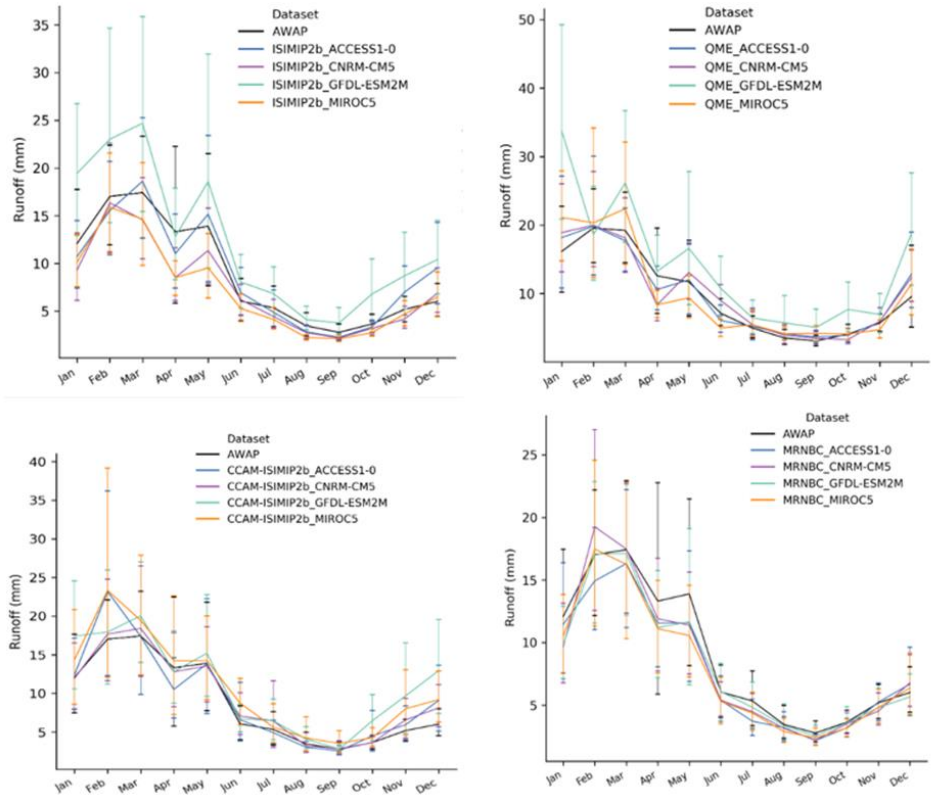

Figure 8.12. Comparison of the mean monthly runoff (mm) for the 16-member ensemble and observed (AWAP) data for the East Coast region (1976–2005)

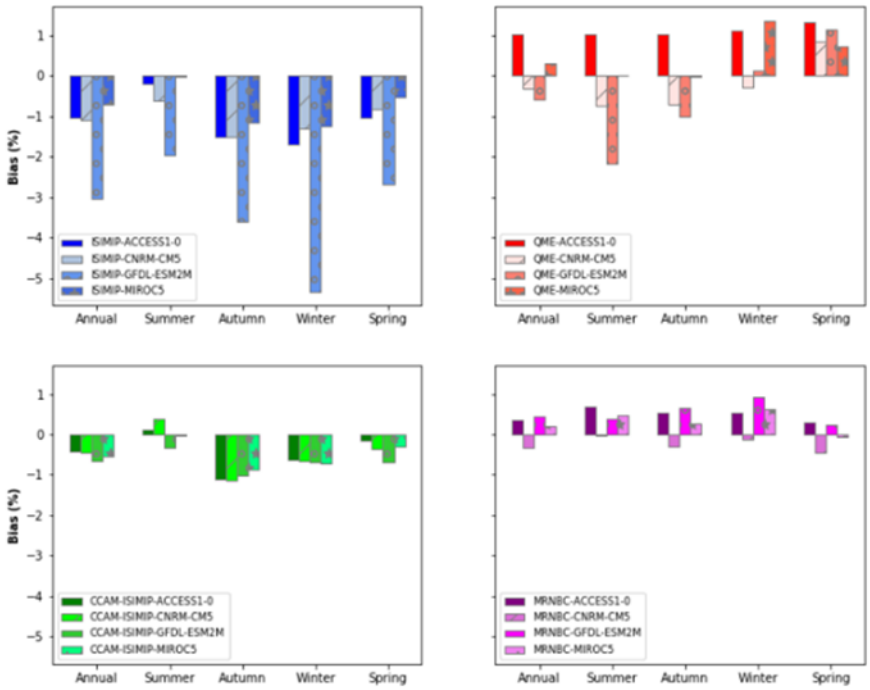

Figure 8.13. Bias (%) in mean annual and seasonal potential evapotranspiration for the East Coast region

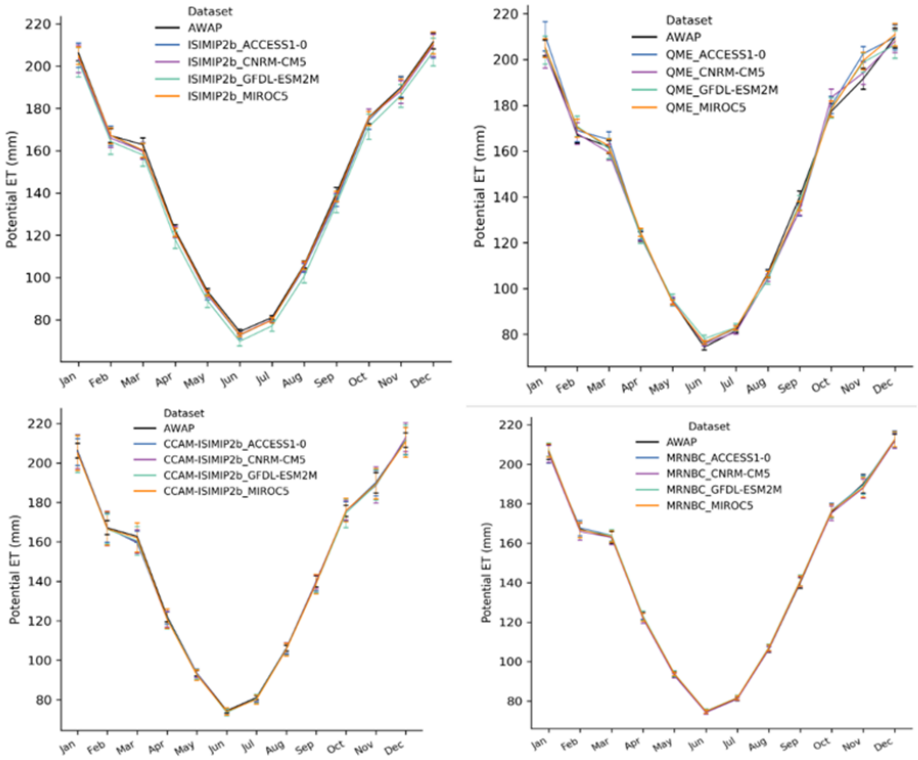

Figure 8.14. Comparison of the mean monthly potential evapotranspiration (mm) for the 16-member ensemble and observed (AWAP) data for the East Coast region (1976–2005)

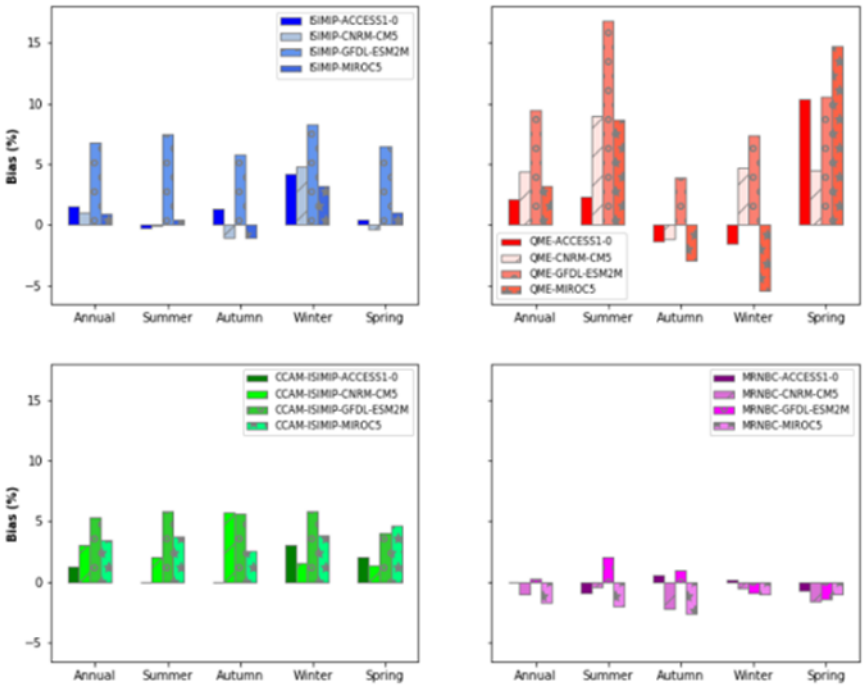

Figure 8.15. Bias (%) in mean annual and seasonal soil moisture for the East Coast region

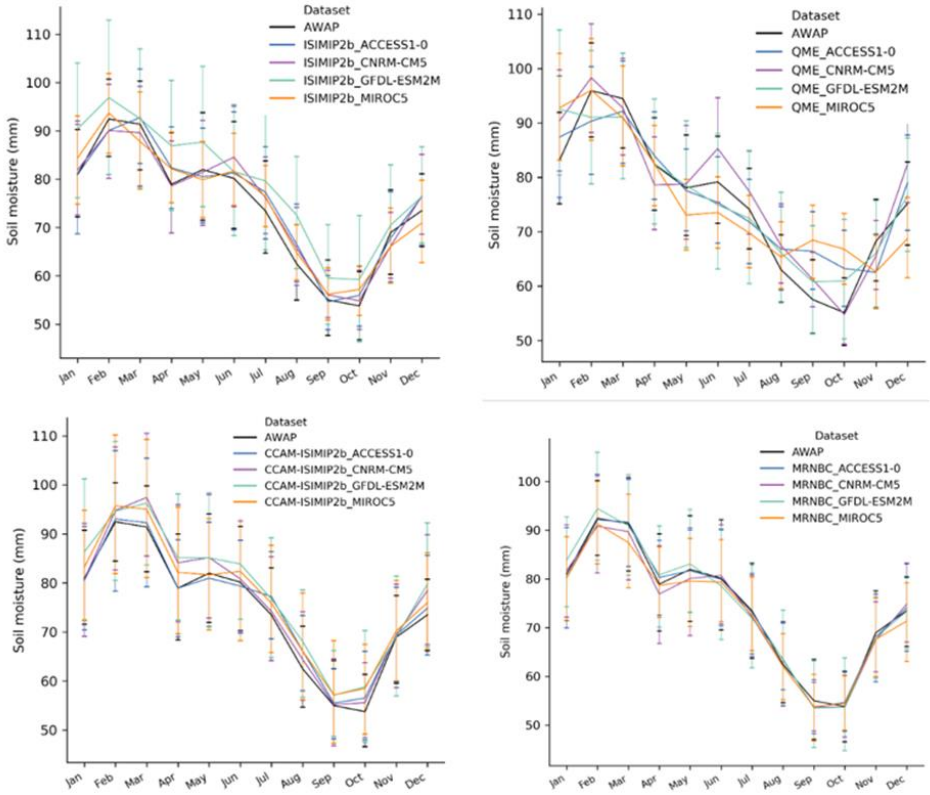

Figure 8.16. Comparison of the mean monthly soil moisture (mm) for the 16-member ensemble and observed (AWAP) data for the East Coast region (1976–2005)